# Foot-and-mouth disease virus VP4: roles in membrane permeability and capsid breathing

Jessica Jane Swanson

Submitted in accordance with the requirements for the degree of Doctor of Philosophy

The University of Leeds

School of Molecular and Cellular Biology

September 2018

The candidate confirms that the work submitted is her own and that appropriate credit has been given where reference has been made to the work of others.

# Acknowledgements

Firstly, I need to thank my wonderful supervisors for 4 years of support and guidance. Toby, thank you for being such a supportive supervisor and for always seeing the positive side. Thank you to my university supervisor Nic Stonehouse for our monthly meetings, her quick and thorough comments on my work and for always making me feel very welcome in Leeds on my annual trips. I was also fortunate enough to have two wonderful co-supervisors, Anusha and Alison, who provided practical support throughout my PhD. Thank you both for making me feel so welcome and offering me help and advice throughout my PhD.

Thank you to both the Picornavirus Molecular Biology and Picornavirus Structure groups. My time in the lab would not have been anywhere near as good without everyone. A special thank you to Joe, Jamie and Chris for all of the good memories of working in Jenner and to Hannah for her organisational help and massive amounts of moral support.

Thank you to Jamie for all of the VP4 discussions which lead to the data presented in chapter 6, which has been carried out by both Jamie and myself. My own contributions, fully and explicitly indicated in the thesis, have been sequence alignments and the size-selectivity membrane permeability assays. The contributions by Jamie were comparison of VP4 structures and membrane permeability assays.

Thank you to all the friends I have made during my PhD. Thank you to Phoebe, Tom, Dana, Ben, Jess, Lisa, Stacey, Grace and everyone else for all the fun over the years. A special thank you to my housemate Laura for being the perfect housemate in my final year.

My final thank you goes to my wonderful family and boyfriend Myles for their support over the past 4 years. I always aspired to do a PhD because my Dad had one and I am grateful for my parent's encouragement along the way. Thank you Myles for always reminding me there was more to life than my PhD and for being there for me anytime.

# Abstract

Foot-and-mouth disease virus (FMDV) is an economically-important picornavirus that infects cloven hooved animals. Entry is a vital step in the virus lifecycle and results in conformational changes in the capsid, including release of the capsid protein VP4. For other picornaviruses, VP4 has been shown to induce membrane permeability and is hypothesised to be involved in the transfer of the viral genome into the cytoplasm using a mechanism which remains poorly understood. The studies presented in this thesis aimed to explore the role of FMDV VP4.

Firstly, characterisation of the membrane permeability induced by FMDV VP4 demonstrated, in contrast to previous work with human rhinovirus (HRV) VP4, that both termini of FMDV VP4 independently induced size-selective membrane permeability. Secondly, the hepatitis B core virus-like particle (VLP) was used to display the N-terminal 15 amino acids of FMDV VP4. Two approaches to displaying this sequence on the VLP were successfully established and taken forward to an immunisation study. Thirdly, characterisation of VP4 reactive antibodies has further alluded to the role of FMDV VP4. Alongside the antibodies generated against the VLPs, antibodies against the N- and C-terminus of VP4 were generated using KLH-peptide conjugates. In contrast to previous studies with antibodies raised against HRV VP4, the FMDV VP4 antibodies did not affect FMDV infectivity or affect FMDV-induced membrane permeability. However, the VP4 antibodies detected FMDV by ELISA, indicating externalisation of VP4 from the capsid. The process of transient VP4 externalisation, termed capsid breathing, has been demonstrated for other picornaviruses and this work indicated capsid breathing occurs in FMDV.

The work presented here indicates that FMDV VP4 plays a role in membrane permeability and capsid breathing. Furthermore, these processes may be shared between different genera of picornaviruses.

# Table of Contents

# List of Figures

# List of Tables

# Abbreviations

| | |
|---|---|
| +ssRNA | positive sense single stranded RNA |
| Å | angstrom |
| µg | microgram |
| µg/mL | microgram per millilitre |
| µl | microlitre |
| µM | micromolar |
| AIDS | acquired immunodeficiency syndrome |
| AiV | aichi virus |
| AMPs | antimicrobial peptides |
| ATP | adenosine triphosphate |
| BHK-21 | baby hamster kidney cells |
| bp | Base pair |
| bus | 3B uridylylation signal |
| CF | carboxyfluorescein |
| CPE | cytopathic effect |
| CRE | cis-acting regulatory element |
| cryo-EM | cryo-electron microscopy |
| CSU | central service unit |
| CVB3 | Coxsackievirus B3 |
| DIVA | differentiation between infected and vaccinated |
| DMSO | dimethyl sulfoxide |
| DNA | deoxyribonucleic acid |
| dsRNA | double stranded RNA |
| *E.coli* | *Escherichia coli* |
| ECL | enhanced chemiluminescence |
| EDTA | ethylenediaminetetraacetic acid |
| eIF1 | eukaryotic initiation factor 1 |

| | |
|---|---|
| eIF3 | Eukaryotic translation initiation factor 3 |
| eIF4A | Eukaryotic translation initiation factor 4A |
| eIF4G | Eukaryotic translation initiation factor 4G |
| ELISA | enzyme-linked immunosorbent assay |
| EM | electron microscopy |
| ERAV | equine rhinitis A virus |
| EVA71 | enterovirus A 71 |
| FBS | foetal bovine serum |
| FD | fluorescein isothiocyanate-linked dextran |
| FHV | flock house virus |
| FITC | fluorescein isothiocyanate |
| FMD | foot-and-mouth disease |
| FMDV | foot-and-mouth disease virus |
| g | gram |
| GFP | green fluorescent protein |
| GST | glutathione S-transferase |
| HA | haemagglutinin |
| HAV | hepatitis A virus |
| HBcAg | hepatitis B core antigen |
| HBc | hepatitis B core |
| Hepes | 4-(2-hydroxyethyl)-1-piperazineethanesulfonic acid |
| HF | high fidelity |
| HIV | human immunodeficiency virus |
| HRP | horse radish peroxidase |
| HRV | human rhinovirus |
| HSG | heparin sulphate glycan |
| IBDV | infectious bursal disease virus |
| IFN β | interferon β |

| | |
|---|---|
| IgG | immunoglobulin G |
| IPTG | isopropyl β-D-1-thiogalactopyranoside |
| IRES | internal ribosome entry site |
| ISG | interferon-stimulated gene |
| ISVP | infectious subviral particle |
| kb | kilobase |
| kDa | kilodalton |
| KLH | keyhole limpet haemocyanin |
| LB | Luria-Bertani |
| LUV | large unilamellar vesicles |
| LV | Ljungan virus |
| M | molar |
| MIR | major immunodominant region |
| mg/mL | milligrams per millilitre |
| mL | millilitre |
| mM | millimolar |
| MLV | multilamellar vesicles |
| mRNA | messenger RNA |
| myr | myristoylation |
| ng | nanogram |
| ng/mL | nanogram per millilitre |
| nm | nanometer |
| nt | nucleotide |
| NTA | nitrilotriacetic acid |
| OD | optical density |
| OPD | o-phenylenediamine dihydrochloride |
| OD600 | optical density at 600 nm |
| ORF | open reading frame |

| | |
|---|---|
| PA | phosphatidic acid |
| PBS | phosphate buffered saline |
| PBS-T | phosphate buffered saline with tween |
| PC | phosphatidylcholine |
| PCR | polymerase chain reaction |
| PDB | protein database |
| PE | phosphatidylethanolamine |
| PFU | plaque forming units |
| PFU/mL | plaque forming units per milliliter |
| PI | preimmune |
| PK | pseudoknots |
| PV | poliovirus |
| PVr | poliovirus receptor |
| RHA | RNA helicase A |
| RNA | ribonucleic acid |
| RNase | ribonuclease |
| rpm | revolutions per minute |
| RPMI | Rosewell Park Memorial Institute media |
| RT | room temperature |
| S | sedimentation coefficient |
| SAFV-3 | saffold virus 3 |
| Scr | Scrambled |
| SD | standard deviation |
| SDS | sodium dodecyl sulphate |
| SDS-PAGE | sodium dodecyl sulphate polyacrylamide gel electrophoresis |
| SOC | super optimal broth with catabolite repression |
| SUV | small unilamellar vesicles |
| SV40 | simian vacuolating virus 40 |

| | |
|---|---|
| SVV | Seneca Valley virus |
| TBE | tris-bovate-EDTA |
| TBS | tris buffered saline |
| $TCID_{50}$ | tissue culture infectious dose 50 % |
| TEM | transmission electron microscopy |
| TMEV | Theiler's murine encephalomyelitis virus |
| TEMED | N,N,N’,N’-Tetramethylethylenediamine |
| UK | United Kingdom |
| UTR | untranslated region |
| V | volts |
| VPg | viral protein genome linked |
| VLP | virus-like particle |
| VNT | virus neutralisation test |
| w/v | weight per volume |
| WT | wild type |
| x g | times gravity |

# Chapter 1 Introduction

# 1. Introduction

Foot-and-mouth disease virus (FMDV) is a member of the *Picornaviridae* family of viruses and belongs to the *Aphthovirus* genus of this family. FMDV is an economically important virus and whilst vaccines exist there are still significant challenges posed by this virus.

The lifecycle of FMDV is split into several stages. First the virus must attach to the host cell via binding of the viral capsid to the receptor, it then enters the cell through endocytosis. Once in the endosome the viral genome has to be transferred across the endosomal membrane and into the cytoplasm. The genome is then translated to produce viral proteins involved in replication and production of progeny viruses. Following the assembly of new viruses, these progeny viruses are released from the infected cell to spread the virus further.

Entry and the subsequent transfer of the genome are key steps in the virus lifecycle and therefore could be a potential target for vaccines and therapeutic treatments for infection. Previous work in the related picornaviruses has suggested that the internal capsid protein VP4 forms a pore which could be involved in the transfer of the genome into the cytoplasm. The aims of this work are to characterise role of FMDV VP4 in membrane permeability and to investigate if antibodies against VP4 are able to protect against FMDV infection.

## 1.1 Foot-and-mouth disease

Foot-and-mouth disease (FMD) is an infectious disease that affects cloven hooved animals including economically important livestock such as cattle, pigs and camels (Grubman and Baxt, 2004, Wernery and Kaaden, 2004). This disease is caused by infection with FMDV. Infection with FMDV leads to the development of lesions in the mouth and on the feet of infected animals and these lesions cause reduced productivity of the animals. Infection with FMDV normally has low mortality rates but can leave animals with permanent damage to tissues, such as the feet and teats. This damage can have lasting effects on the reproductive ability of the herd and result in lameness (James and Rushton, 2002, Alexandersen *et al*., 2003). Infected animals have reduced weight gain, which when combined with lameness and reproductive issues, can affect food security and local trade (Knight-Jones and Rushton, 2013). Currently several countries have been declared FMD free either with or without the use of vaccination (e.g. countries within Europe) but FMD is still

present in countries in Africa and Asia (figure 1.1)

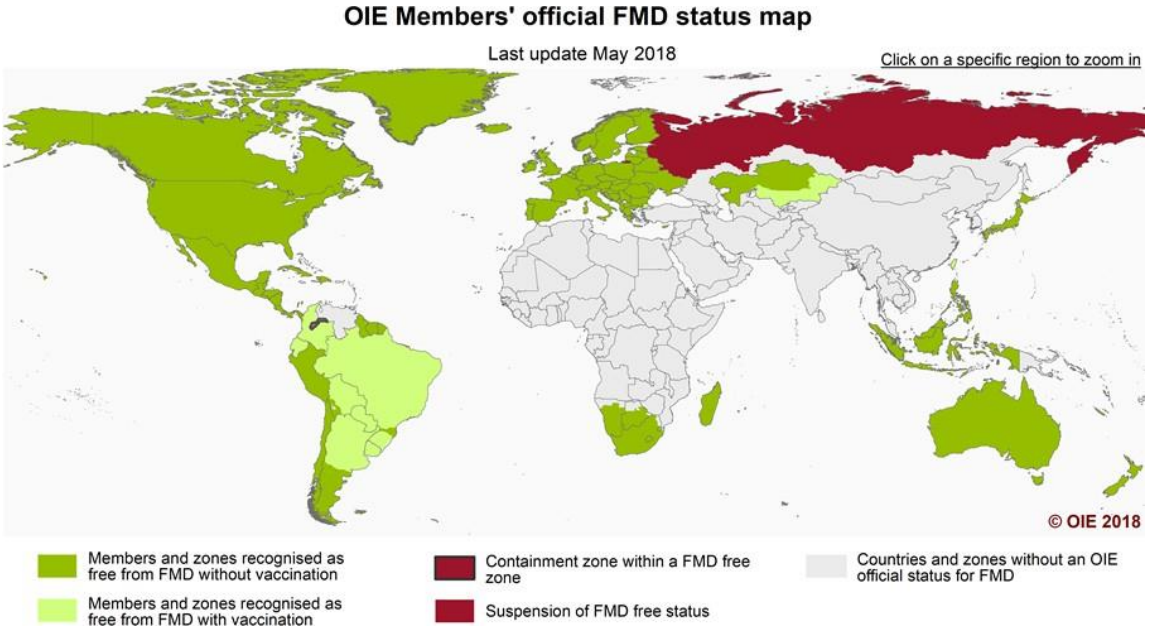


**Figure 1. 1: FMD status worldwide as of May 2018.**

Countries that are shown in green are free from FMD, either with or without the use of vaccination. Countries shown in red are currently not deemed to be FMD free. Countries shown in grey do not have a confirmed OIE official status for FMDV. Map obtained from: http://www.oie.int/en/animal- health-in-the-world/official-disease-status/fmd/en-fmd-carte/

## 1.1.1 Economic impact of FMDV

The presence of FMDV in a country can have a severe economic impact. In countries declared as FMDV-free, such as the UK, an outbreak can have huge costs to the country. It is estimated that the 2001 FMDV outbreak in the UK cost the agriculture industry about £3.1 billion and the tourism industry about £3.2 billion (Thompson *et al*., 2002). Obtaining FMDV-free status for a country is very beneficial as it allows the country to trade meat products without trade restrictions (Knight-Jones and Rushton, 2013). The maintenance of the FMDV-free status requires stringent control policies, often including strict trade guidelines and immediate culling of infected and at-risk animals. FMDV also has severe economic impacts on countries where infection is endemic, such as several African and Asian countries. The prevalence of FMDV in these countries results in limited trade opportunities as they cannot trade live animals, and in some cases fresh meat products, with FMDV-free countries (James and Rushton, 2002).

### 1.1.2 FMDV control

There are 7 distinct serotypes of FMDV (A, C, O, Asia1, SAT 1(South African Territories 1), SAT 2 and SAT 3) and there are high levels of genetic variation within each serotype (Grubman and Baxt, 2004). Serotype A is considered the most diverse and contains 3 geographically distinct topotypes and across these there are 26 distinct genotypes (Knowles and Samuel, 2003, Mohapatra *et al*., 2011). This creates a problem for vaccination programs as there is little cross-protection from the vaccine between different genotypes of the same serotype.

Another challenge for FMDV vaccination programs is the differentiation between infected and vaccinated animals (DIVA) as the vaccine used is an inactivated virus vaccine and therefore the immune response generated is against the whole particle. This is particularly important as some animals recover from the disease and can act as carriers (Moonen and Schrijver, 2000). A DIVA assay is normally done by looking for the presence of antibodies against the non-structural proteins of FMDV as these should not have been produced when vaccinated because the inactivated virus does not replicate (Jamal and Belsham, 2013).

## 1.2 Picornavirus Classification

FMDV is a member of the genus *Aphthovirus* belonging to the family *Picornaviridae.* The *Picornaviridae* family contains 80 species which are classified into 35 genera including *Aphthovirus*, *Cardiovirus*, *Enterovirus*, *Megrivirus*, *Kobuvirus*, *Parechovirus*, *Sapelovirus* and *Senecavirus* (genera shown on figure 1.2) (Zell, 2018). The classification of the genera is based upon the genome organisation of the member viruses. The most studied genus of the *Picornaviridae* is the *Enterovirus* genus which includes several important human pathogens such as poliovirus (PV), human rhinovirus (HRV) and enterovirus 71 (EVA71).

The *Picornaviridae* belongs to the order *Picornavirales*, which is a group of positive sense single stranded RNA (+ssRNA) genome viruses. The viral genome has a highly structured 5’ region with a virus-encoded protein (VPg) attached and a 3’ poly(A) region. (Le Gall *et al*., 2008). There are several other families of viruses within the *Picornavirales* including some that infect plants, such as *Comoviridae* and *Potyviridae*, and some that infect insects, such as *Discistroviridae* (Le Gall *et al*., 2008).

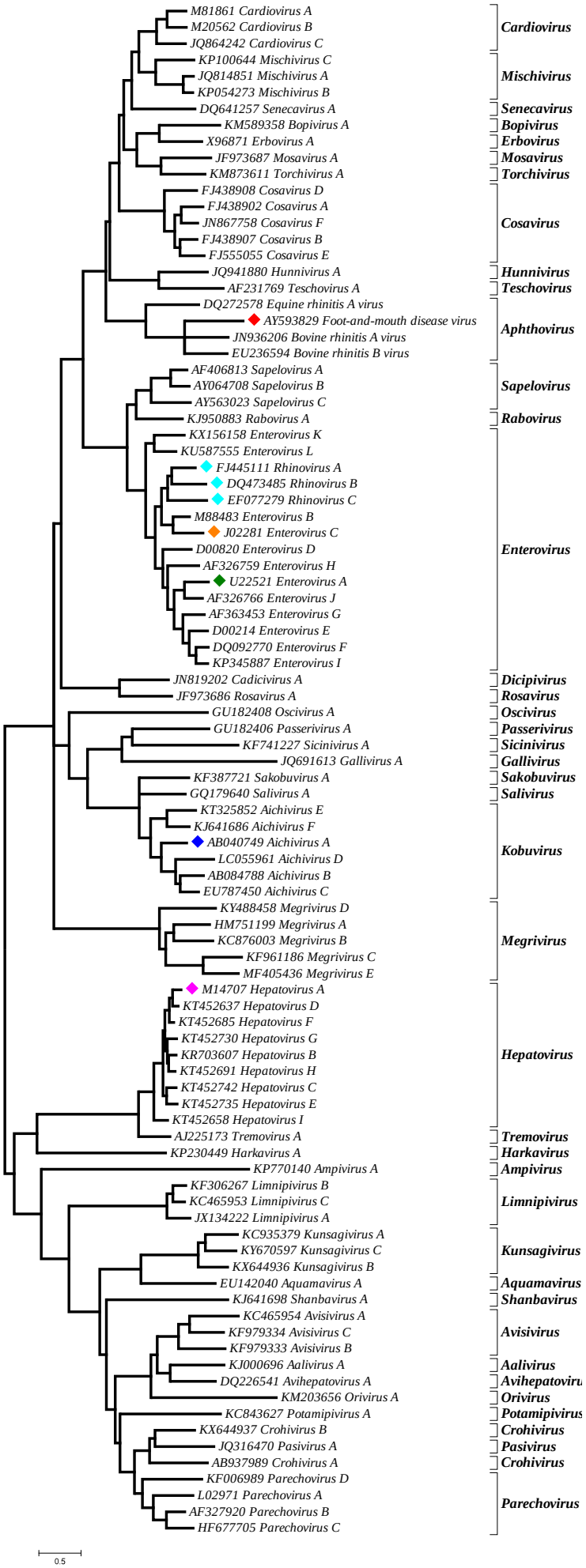


**Figure 1. 2: Molecular phylogenetic analysis of the P1 capsid of picornaviruses by the Maximum Likelihood method.**
The evolutionary history was inferred by using the Maximum Likelihood method based on the Le and Gascuel model (Le and Gascuel, 2008). The tree with the highest log likelihood (-80323.3858) is shown. The tree is drawn to scale, with branch lengths measured in the number of substitutions per site. The analysis involved 94 amino acid sequences representing each of the currently classified picornavirus species which are grouped into 40 genera. All positions with less than 95% site coverage were eliminated. That is, fewer than 5 % alignment gaps, missing data, and ambiguous bases were allowed at any position. There were a total of 513 positions in the final dataset. Evolutionary analyses were conducted in MEGA7 (Kumar et al., 2016). The taxonomic positions of the following viruses are highlighted by coloured diamonds: green, enterovirus A71 (*Enterovirus A*); orange, poliovirus 1 (*Enterovirus C*); cyan, human rhinoviruses (*Rhinovirus A*, *Rhinovirus B*, *Rhinovirus C*); red, foot-and-mouth disease virus (*Foot-and-mouth disease virus*); pink, hepatitis A virus (*Hepatovirus A*); blue, Aichi virus (*Aichivirus A*). Phylogenetic tree kindly provided by Nick Knowles, The Pirbright Institute.

## 1.3 FMDV Genome organisation

FMDV has a positive sense single stranded RNA genome, which contains ~8500 nucleotides (nt). Like other picornaviruses, the FMDV genome is sufficient for FMDV infection if the genome is delivered into the cell correctly (Belsham and Bostock, 1988). The FMDV genome consists of the 5′ untranslated region (UTR), a single open reason frame (ORF) and the 3′ UTR (shown in figure 1.3). The 5′ UTR contains several important RNA structures and has a genome linked viral protein (VPg) on the 5′ end. The 3′ UTR also contains RNA stem loops and a poly(A) region (shown in figure 1.3). The polyprotein encoding region is divided up into 3 regions P1, P2 and P3. These encode structural proteins (P1) and non-structural proteins (P2 and P3) and will be discussed further in section 1.5.2.

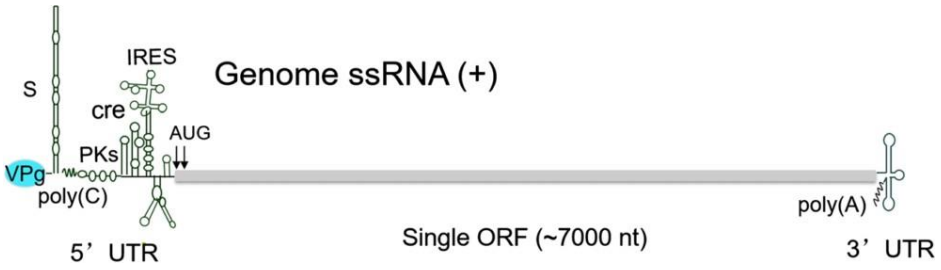


**Figure 1. 3**: **Schematic of the genome structure of FMDV.**

The genome consists of a single open reading frame (ORF) of about 7000 nt and two UTRs with important RNA structures. The 5′ UTR has a covalently bound viral protein (VPg) and contains the internal ribosome entry site (IRES) and other RNA structures. The labelled RNA structures in the 5′ UTR are the S-fragment (S), the poly (C) region, pseudoknots (PK). The 3′ UTR contains two essential stem loops and a poly (A) region. Figure adapted from (Gao *et al*., 2016)

### 1.3.1 5′ UTR

The 5′ UTR of FMDV is over 1300 nt long and contains 5 structured RNA regions. From the 5′ end the RNA regions are; the S-fragment, poly(C) tract, multiple pseudoknots, cis-acting regulatory element (CRE) and the internal ribosome entry site (IRES). The S-fragment contains approximately 350 nt and forms a long stem loop through base pairing (Newton *et al*., 1985). The S-fragment is important for virus replication. One possible way the S-fragment could be involved in virus replication is through interaction with the cellular RNA helicase A (RHA) as depletion of RHA using small interfering RNA constructs from cells resulted in inhibited FMDV replication (Lawrence and Rieder, 2009). The S-fragment may also

play a role in controlling the host immune response to FMDV infection as cells transfected with a truncated S-fragment induce higher levels of interferon β (IFN-β) and interferon-stimulated genes (ISGs) compared to cells transfected with a full length fragment (Kloc *et al*., 2017).

Following the S-fragment is the poly(C) tract (about 150-200 nt in length) and a stretch of RNA that forms 2-4 pseudoknots, the role of these is unclear. The poly(C) tract is required to be above a minimum length to allow virus recovery following transfection of cells with an infectious plasmid, suggesting it plays an important but yet uncharacterised role (Zibert *et al*., 1990).

Beyond the pseudoknots are two important RNA structures, the CRE and the IRES. The CRE is a highly conserved stem loop of 55 nt. The CRE has been shown to be essential for FMDV replication as mutants of the AAACA site in the loop region had a slower rate of replication and reverted back to wild type (Mason *et al*., 2002). The CRE is responsible for the uridylylation of the 3B proteins, also know as viral protein genome linked (VPg), which is required to allow VPg to act as a primer for replication. Therefore, the CRE is known as the 3B uridylylation signal (bus) in FMDV and has been demonstrated to act in trans to uridylylate 3B (see section 1.4 for the role of 3B uridylylation) (Tiley *et al*., 2003, Nayak *et al*., 2005).

The IRES is a highly structured region of RNA that is essential for cap-independent translation of the viral genome. This is about 450 nt in length and contains 5 main domains with several stem loops. All 5 domains are important and domains 3 and 4 are essential. Domain 3 contains conserved motifs, including a GNRA motif which has been shown to be essential for IRES activity as this region did not tolerate substitution mutations (Lopez de Quinto and Martinez-Salas, 1997). Within the GNRA motif the N position can contain any nucleotide and the R position must contain a purine. Domain 4 has a binding site for host initiation factor 4G (eIF4G) and mutations at the base of domain 4 prevent eIF4G binding. The mutations that prevent eIF4G binding have been demonstrated to prevent IRES-dependent translation showing this interaction is essential for translation (Lopez de Quinto and Martinez-Salas, 2000).

### 1.3.2 3′ UTR

The 3′ UTR contains two important stem loop structures and a poly (A) tail. The two stem loops are formed from a 90 nt region of RNA and if the stem loops are removed it is not possible to recover virus (Saiz *et al*., 2001). The 3' UTR has been shown to affect the activity of the IRES, indicating it plays an important role in viral replication (Garcia-Nunez *et al*., 2014).

## 1.4 Translation and replication of the FMDV genome

The translation of the viral genome into polyproteins is required to advance the virus lifecycle by producing progeny virus particles. Translation is a cellular process that occurs constantly within living cells. The normal translational process in cells starts with the recruitment of a translation initiation complex to an mRNA via an $m^7$GpppN modified base at the 5' end of the RNA before recruitment of the ribosome and subsequent translation of the mRNA. The $m^7$GpppN modified base is also known as a cap and therefore normal cellular translation is known as cap-dependent translation (Hinnebusch, 2014).

Translation of the FMDV genome is carried out in a cap-independent manner and is initiated by the IRES found in the 5' UTR of the genome (IRES described in section 1.3.2.2) (Belsham and Brangwyn, 1990). FMDV is able to utilise cap-independent translation as the viral leader protease ($L_{pro}$) cleaves eIF4G, which shuts off host translation (Devaney *et al*., 1988). While the cleaved form of eIF4G is not sufficient for normal eukaryotic translation, cleaved eIF4G is essential for FMDV replication. Cleaved eIF4G is vital for the formation of the 48S ribosomal translation initiation complex via the association of host initiation factors, including eIF4A, eIF1 and eIF3, with the IRES. The C-terminal portion of cleaved eIF4G associates with eIF4A, eIF1 and eIF3 and these factors are required for the formation of the 48S complex (Andreev *et al*., 2007). The host initiation factors then bind the IRES, via the cleaved eIF4G. The interaction of cleaved eIF4G and the IRES is promoted by eIF4A as it has been demonstrated that inclusion of eIF4A in toeprinting assays increased eIF4G binding to the IRES (Pilipenko *et al*., 2000).

Alongside translation, replication of the virus genome must occur to produce genomes of progeny viruses. As the FMDV genome exists as a single stranded positive sense RNA the replication of this must initially involve the production of a negative sense template from which more positive strand RNA genomes can be

produced. Production of both positive and negative RNA strands is carried out by the 3D RNA-dependent RNA polymerase ($3D_{pol}$) encoded within the FMDV polyprotein. The atomic structure of $3D_{pol}$ has been solved and it has been shown to contain the characteristic finger, palm and thumb domains associated with a polymerase (Ferrer-Orta *et al*., 2004). Prior to replication VPg is uridylylated by the CRE, which allows VPg to act as a primer for replication. VPg binds to the central cavity of the polymerase to start replication of the genome (Ferrer-Orta *et al*., 2006).

## 1.5 FMDV polyprotein processing

The FMDV genome is translated as a single polyprotein, which undergoes both co-translational and post-translational modifications to produce 14 viral proteins, 4 structural proteins (VP1-4) and 10 non-structural proteins (L protease, 2A, 2B, 2C, 3A, 3B (1-3), 3C protease and 3D polymerase) (shown in figure 1.4) (Rueckert and Wimmer, 1984).

### 1.5.1 Polyprotein cleavage

FMDV contains two viral proteases, leader protease ($L_{pro}$) and 3C protease ($3C_{pro}$), which are involved with the cleavage of the polyprotein. $L_{pro}$ is a papain-like protease which is autocatalytically cleaved from the polyprotein releasing the P1, P2 and P3 regions of the polyprotein (Strebel and Beck, 1986, Gorbalenya *et al*., 1991). $3C_{pro}$ is a chymotrypsin-like cysteine protease responsible for the release of the majority of the viral proteins (Vakharia *et al*., 1987, Birtley *et al*., 2005).

FMDV does not have a 2A protease, as found in the enteroviruses, but instead the 2A protein of FMDV initiates cleavage of the P1 structural region via a ribosome skipping mechanism. This process results in the hydrolysis of the peptidyl(2A)-tRNA ester linkage within a sequence in the C-terminus of 2A. Ribosome skipping results in the premature termination of translation in the ribosome with the potential for the re-initiation of translation to produce the P2 and P3 regions (Donnelly *et al*., 2001). The final maturation cleavage to form VP4 and VP2 occurs within the virion and is likely autocatalytic in nature though the process is not fully understood (Arnold *et al*., 1987). In some picornaviruses, such as the kobuviruses and parechoviruses, the maturation cleavage does not take place and these viruses have VP0 in the mature capsid (Zell, 2018).

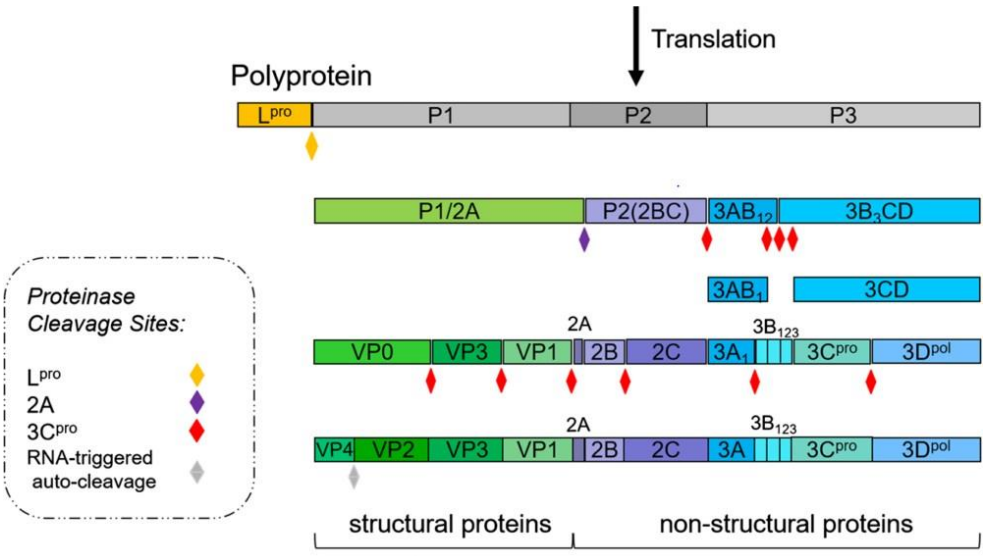


**Figure 1. 4**: **Schematic of the polyprotein processing of the FMDV polyprotein.**

Following translation the FMDV polyprotein and autocatalytic removal of $L_{pro}$, the FMDV polyprotein has three domains; P1, P2 and P3. P1-2A is released from the other regions through the ribosome skipping activity of 2A (indicated by the purple diamond). The proteins in P1-2A, P2 and P3 are cleaved by $3C_{pro}$ (indicated by the red diamond). VP0 is then cleaved into VP2 and VP4 during the final step of capsid maturation though an autocatalytic event (indicated by the grey diamond). Figure adapted from (Gao *et al*., 2016).

## 1.5.2 Viral proteins

After processing of the viral polyprotein 14 viral proteins are produced. The structural proteins encoded by the P1-2A region go on to form the virus capsid and will be discussed further in section 1.6. The viral protease $L_{pro}$ plays an important role in the translation of the viral genome by cleaving eIF4G (discussed in section 1.4). The roles of $3C_{pro}$ and 2A in polyprotein processing are discussed in section 1.5.3. The other 7 proteins will be discussed here.

The P2 region of the FMDV polyprotein encodes 3 proteins; 2A, 2B and 2C. Following disruption of polyprotein translation by 2A, the 2BC precursor is cleaved from the remaining polyprotein by 3C pro and is then further processed into 2B and 2C (Grubman *et al*., 1984). The 2BC protein has been shown to inhibit trafficking to the cell surface. The inhibition of trafficking has been demonstrated to require both 2B and 2C and cannot be replicated through single expression of either 2B or 2C (Moffat *et al*., 2005, Moffat *et al*., 2007). The role of free 2B is not fully understood. However, a recent study has shown 2B localises to the endoplasmic reticulum and may function as a viroporin as it was able to increase membrane permeability in

both bacterial and mammalian cells (Ao *et al*., 2015). 2C is a component of the virus replication complex and has been shown to be an AAA+ ATPase which adopts a hexameric conformation when ATP and RNA bind (Sweeney *et al*., 2010).

The P3 region encodes 6 proteins; 3A, $3B_1$, $3B_2$, $3B_3$, 3C pro and 3D pol. The non-structural protein 3A has been implicated in playing a role in the host range that FMDV can infect. Deletion of some of the 3A sequence results in FMDV that is attenuated in cattle but pathogenic in pigs (O'Donnell *et al*., 2001). Variation in 3A has been observed in a naturally occurring outbreak in Taiwan in 1997 that had the unusual feature of being pathogenic in pigs but not cattle, indicating this role in host range is important in the field (Beard and Mason, 2000). The P3 region also encodes 3 copies of 3B, also known as VPg, which is found at the 5' end of the genome (Sangar *et al*., 1977). It is not clear why FMDV has 3 copies of 3B but all 3 can be incorporated into new genomes suggesting they all play a role in the virus lifecycle (King *et al*., 1980). Recently, it has been shown that while all 3B proteins can be used as a primer for replication, the $3B_3$-3C junction is essential for replication (Herod *et al*., 2017).The remaining two proteins in P3 are $3C_{pro}$ and $3D_{pol}$ and these have been discussed in sections 1.5.1 and 1.4 respectively.

## 1.6 FMDV Capsid

Once the viral genome has been replicated and the P1-2A region of the genome has been liberated from the polyprotein the P1-2A region must be cleaved further to form the 4 capsid proteins and assemble into new virus particles, allowing the formation and release of progeny virus particles.

### 1.6.1 FMDV assembly

The process of FMDV assembly is not fully understood and the process infers similarities from the more advanced understanding of assembly in enteroviruses, such as PV. FMDV capsid assembly starts with the processing of the P1-2A polyprotein by $3C_{pro}$, resulting in the production of three capsid proteins VP0, VP1 and VP3. Following this cleavage the capsid proteins are processed into protomers with the assistance of the cellular chaperone Hsp90 (Newman *et al*., 2018). A pentamer is then formed from 5 protomers (figure 1.5). Pentamer formation requires the presence of the N-terminal fatty acid myristate group on VP0 and protomers lacking myristoylation are unable to form pentamers correctly (Chow *et al*., 1987, Goodwin *et al*., 2009).

The 12 pentamers assemble as an immature virus particle which may contain RNA or be a naturally occurring FMDV empty particle. A virion encapsulating the viral RNA then undergoes the autocatalytic cleavage of VP0 to produce VP2 and VP4 (shown in figure 1.5) (Arnold *et al*., 1987). The atomic structure of FMDV has been solved both as an empty particle and a RNA-containing virus particle by X-ray crystallography. These show no difference in the arrangement of the outer capsid proteins following cleavage of VP0, but do show changes to the orientation of internal N-terminus of VP2 and capsid protein VP4. The conformational changes resulting from VP0 cleavage lead to a more stable capsid (Curry *et al*., 1997).

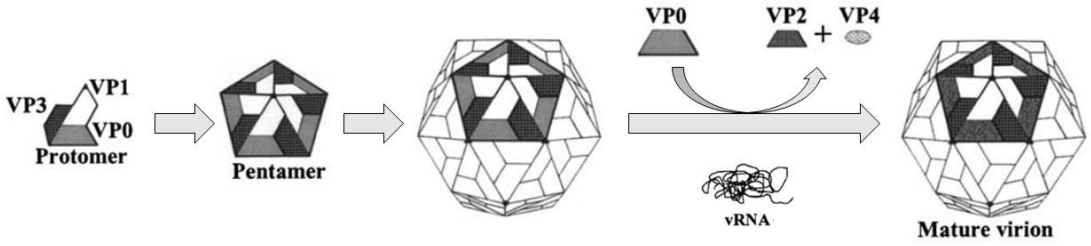


**Figure 1. 5**: **Schematic showing the assembly of the FMDV capsid.**

Following the cleavage of the P1-2A region of the polyprotein VP1, VP3 and VP0 form protomers. Five protomers then assemble into a pentamer and 12 pentamers assemble into a virus capsid. In the presence of viral RNA (vRNA) the VP0 capsid protein undergoes an autocatalytic cleavage to yield VP2 and VP4, resulting in a mature virion. Figure adapted from (Clavijo *et al*., 2004).

## 1.6.2 FMDV capsid structure

The atomic structure of FMDV was first solved in 1989 (Acharya *et al*., 1989). The FMDV capsid contains the 4 structural viral proteins. The capsid proteins VP1, VP2 and VP3 are of a similar size and share a common protein fold. The structure of the small capsid protein VP4 is not fully resolved but it appears mainly internal.

The protein fold formed by VP1, VP2 and VP3 is an 8-stranded, trapezoidal β-barrel, which is composed of 8 β strands. The 8 β strands come together to form two 4-stranded β sheets which form the outer edges of the wedge of the trapezoid. Between the β strands there are variable loops of difference lengths. At the apex of the wedge the variable loops are short but on the outer edge of the trapezoid the variable loops are much longer (figure 1.5) (Acharya *et al*., 1989, Fry *et al*., 2005).

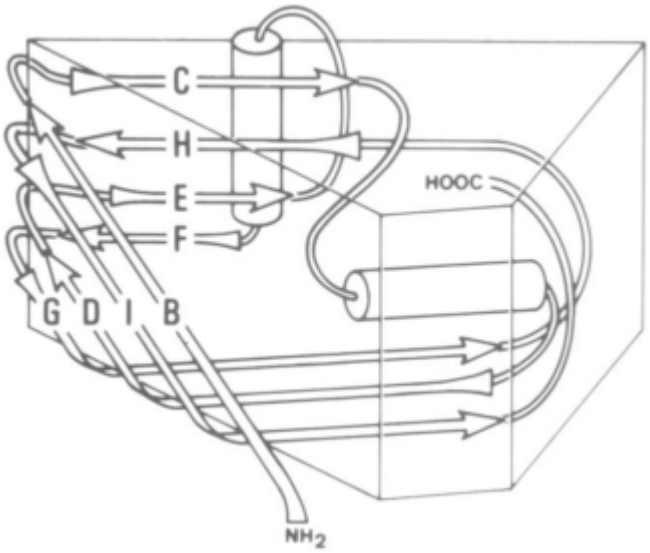


**Figure 1. 6: Schematic showing the fold of VP1, VP2 and VP3.**

VP1, VP2 and VP3 share a common fold, which is a β-barrel in the shape of an 8-stranded trapezoid. This structure has two 4-stranded β sheets. One β sheet is composed of strands G, B, I and B. The other β sheet is composed of strands C, H, E and F. Short variable loops are found between the sheets at the apex of the wedge formed by the β sheets and long variable loops are found at the opposite side, along with the C-terminus of the protein. Figure adapted from (Filman *et al*., 1989).

FMDV has a pseudo T=3 (p=3) icosahedral capsid. An icosahedron is formed of twelve triangles and where each of the triangles meet there is a 5-fold axis. Within each of the triangular sides of the icosahedron it is possible to have three identical units, orientated around a central point in the triangular facet and this provides a 3-fold axis of symmetry. Therefore, if each of the icosahedral faces of a virus capsid contains 3 virus capsid proteins, the virus capsid would be composed of 60 capsid proteins.

The triangulation number (T number) of an icosahedral capsid is calculated by mapping the icosahedral capsid onto a hexagonal lattice and establishing the distance travelled between two 5-fold axis through two vectors, h and k. This allows the T number to be calculated using the equation $T=h^2+hk+k^2$ (Caspar and Klug, 1962). The T number reflects the number of proteins that make up a single unit of the virus capsids which then form the 3 fold axis within the icosahedral capsid. In the case of picornaviruses, which has T= pseudo 3, there are three capsid proteins in each capsid unit. T numbers assume identical capsid proteins and as picornavirus capsids have 3 main capsid proteins which share similar structures

but are not identical the T number assigned is a T= pseudo 3. This indicated the capsid structure is the same as T=3 but is not composed of identical capsid subunits.

The FMDV capsid has three axis of symmetry, a five-fold, three-fold and two-fold axis (indicated on figure 1.7). At the five-fold axis there are 5 copies of VP1 and at the three-fold axis there are 3 copies of both VP2 and VP3 which alternate around the axis. The N-terminus of VP4 is found at the 5-fold and the C-terminus is located at the three-fold (Acharya *et al*., 1989, Fry *et al*., 2005).

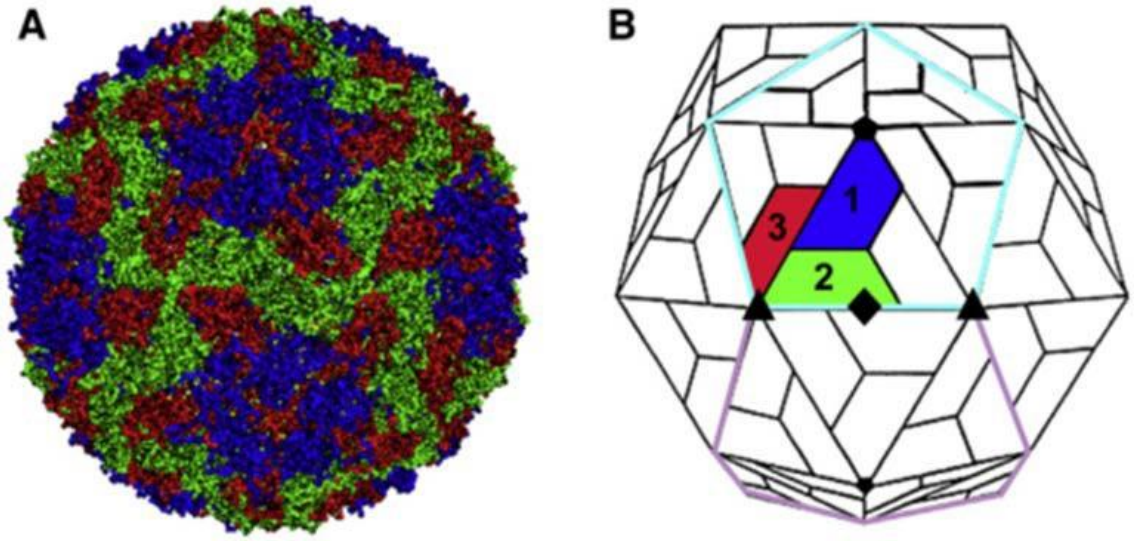


**Figure 1. 7**: **Structure of the FMDV capsid**

The FMDV capsid structure and a schematic showing some of the key features. (A) The crystal structure of the C-S8c1 FMDV particle (as published by (Lea *et al*., 1994)) showing VP1 (blue), VP2 (green) and VP3 (red). (B) Schematic showing the position of a protomer containing VP1, VP2 and VP3 using the same colours as (A). These come together to form a pentamer, outlined in cyan. The FMDV has three axis of symmetry which are indicated as follows: fivefold axis (pentagon), threefold (triangle) and twofold (diamond). Figure adapted from (Rincon *et al*., 2014).

## 1.6.3 Capsid breathing

The structural data obtained for the FMDV capsid has indicated that the small capsid protein VP4 is located on the interior of the capsid with some regions being disordered (Acharya *et al*., 1989). However, there has been evidence from several studies that the rigid structures identified by techniques such as x-ray

crystallography and cryo-EM may be missing the dynamic nature of the picornavirus capsids.

An early indication that the picornavirus capsid might be more dynamic than indicated by the structural data was the discovery that antisera against the N-terminus of PV VP1 and whole PV VP4 peptide was able to neutralise PV. This result indicated that these “internal” sequences had to be displayed on the surface of the virus capsid (Li *et al*., 1994). It has been possible to obtain structures of this using fragments of a monoclonal antibody that binds the N-terminus of VP1, confirming the N-terminus of VP1 was externalised near the twofold axis (Lin *et al*., 2012). The transient externalisation of internal capsid protein sequences, such as VP4, has been termed capsid breathing. The capsid breathing phenomenon demonstrates that virus capsids are dynamic structures. Therefore, capsids exist in a metastable state, primed to undergo the appropriate conformation changes to release the viral RNA when exposed to suitable triggers.

To date the evidence of capsid breathing has been based predominantly on studies using viruses from the enterovirus genus. However, there is evidence from the aphthovirus equine rhinitis A virus (ERAV) that this process occurs in the aphthoviruses. Prior to obtaining atomic resolution structures of ERAV, crystals were formed at low pH, forcing uniform conformational changes within the population, and this allowed the formation of an altered particle. The structure of the altered particle showed the N-terminus of VP2 becomes disordered under low pH. Therefore, it is possible that the N-terminus of FMDV VP2 is the analogous region to the N-terminus of VP1 exposed during breathing in enteroviruses and is externalised alongside the N-terminus of VP4 (Tuthill *et al*., 2009).

## 1.7 Virus entry

One of the most challenging parts of the infection cycle for a virus is obtaining entry to the host cell. If a virus is unable to pass the host barriers, such as the physical barrier presented by cellular membranes, then infection cannot occur as viral replication is reliant on the host cell machinery. In general, the process of viral entry contains three key steps receptor binding, uptake of the virus into cellular vesicles and uncoating of the virus particle to release the genome for replication. For example, there is evidence that HIV may enter the host cell at the plasma membrane (Wilen *et al*., 2012).

The first step of entry requires the binding of the virus to a cellular receptor, which can be considered any molecule that the virus particle can interact with, and results in the internalisation of the virus. A wide range of cellular receptors are utilised for virus entry. After receptor binding most viruses enter through cellular vesicular trafficking system and this is often through clathrin-mediated endocytosis but some viruses utilise clathrin independent mechanisms such as micropinocytosis and caveolin-mediated endocytosis.

In order to deliver the viral genome to the site of replication, often distinct sites within the cytosol to the nucleus, the virus must cross the vesicle membrane. In the case of enveloped viruses, the viral envelope fuses with the host membrane allowing passage of the viral nucleocapsid into the cytoplasm to continue with the virus lifecycle (illustrated in figure 1.8). For non-enveloped viruses, such as picornaviruses, this step presents a challenge as they cannot use membrane fusion. Non-enveloped viruses have been shown to use mechanisms of indiscriminate complete membrane disruption or controlled membrane permeabilisation events in order to allow the movement of the viral genome into the cytoplasm (illustrated in figure 1.8). This step can often coincide with the third main step of entry, uncoating, as the conformational changes that occur to allow membrane penetration are often part of the uncoating process. Once the virus has undergone uncoating the free genome is able to replicate and produce new viral proteins, allowing the continuation of the virus lifecycle.

### 1.7.1 Enveloped virus entry

Entry into the cell for enveloped viruses is well-studied. Generally, after receptor binding viruses are taken up into the endocytic pathway and following a triggering step the viral envelope will fuse with the host membrane and this process occurs using fusion proteins on the envelope of the virus particle. The fusion of two membranes proceeds through the process shown in figure 1.9. Initially the membranes come together and form an intermediate hemifusion stage where one of the bilayers of the membrane has fused but the second bilayer is yet to fuse. The fusion of viral and host membranes can be a pH-dependent or pH-independent phenomenon and this process is used by viruses such as influenza A and HIV.

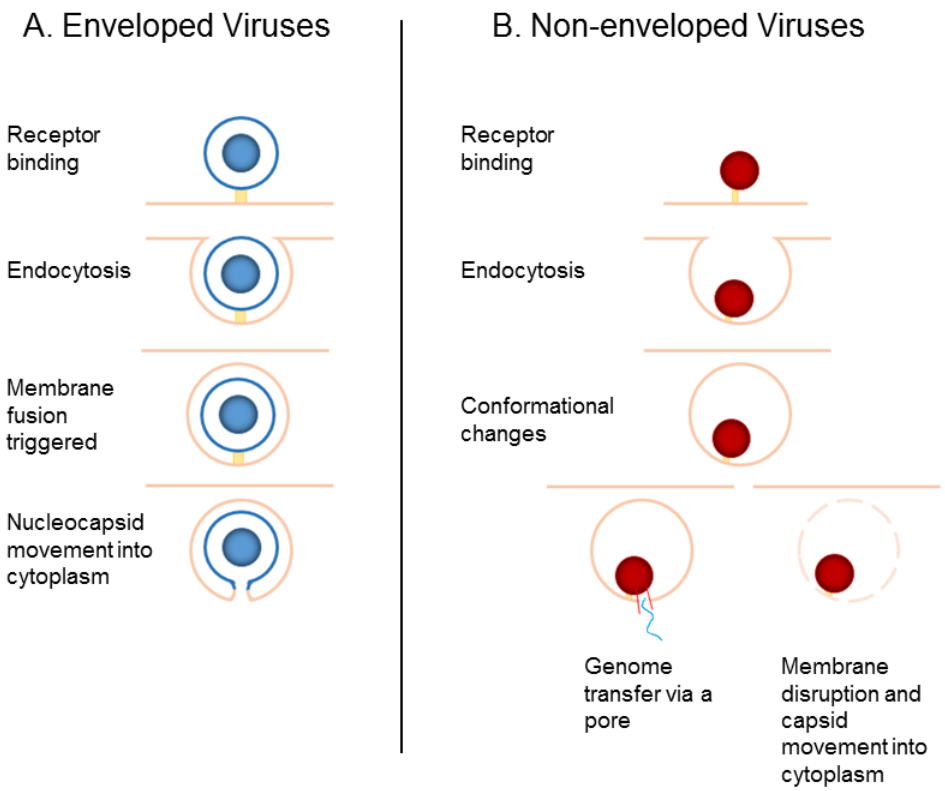


**Figure 1. 8**: **Schematic showing the entry process of enveloped and non-enveloped virus entry**

In general both enveloped (A) and non-enveloped (B) viruses undergo the same first two steps of entry, receptor binding followed by endocytosis. (A) Once within the endocytic vesicle or endosome enveloped viruses initial membrane fusion using fusion proteins within the viral envelope. The process of membrane fusion then allows the viral nucleocapsid to transfer across the cellular membrane to complete the virus lifecycle. (B) In general alongside receptor binding and endocytosis non-enveloped viruses undergo a conformational change in the capsid. This allows the virus to continue in one of two ways. Firstly the virus may penetrate the endosomal membrane by forming a pore to allow the viral genome to enter the cytoplasm and it is likely the conformational changes that occur allow capsid proteins to mediate this. Secondly the virus may trigger complete disruption of the cellular membrane and this is also likely to be mediated by capsid proteins released during the conformational changes.

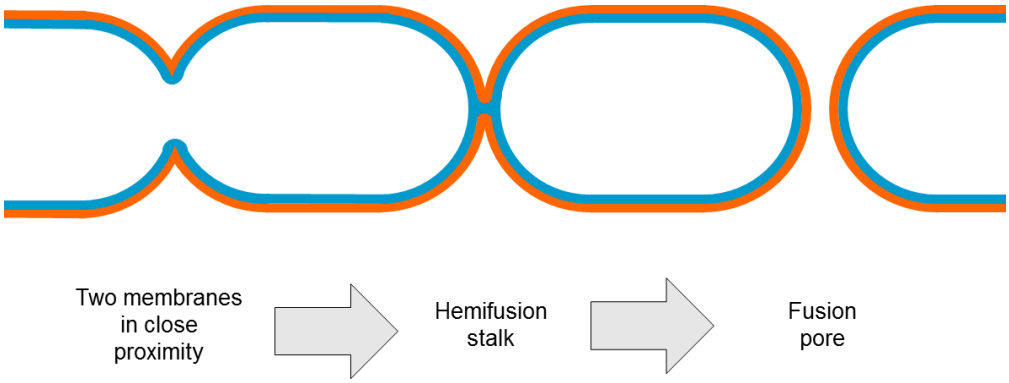


**Figure 1. 9: Schematic showing the fusion of two lipid bilayers**

Membrane fusion occurs through two lipid bilayers coming close together. The internal layers of the bilayer (shown in teal) then fuse before the outer layers (shown in orange) forming a hemifusion stalk. The outer layers then form and this makes the fusion pore.

Enveloped viruses have fusogenic proteins to mediate the process of membrane fusion. Fusion proteins are found on the outer surface of the virus envelop in a fusion-competent state but are often shielded before fusion and are exposed due to conformational changes induced by receptor binding or changes in pH. There are three classes of fusogenic membrane glycoproteins that have been identified; class I, class II and class III.

Class I fusogenic peptides exist as trimeric structures and require a proteolytic cleavage to free an N-terminal fusion peptide during assembly and maturation of the virus. The trigger for fusion of class I fusogenic peptides is often either low pH or the binding of a nearby attachment protein or subunit to the host cell. Following fusion, class I fusion proteins assume a six helix bundle structure. Examples of class I fusion proteins are influenza haemagglutinin (HA) and paramyxovirus F protein (White *et al*., 2008, Plemper, 2011, Harrison, 2015).

Class II fusion proteins have a high β-sheet content and form structures that are parallel to the viral envelope until triggering of fusion by low pH induces a conformational change resulting in the formation of trimeric structures that project from the viral envelope. The low pH trigger released an internal fusion loop within the fusion protein and this is presented to the target membrane, allowing membrane fusion. An example of a class II fusion protein is the E protein of dengue virus (White *et al*., 2008, Plemper, 2011, Harrison, 2015).

Class III fusion proteins combine elements of both class I and class II fusion proteins. These exist as trimeric structures both before and after fusion. Similar to class II fusion proteins these contain a fusion loop within the structure rather than a fusion peptide, as for class I. Membrane fusion by class III fusion proteins is triggered by low pH and post fusion these proteins take on a similar six helical bundle to the class I fusion proteins. An example of a class III fusion protein is the gB of herpes simplex 1 virus (White *et al*., 2008, Plemper, 2011, Harrison, 2015).

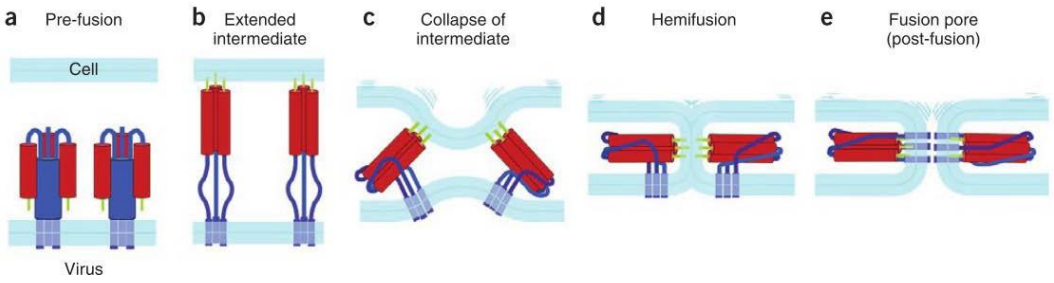


**Figure 1. 10: Progression of fusion pore formation induced by a viral fusion proteins**

(a) The fusion protein in pre-fusions state with the fusion sequences shielded (shown in green). (b) During the entry process the fusion protein is triggered through a conformational change induced by receptor binding or pH change and this released the fusion sequences and allows the formation of an extended intermediate that bridges the two membranes. (c) The extended intermediate then collapses which draws the two membranes together. (d) The collapsed intermediates result in the formation of a hemifusion stalk where the internal membranes are fused but the outer layer is not. (e) A final structural rearrangement results in the formation of the post-fusion protein and completed membrane fusion. The fusion pore then allows the virus nucleocapsid to move into the cytoplasm. Figure adapted from (Harrison, 2008).

## 1.7.2 Non-enveloped virus entry

In comparison to the entry of enveloped viruses the entry mechanisms of non-enveloped viruses are less well studied. Non-enveloped viruses lack a viral envelope and therefore cannot utilise the mechanism of membrane fusion to move beyond the endocytic pathway. Two mechanisms for crossing the membrane barrier have been identified for this group of viruses. Firstly, small peptides have been identified that can cause complete disruption of membranes, for example adenovirus VI peptide. Secondly, small peptides that are able to initiate a controlled permeabilisation of membranes though pore formations. An example of such a

peptide that use this second approach is reovirus µ1. The majority of evidence from picornaviruses such as PV and HRV indicate that picornaviruses utilise the second of these approaches and will be discussed in section 1.8.4. Three viral proteins from non-enveloped viruses involved in membrane permeabilisation or disruption are discussed below and a discussion of features that are common between them will follow.

### 1.7.2.1 Adenovirus VI

Adenovirus attaches to the cell via a primary receptor, such as coxsackie and adenovirus receptor (CAR) or heparan sulphate glycosaminoglycans (Bergelson et al., 1997, Dechecchi et al., 2001). Following attachment, internalisation of adenovirus is triggered by the binding of the secondary receptor, $\alpha_v$ integrin, through an Arg-Gly-ASp (RGD) motif found on the penton protein, the major component of the capsid (Neumann *et al*., 1988, Wickham *et al*., 1993). Binding to integrin triggers internalisation by clathrin-mediated endocytosis and transportation to the early endosomes (Nemerow, 2000).

Early studies demonstrated that adenovirus virus particles could be seen in the cytosol of infected cells, indicating adenovirus could be utilising large scale membrane destruction to escape the endosome (Morgan *et al*., 1969). The membrane disruption induced by adenovirus has been shown to require low pH in liposome permeability assays, either through pre-treating virus or carrying out the assay at low pH (Blumenthal *et al*., 1986, Wiethoff and Nemerow, 2015). The requirement for low pH could be removed if uncoating of adenovirus was triggered through heating the virus, suggesting the membrane permeability induced by adenovirus is linked to a conformational change during uncoating.

The small capsid protein VI has been demonstrated to be essential for adenovirus-induced membrane disruption and endosomal penetration by adenovirus can blocked by antibodies against the VI precursor (Maier *et al*., 2010). The VI protein is a small capsid protein which is released from a precursor protein, pVI, during maturation of the virus particle by adenovirus proteinase (AVP) (Diouri *et al*., 1996, Wiethoff and Nemerow, 2015). VI is located near the penton base in the mature virus particle and is released from the capsid (Wiethoff *et al*., 2005, Wiethoff and Nemerow, 2015).

Analysis of the VI sequence indicated the presence of an N-terminal α-helix, which has been shown to induce membrane disruption, independent of the rest of the protein (Maier *et al*., 2010). The helix has been shown to be essential for membrane penetration as removing the helix prevents membrane permeability (Maier *et al*., 2010). Additionally, a single mutation within the α-helix, L40Q, results in decreased virus infectivity and decreased virus membrane penetration (Moyer *et al*., 2011). However, the region of VI following the N-terminal helix also contains three α-helices and has been shown to induce membrane penetration when targeted to the membrane using a His-tag and nickel containing lipids (Maier and Wiethoff, 2010). Therefore, the mechanism of membrane permeability by adenovirus VI is not fully understood and may involve more than one of the α-helices identified in the sequence.

### 1.7.2.2 Flock house virus γ peptide

The flock house virus (FHV) capsid is initially composed of α protein, which undergoes an autocatalytic cleavage during virus maturation to form the major capsid protein β and a small peptide, γ, (Hosur *et al*., 1987). The maturation cleavage is essential and preventing it through mutation of a key residue prevents virus entry at a step after cell attachment (Schneemann *et al*., 1992). After the maturation cleavage γ associates with the viral RNA on the internal surface of the capsid via the C-terminus of the protein (Fisher and Johnson, 1993).

FHV enters via the endocytic pathway and low pH in the endosome has been shown to be important for FHV entry (Odegard *et al*., 2009). The requirement for low pH has also been demonstrated *in vitro* as membrane permeability induced by FHV increased when mixed with liposomes at pH 6 compared to pH 7 (Odegard *et al*., 2009). It is likely that the lowering pH triggers uncoating and entry intermediates of FHV have been identified that lack the γ peptide, indicating γ is released during the uncoating process (Walukiewicz *et al*., 2006).

Most of the studies looking at the membrane permeability induced by γ have used a 21 amino acid peptide representing the N-terminus of γ (termed $\gamma_1$) as this region has been identified as α-helical in structural studies (Fisher and Johnson, 1993). Studies using liposomes as a model membrane have shown that the $\gamma_1$ peptide can induce membrane permeability *in vitro*. However, $\gamma_1$ does not insert into the membrane so it is unlikely this membrane permeability is due to the formation of a pore (Bong *et al*., 2000). Despite the N-terminal membrane permeabilising

ability, it has become evident that membrane penetration by FHV requires the C-terminal domain (Banerjee and Johnson, 2008, Bajaj *et al*., 2016). Therefore, the mechanism of the membrane permeability induced by the γ peptide is not fully understood.

### 1.7.2.3 Reovirus μ1

The reovirus capsid protein μ1 is found as part of a heterohexamer composed of 3 copies of μ1 and 3 copies of σ3 (Liemann *et al*., 2002). During entry the virus particle undergoes a transition from virus particle to infectious subviral particle (ISVP) as a result of exposure to host proteases, such as those found in the intestinal lumen (Bodkin *et al*., 1989). As part of the transition from virus to ISVP the σ3 protein is proteolytically removed from the capsid, revealing μ1 (Joklik, 1972). The ISVP undergoes a further transition to the ISVP* after incubation at physiological temperatures and during this transition μ1 undergoes a conformations change that is required to induce membrane permeability (Chandran *et al*., 2002). Membrane penetration by reovirus has been shown to occur alongside the transition to the ISVP* (Agosto *et al*., 2006).

The μ1 protein is myristoylated at the N-terminus of the protein and during entry μ1 undergoes two cleavage events to produce 3 peptides (Nibert *et al*., 1991, Nibert and Fields, 1992). One cleavage results in the production of the ϕ peptide from the C-terminus of μ1, which contains an amphipathic helix (Nibert and Fields, 1992). The ϕ is not required for membrane penetrating ability as preventing this cleavage by incubating the cells with $NH_4Cl$, which prevents the cleavage of μ1 to produce ϕ, does not prevent infection (Chandran *et al*., 1999).

The second cleavage occurs autolytically and liberates a short N-terminal peptide, termed μ1N, which retains the myristoylation modification of the original μ1 protein (Nibert *et al*., 1991). The μ1N peptide is released from the particle during conversion of the ISVP to the ISVP* (Chandran *et al*., 2002). A synthetic myristoylated μ1N peptide has been shown to induce size-selective membrane permeability as release of 40 kDa FITC-linked dextrans was limited in comparison to the release of a small fluorescent dye, indicating the membrane permeability induced is size-selective (Zhang *et al*., 2009).

Prevention of the cleavage of μ1N by introducing a mutation (N42A) in μ1 generated ISVPs that had reduced infectivity and lacked haemolytic activity, indicating that the μ1 cleavage is vital for the progression of reovirus infection (Odegard *et al*., 2004).

Following this study, free µ1 with the N42A mutation was shown to induce membrane permeability similar to wild type using liposomes, suggesting that while the cleavage of µ1 is vital in the context of virus entry, possibly due to the conformation of µ1 within the virus particle, it may not be essential for the membrane penetration ability of µ1 (Zhang *et al*., 2009).

### 1.7.2.4 Shared features of non-enveloped membrane penetrating proteins

The viral proteins responsible for membrane penetration events by diverse non-enveloped viruses share several features. These proteins are often small proteins or peptides which lack sequence similarity that are released from a capsid precursor during the maturation of the virus capsid or early stages of entry. For example the release of γ as a result of the autocatalytic cleavage of α during FHV maturation. Inhibition of the viral cleavage has been shown to prevent formation of infectious virus for several of non-enveloped viruses supporting the requirement for the release of these peptides for successful production of virus. Structurally, these components of non-enveloped virus are often found internally, such as the γ protein of FHV which associates with the viral genome, or masked to prevent premature triggering, such as µ1 being masked by σ3 in the reovirus capsid.

Another key similarity is the requirement for externalisation or release of the membrane-penetrating peptide. This seems to regularly occur due to conformational changes often induced by pH changes within the endocytic pathway or proteolytic removal of masking proteins. The externalised internal proteins of several non-enveloped viruses (discussed above for reovirus µ1, adenovirus VI and FHV γ) have been shown to interact with membranes using the well-established technique of using liposomes as model membranes.

## 1.8 FMDV entry and the role of VP4

### 1.8.1 Receptor binding and endocytosis

The cellular receptor of FMDV has been identified as integrin and the major integrin utilised in cattle has been identified as the integrin $\alpha_v\beta_6$ (Jackson *et al*., 2000). Integrins are a large family of glycoproteins found on the cell surface and are known to play a role in the entry of a range of viruses, such as Epstein-Barr virus and HIV-1 (Hynes, 1992, Hutt-Fletcher and Chesnokova, 2010, Cicala *et al*., 2011).

Integrins are heterodimers that are formed of α and β subunits and there have been 24 αβ heterodimers identified utilising 18 α and 8 β subunits (Pan *et al*., 2016). The structure of integrins has shown that each subunit consists of a globular head and two leg regions which are inserted into the plasma membrane. Therefore, integrins have three main domains; the extracellular domain, transmembrane domain and cytoplasmic domain. Integrins play several important roles in cellular processes, such as cell proliferation and cell adhesion (reviewed in Pan *et al* 2016).

The integrin $\alpha_v\beta_6$ has been proposed as the natural receptor in cattle because it is expressed in epithelial tissue, which is the site of FMDV infection (Breuss *et al*., 1993). While $\alpha_v\beta_6$ may be the preferred receptor of FMDV, the virus has also been shown to use other integrin receptors such as $\alpha_v\beta_1$, $\alpha_v\beta_3$ and $\alpha_v\beta_8$ (Jackson *et al*., 2002, Jackson *et al*., 2004, Duque *et al*., 2004). FMDV binds to integrin via the Arg-Gly-Asp (RGD) motif located on the externalised GH loop of VP1 (Logan *et al*., 1993, DiCara *et al*., 2008). This is a classical integrin binding motif and can be found in other viral and host proteins known to interact with integrin, such as fibronectin and the penton protein from adenovirus (D'Souza *et al*., 1991, Hynes, 1992, Wickham *et al*., 1993). In addition to using integrin as a receptor, cell-culture adapted FMDV is able to utilise heparin sulphate glycan (HSG) as an alternative receptor for cells which lack integrin (Jackson *et al*., 1996).

Once FMDV has bound to a cellular receptor the virus is internalised through endocytosis. FMDV entry in epithelial cells has been shown to be via clathrin-mediated endocytosis (Berryman *et al*., 2005). Cell-culture adapted FMDV has been shown to utilise the clathrin-independent caveolin endocytic pathway (O'Donnell *et al*., 2005). The difference in endocytic pathway used could be due to differences in receptor usage between FMDV infecting epithelial cells and using a cell-culture adapted virus in cultured cells. FMDV has been shown to traffic through the endosome system and infection cannot progress without endosomal acidification (Berryman *et al*., 2005).

## 1.8.2 Capsid rearrangements within the endosome

As previously discussed in section 1.6.3 picornaviruses undergo the process of capsid breathing. This metastable state allows the virus capsid to be both sufficiently stable to protect the viral genome from environmental damage, and primed to release the viral genome, should the required stimuli trigger release. The stimuli required for picornavirus uncoating and genome release varies between viruses. For

some, the predominant trigger is receptor binding and this is the case for PV. For other picornaviruses, such as FMDV, receptor binding has little effect and it is likely that the acid sensitivity of the virus particle is responsible for inducing conformation changes. There are also picornaviruses that require a combination of the two, such as HRV16 and HRV2 (Nurani *et al*., 2003).

The entry steps following endocytosis are poorly characterised for FMDV. FMDV is very sensitive to low pH, with reports of virions dissociating in conditions below pH 6.8, making it unlikely that the particle would stay intact for long within the acidic conditions in an early endosome (Brown and Cartwright, 1961, Hu *et al*., 2015). It has been observed that on exposure to low pH, FMDV virions completely dissociate resulting in the release of VP4 and the RNA (indicated in figure 1.11B) (Burroughs *et al*., 1971).

However, there is evidence from the aphthovirus ERAV, which also undergoes dissociation at low pH, that an intermediate particle is formed (Tuthill *et al*., 2009). This was demonstrated by comparing the structure of ERAV crystallised at low pH with that at a neutral pH (Tuthill *et al*., 2009). Recent work in the laboratory has shown that it is also possible to capture an intermediate particle of FMDV when FMDV was incubated at low pH in the presence of formaldehyde (Gold *et al*, manuscript in preparation). These studies indicate that it is possible that aphthovirus entry progresses in a similar way to enterovirus entry, through the initial conformation change induced by an environmental trigger to generate an intermediate particle.

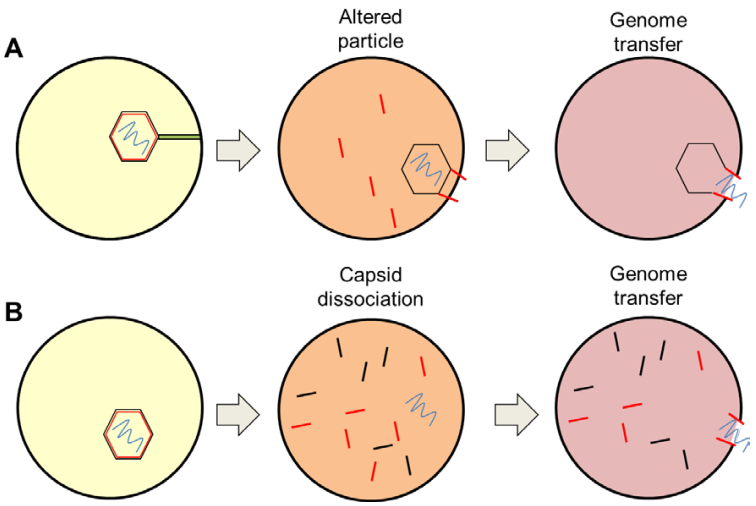


**Figure 1. 11: Schematic showing the comparison of proposed the entry process of enteroviruses and aphthoviruses**

Following endocytosis the virus particle proceeds through the endosomes. The pH of the vesicles decreases, indicated by the colour change from yellow to red in the schematic. Due to receptor binding or a decrease in pH, (A) the enteroviruses undergo a conformational change, releasing VP4 or (B) the aphthovirus capsid dissociates. For both genera it is proposed that the free VP4 forms a pore through which the virus genome is transferred out of the endosome.

As aphthoviruses are likely to form an entry intermediate, the well-characterised structural rearrangements of the enteroviruses are important to consider as similar changes may be occurring transiently in the aphthovirus capsid. During enterovirus entry an external stimuli, for example receptor binding in PV, triggers a conformational change in the capsid. The conformational change results in the formation of an altered particle, “A” particle, which has the N-terminus of VP1 externalised and VP4 is expelled from the capsid (Figure 1.11A) (De Sena and Mandel, 1977, Fricks and Hogle, 1990). The altered particle still contains the viral RNA and a further event occurs allowing the movement of the genome across the endosomal membrane (genome transfer is discussed in section 1.8.3) (De Sena and Mandel, 1977). Once the genome is expelled an empty particle is left behind which lacks RNA (Fricks and Hogle, 1990). Therefore, enterovirus entry consists of an environmental trigger, receptor binding or pH, triggering the formation of an intermediate RNA-containing A particle and then subsequent RNA genome transfer into the host cell (illustrated in figure 1.11). After this has occurred an empty particle is left behind.

The A particle can be isolated from PV infected cells and therefore is a naturally occurring uncoating intermediate (Fricks and Hogle, 1990). The altered particle has a sedimentation coefficient of 135S which is lower than that of the virus particle (160S) (De Sena and Mandel, 1977). The A particle is antigenically different from the virus particle and had increased sensitivity to proteases compared to the virus particle (Fricks and Hogle, 1990).

The A particle has undergone significant structural rearrangements, resulting in the loss of VP4, externalisation of the N-terminus of VP1 and the expansion of the capsid. The externalisation of the N-terminus of VP1 has been demonstrated by the reactivity of A particles with antibodies against the N-terminus of VP1 at 4°C, whereas virus does not (Curry *et al*., 1996). The site of externalisation of the N-terminus of VP1 in the altered particle has been investigated by comparing the structure of a PV altered particle with a PV altered particle lacking the first 31 amino acids of VP1. The comparison of the two particles showed that the N-terminus of VP1 emerged near a feature known as the “propeller tip”, which is located near the 3-fold axis of the virus capsid, and not at the fivefold axis as previously thought (Bubeck *et al*., 2005).

The A particle has been shown to be expanded by 4 % compared to the virus particle and the expansion is due to the rearrangement of the structural proteins (Belnap *et al*., 2000, Levy *et al*., 2010). Through the conformational changes to the capsid proteins, the hydrophilic virion is converted into a hydrophobic A particle that is able to interact with cellular membranes (Danthi *et al*., 2003). This is particularly interesting as it suggests the A particle would be capable of tethering the particle to the membrane, which would be an important requirement for the controlled transfer of the viral genome into the cytoplasm (discussed in section 1.8.3). The empty particles have a similar structure to the altered particle but lack viral RNA (Hewat *et al*., 2002).

The structural changes induced by uncoating have recently been investigated for another member of other picornavirus family. The recent study looking at the cardiovirus human saffold virus 3 (SAFV-3) has shown that when uncoating was triggered artificially by heating to 42 °C for 2 min an altered particle was formed which lacks VP4. Within this sample approximately 1 % of the capsids had converted to empty particles. The A particles generated were found to dissociate quickly when left at room temperature (Mullapudi *et al*., 2016).

Another important group of picornaviruses to consider are the viruses that do not undergo the VP0 cleavage and as such cannot release VP4 during entry. Two examples of this are the kobuviruses, such as aichi virus (AiV), and the parechoviruses, such as Ljungan virus (LV). Recently the effect of artificially forcing uncoating has been investigated for AiV. Uncoating was obtained by heating AiV to 53°C for 10 min and this resulted in the formation of empty particles which were shown to have an expanded capsid and changes to the pentamer interface. The empty particles did not dissociate after heating (Sabin *et al*., 2016).

As there is evidence from work on ERAV that aphthoviruses may indeed undergo entry via an intermediate particle it is possible that there is a common mechanism across picornaviruses during entry. This would consist of an environmental trigger inducing a conformational change to allow the formation of an intermediate particle. The formation of the intermediate would allow genome transfer to occur and following this the intermediate either exists as an empty particle or dissociates.

### 1.8.3 Genome transfer

One of the main roles of a virus capsid is as a vehicle for delivering the viral genome into susceptible cells to allow replication and production of progeny virus. In the case of picornavirus entry it is probable that the structural rearrangements resulting in the formation of entry intermediates are linked to the release of the genome from viruses. Little is known about this part of the FMDV lifecycle, but there are tantalising insights provided from experiments using the enteroviruses.

There is structural evidence that the virion is attached to the membrane during the genome transfer step. Liposomes containing lipids with a nickel-charged nitrilotriacetic acid (NTA) head group were decorated with a recombinant poliovirus receptor (PVr) with a C-terminal Histidine-tag and mixed with PV. This allowed PV to undergo the necessary conformational changes induced by receptor binding to trigger uncoating and therefore genome transfer. The resulting cryo-electron tomography (cryo-ET) reconstructions demonstrated the formation of an umbilicus joining the altered particle to the liposome (Strauss *et al*., 2013). Recently, new structural techniques have been developed that utilise nanodiscs to provide the lipid bilayer and receptor. This technique has been used, alongside a technique called symmetry-mismatch reconstruction to generate a 7.8 Å asymmetric reconstruction of the altered particle of the enterovirus coxsackievirus B3 (CVB3). The asymmetric reconstruction shows a density linking the virion to the membrane of the nanodisc and this appears to emerge through the three-fold axis or the propeller tips near the

three-fold axis (Lee *et al*., 2016). It is interesting to note that when icosahedral averaging was applied to these CVB3 particles an icosahedral particle was obtained at 3.9 Å but the asymmetry was lost, which raises the question whether previous structures of altered particles may also show some asymmetry that has been lost through averaging.

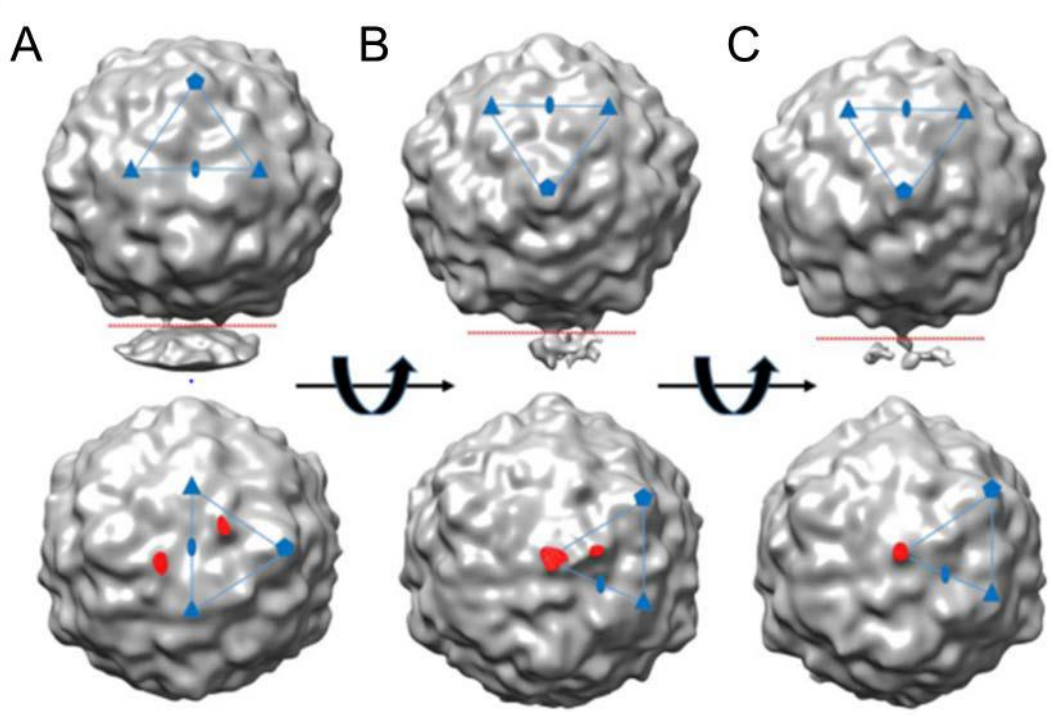


**Figure 1. 12**: **Protein extensions formed between coxsackievirus B3 and receptor-decorated membranes during formation of an asymmetric entry intermediate.**

Three distinct structures with protrusions from the virion to the membrane were identified after asymmetric averaging of the structure of coxsackievirus B3 in complex with receptor and membrane. The three structures are (A) two protrusions at the propeller tips across the twofold axis, (B) two protrusions with one at the threefold axis and the second at the propeller tip and (C) a single protrusion exiting at the threefold axis. The top panel shows the virion linked to the membrane via the observed densities. The second panel then show a cross section through the join (indicated by the red line) and the red indicated where on the virion surface the densities can be found. For all images the axis of symmetry are indicated by the blue lines and symbols. The axis are indicated as follows; fivefold (pentamer), threefold (triangle) and twofold (diamond). Figure reproduced from (Lee *et al*., 2016).

There is evidence that the transfer of the viral genome proceeds in a controlled manner and the genome unfolding is required for this to occur. This has been demonstrated by producing PV in the presence of the Syto82 dye, which binds to double-stranded RNA (dsRNA), which would only be found in secondary structures within the folded PV genome. During entry the signal for Syto82 was reduced, indicating the dye had been released from the dsRNA, which would require the

genome to become unfolded. When the experiment was repeated in the presence of an inhibitor of receptor-induced conformational changes and the subsequent entry steps, there was no loss of signal. This indicates the signal was lost due to the step of genome transfer (Brandenburg *et al*., 2007). The requirement for unfolded RNA may explain the observation that the length of RNA found in a PV particle undergoing genome transfer varies (Bostina *et al*., 2011). The rate of exit may vary as secondary structure is unfolded, causing the process to pause. In addition to this it has been demonstrated that the genome of HRV2 exits the virus from the 3' end as the 5' end. This was determined by forming altered particles and following cross-linking of the capsid any externalised RNA was digested away. The protected RNA remaining within the virion was then sequenced and found to be exclusively from the 5' of the viral genome (Harutyunyan *et al*., 2013). These studies indicate that the viral genomes are expelled in a controlled and precise manner and the requirement for unfolding could be linked to the formation of a pore in the endosomal membrane would facilitate this controlled release.

The linkage to the membrane is likely to be the formation of a pore to shield the viral genome from the contents of the endosome. A recent study has shown that during entry the viral RNA is shielded from RNase as it is transferred into the liposome (Groppelli *et al*., 2017). This study went on to show that the viral genome was also protected when PV infection occurred in media containing RNase (Groppelli *et al*., 2017).

As previously mentioned it is possible that there is a conserved mechanism of picornavirus entry that requires conformational changes within the capsid to form an intermediate particle, regardless of the stability of the particle after RNA release. It is interesting to consider beyond this that there is likely to be a conserved mechanism of genome transfer from the intermediate particle prior to the formation of an empty particle or complete dissociation of the capsid. To date most of the evidence pointing towards the formation of an umbilicus structure linking the virus to a membrane has been generated using enteroviruses. Recently it has been shown that infection by ERAV is not affected by RNase in the media (Groppelli *et al*., 2017).This development, combined with the low pH intermediate captured for ERAV, could suggest that aphthovirus entry progresses in a similar way to the enteroviruses but after RNA transfer the particle dissociated.

## 1.8.4 Membrane permeability

As discussed in section 1.7.2, one of the crucial steps in non-enveloped viruses is the ability of the virus to penetrate the host membrane to allow passage of the genome to the site of replication. It can be envisaged that prior to infection the virus capsid exists in a metastable state that undergoes transient capsid breathing, allowing the externalisation of the N-termini of VP1 and VP4. On receipt of a suitable trigger, the structural changes in the capsid lead to the permanent externalisation of the N-terminus of VP1 and the loss of VP4 from the capsid and this conformational change is linked to the membrane penetration of the virus. Therefore, this has led to the suggestion that either VP1 or VP4 acts like the membrane penetrating peptides described in 1.7.2.

Initial work showed that the N-terminus of VP1 was able to bind PV to liposomes (Fricks and Hogle, 1990). But a recent study has shown using a peptide of the N-terminal 24 amino acids of VP1 that this region of VP1 lacks the ability to permeabilise liposomes (Panjwani *et al*., 2016). This leads to the notion that the N-terminus of VP1 does not play a role in penetrating the membrane but may play a role in tethering the virus to the membrane and could be involved in the formation of the umbilicus.

During the conformational rearrangements of enteroviruses, cardioviruses and aphthoviruses (discussed in section 1.8.2) VP4 is released and there is mounting evidence that VP4 is the small capsid protein responsible for membrane penetration, as seen in other non-enveloped viruses (section 1.7.2). VP4 has been shown to be myristoylated and the presence of a myristate group on a protein is often linked to proteins that are targeted to membranes (discussed further in section 3.1) (Chow *et al*., 1987). VP4 has been shown to associate with liposome membranes following incubation of PV with PVr decorated liposomes (Tuthill *et al*., 2006). This shows that following formation of an altered particle that the expelled VP4 relocates into the nearby membrane and therefore could play a role in the formation of the umbilicus and subsequent genome transfer steps.

The essential role of VP4 in entry is highlighted through studies into a lethal mutation found in PV VP4. The substitution of threonine-28 for a glycine has been shown to form progeny viruses when transfected into cells. The mutant PV viruses can progress through the initial steps of entry and were shown to associate with membranes. These viruses were not able to undergo the genome transfer step

required to continue infection, indicating VP4 plays a vital role in the genome transfer stage of PV (Moscufo *et al*., 1993). Following this study the characterisation of the lethal mutation showed that the T28G mutant particles were unable to form ion channels when compared to wild type or viable mutants (Danthi *et al*., 2003). This provides evidence that wild type VP4 forms a channel in a membrane and suggests VP4 membrane permeability is vital for virus entry.

Studies on the VP4 from both HRV and hepatitis A virus (HAV) have shown that both these proteins are capable of inducing membrane permeability using liposomes as a model membrane system (Panjwani *et al*., 2014, Shukla *et al*., 2014). In addition to these picornaviruses the VP4 protein of the distantly related discistrovirus triatomavirus has also been identified as inducing membrane permeability (Sanchez-Eugenia *et al*., 2015). For all of these VP4 studies the ability of the membrane permeability to selectively release fluorescein isothiocyanate (FITC)-linked dextrans (FDs) of known molecular weights has been evaluated and it has been shown that all of these proteins are able to induce size-selective membrane permeability (Panjwani *et al*., 2014, Shukla *et al*., 2014, Sanchez-Eugenia *et al*., 2015). The ability of VP4 to form a size-selective opening in a membrane is further supported by electron microscopy images that showed GST-tagged recombinant HRV VP4 is able to form ring-like structures containing 5 or 6 copies of VP4 and this is consistent with pore formation. The membrane permeability of HRV VP4 has been further characterised and has been attributed to the N-terminus of VP4 (Panjwani *et al*., 2016).

Recently a study in the laboratory has characterised the interaction of FMDV with liposomes. This study has shown that FMDV is capable of permeabilising liposomes in a size-selective manner and that the permeability induced is enhanced when the virus is exposed to low pH. The low pH at which membrane permeability is enhanced coincides with the pH at which FMDV releases the viral genome, indicating a link between membrane permeability and genome transfer (Gold *et al*, manuscript in preparation). This work indicates that FMDV also interacts with membranes in a controlled and size-selective manner which is similar to the membrane interactions characterised for other picornavirus VP4 proteins.

The release of VP4 occurs across multiple genera of picornaviruses and occurs as an outcome of the capsid rearrangements involved in genome transfer, regardless of the formation and stability of an intermediate. The evidence from structural studies of genome transfer and molecular studies into how the genome is transferred

indicate that this process requires some means of controlled exit from the virion. Therefore, it is possible that the membrane permeability induced by VP4 is due to its vital role in forming a pore to allow genome transfer. This is supported by the pore structures documented previously (Panjwani *et al*., 2014). To date the VP4 protein of an aphthovirus has not been investigated for the ability to induce membrane permeability. This would help shed light on whether the membrane permeability induced by all picornavirus VP4 proteins utilise the same mechanism. Alternatively there could be a shared requirement for VP4-induced membrane permeability but the mechanisms of this could vary across the family.

## 1.9 Picornavirus VP4 as a novel target

Evidence from PV has indicated that VP4 plays an essential role in the entry of the virus as the T28G mutation discussed in section 1.8.4 has been shown to prevent infection (Moscufo *et al*., 1993). Alongside this the VP4 protein is highly conserved between viruses of the same species. These two observations make VP4 an interesting target for picornaviruses.

Early evidence that VP4 could be an exciting neutralising target came from a study where antisera against a synthetic VP4 peptide was shown to neutralise PV infection (Li *et al*., 1994). This discovery was unexpected as all prior studies had indicated that VP4 was the internal capsid component and provided the early evidence of the transient externalisation of VP4 through breathing (discussed in section 1.6.3). The induction of neutralising antibodies is a goal for tackling many infectious diseases and as such identifying sequences with high levels of conservation is important.

Further studies have shown that antibodies against the N-terminus of HRV VP4 are also able to neutralise virus infectivity (Katpally *et al*., 2009, Panjwani *et al*., 2016). Antisera raised against the N-terminal 30 amino acids of HRV14 VP4 was shown to be able to neutralise other serotypes of HRV, HRV16 and HRV29, indicating the N-terminus of HRV14 VP4 elicits a cross-serotypic neutralising response (Katpally *et al*., 2009). To date work investigating VP4 as a novel target has focused on the VP4 proteins of enteroviruses and a study has shown that antibodies against HRV VP4 can reduce both HRV infectivity and HRV-induced membrane permeability in liposomes (Panjwani *et al*., 2016).

As cross-serotypic neutralisation has been observed for VP4-specific antibodies, an attempt has been made to harness these antibodies by displaying the N-terminal 20 amino acids of EVA71 VP4 on a virus-like particle (VLP). This sequence was displayed on the major immunodominant region of the well-established hepatitis B core (HBc) VLP (VLP system detailed in section 4.1). The serum from mice immunised with the VP4N20-displaying VLP was able to neutralise different genotypes of EVA71 *in vitro* and neutralise virus and protect neonatal mice from infection (Zhao *et al*., 2013). This study begins to translate the cross-serotypic response to VP4 identified earlier in HRV into a potential novel target for picornaviruses by displaying it on a well-characterised VLP.

## 1.10 Aims of PhD

Previous work on the entry of picornaviruses has predominantly focused on the entry of enterovirus and as such little is known about the role of the FMDV capsid protein VP4 and how this compares to the previously described role of other picornavirus VP4 proteins. In this thesis I have followed on from work in the group that has characterised the ability of FMDV to induce membrane permeability. I have investigated the role of the ability of FMDV sequences to induce membrane permeability and characterised two panels of FMDV VP4-specific antibodies. The overall aim of this thesis is to further the understanding of the role of FMDV VP4 in the processes of membrane permeability and capsid breathing. The specific objectives of this project are:

- To characterise the pore forming ability of FMDV VP4 using peptides and liposomes
- To generate HBc VLPs displaying VP4N15 using two display approaches
- To compare the antibody response to FMDV VP4 and determine if antibodies against FMDV VP4 can neutralise virus infection
- To investigate the phenomenon of virus breathing in FMDV

# Chapter 2 Materials and Methods

# 2. Materials and Methods

## 2.1 General materials

### 2.1.1 Bacterial strains

*Escherichia coli* (*E.coli*) XL-10 gold ultracompetent bacteria were purchased from Agilent, genotype TetrD(mcrA)183 D(mcrCB-hsdSMR-mrr)173 endA1 supE44 thi-1 recA1 gyrA96 relA1 lac Hte [F´ proAB lacIqZDM15 Tn10 (Tetr) Amy Camr] and used for cloning purposes.

*E.coli* BL21 (DE3) were purchased from New England Biolabs (NEB), genotype fhuA2 [lon] ompT gal (λ DE3) [dcm] ∆hsdS (λ DE3 = λ sBamHIo ∆EcoRI-B int::(lacI::PlacUV5::T7 gene1) i21 ∆nin5) and used for protein expression.

One Shot TOP10 chemically competent *E.coli* (Invitrogen) were used with the Zero Blunt TOPO cloning kit. The genotype of these is F- *mcrA* Δ( *mrr-hsd*RMS-*mcr*BC) Φ80*lac*ZΔM15 Δ *lac*X74 *rec*A1 *ara*D139 Δ( *araleu*)7697 *gal*U *gal*K *rps*L (StrR) *end*A1 *nup*G.

### 2.1.2 Cell lines

BHK-21 cells were maintained in the lab for the plaque assays and were used at passages between 65-95.

### 2.1.3 Plasmids

The plasmid CoHBc190 C61A for expressing the hepatitis B core protein was kindly provided by Dr Sam Stephen at the University of Leeds. The CoHBc190 C61A plasmid encodes the full length hepatitis B core antigen protein with a mutation from cysteine to alanine at amino acid 61 and is based on a pET 28b backbone (Peyret *et al*., 2015). The hepatitis B core protein encoded has been modified to include restriction sites at the major immunodominant region. This region is called the FAGAS region.

The pCR™-Blunt II-TOPO plasmid (Invitrogen) was used for the TOPO cloning of the native GeneArt string before insertion into the CoHBc190 plasmid. This plasmid is part of the zero blunt TOPO PCR cloning kit (Invitrogen).

## 2.1.4 Antibodies

Commercial monoclonal antibody anti-HBcAg 10E11 (Abcam) (dilution 1:1000) was used to detect expressed VLPs. Commercial rabbit anti-mouse HRP-conjugated antibody (Santa Cruz) was used as a secondary for western blots (dilution 1:2000). Commercial rabbit anti-mouse HRP-conjugated antibody (DAKO) (dilution 1:2000) and goat anti-rabbit HRP-conjugated antibody (Biorad) (dilution 1:5000) was used as a secondary for ELISA at the dilutions stated.

Polyclonal rabbit serum against the myrVP4N45 and VP4C45 peptides were generated by Envigo. This was produced against KLH-peptide conjugates (Peptide Synthetics) and two rabbits were immunised for each peptide.

## 2.1.5 Lipids

Phosphatidic acid (PA), phosphatidylcholine (PC) and phosphatidylethanolamine conjugated to rhodamine (PE) lipids were bought from Avanti Polar Lipids in chloroform at 10 mg/ Cholesterol was purchased powdered and made up to the same concentration in chloroform.

## 2.1.6 Synthetic peptides

### 2.1.6.1 Peptides for liposome assays

Synthetic peptides were ordered from Peptide Synthetics for use in membrane permeability and FD release assays. These were designed using the O1 kaufbeuren FMDV sequence and represent the N- and C-terminus of FMDV VP4. These peptides also included a poly lysine region for increased solubility. Sequences shown in table 2.1.

### 2.1.6.2 Peptides for peptide attachment onto HBc

A synthetic peptide was ordered from Peptide Synthetics for attachment onto the HBcAg VLPs. This included the N-terminal 15 amino acids of the O1 kaufbeuren FMDV VP4 sequence and a tag designed to attach the peptide onto the MIR of the HBcAg protein. Sequences shown in table 2.1.

### 2.1.6.3 KLH-peptide conjugates for polyclonal serum

KLH-peptide conjugates were ordered from Peptide Synthetics to be used in raising polyclonal serum in rabbits and as a control for the mouse study. Sequences shown in table 2.1.

| **Name of peptide** | **Sequence** |
|---|---|
| myrVP4N45 | *myr*GAGQSSPATGSQNQSGNTGSIINNYYMQQYQNSMDTQLGDNAISGKKKKKK |
| myrVP4N30 | *myr*GAGQSSPATGSQNQSGNTGSIINNYYMQQYKKKKKK |
| myrVP4N15 | *myr*GAGQSSPATGSQNQSKKKKKK |
| VP4N45 | GAGQSSPATGSQNQSGNTGSIINNYYMQQYQNSMDTQLGDNAISGKKKKKK |
| myrVP4N15 –Spike tag | *myr*GAGQSSPATGSQNQSKKKKKKHHHHHH**GSLLGRMKGA** |
| myrVP4N45-KLH | *myr*GAGQSSPATGSQNQSGNTGSIINNYYMQQYQNSMDTQLGDNAISGKKKKKKC-KLH |
| myrVP4N15-KLH | *myr*GAGQSSPATGSQNQSKKKKKKC-KLH |
| VP4C45-KLH | KLH-CKKKKKKNAISGGSNEGSTDTTSTHTTNTQNNDWFSKLASSAFSGLFGALLA |
| VP4C45 | KKKKKKNAISGGSNEGSTDTTSTHTTNTQNNDWFSKLASSAFSGLFGALLA |
| VP4C30 | KKKKKKSTHTTNTQNNDWFSKLASSAFSGLFGALLA |
| VP4C15 | KKKKKKLASSAFSGLFGALLA |
| Scrambled VP4N45 | GQNSSQQQSDMQGSAGSDTGPSLINTNNGQMYYAYTQNAGGNSIIKKKKKK |
| Scrambled myrVP4N45 | *myr*GQNSSQQQSDMQGSAGSDTGPSLINTNNGQMYYAYTQNAGGNSIIKKKKKK |
| Scrambled VP4C45 | KKKKKKFQTNDTTLTLTNANNNTSASKSSASHSDSIGGFFGLWTAGGALES |

**Table 2. 1: Sequences of FMDV O1 Kaufbeuren VP4 peptides.**

VP4 peptides were used for membrane permeability, attachment to the HBc VLPs and production of polyclonal antibodies. The presence of a myristate group is indicated by the *myr* abbreviation. The orientation of the peptides attached to KLH are indicated by the KLH at the terminus linked to KLH. The tag for attachment to HBc VLPs is highlighted in bold.

### 2.1.7 Viruses

FMDV O1Manisa was used for all virus work. This virus was chosen as it is the same virus used for previous characterisation of FMDV induced membrane permeability. It had also been extensively characterised so the precise pH at which the capsid dissociated was known. The virus was grown and purified from a stock provided by Dr Sarah Gold. This virus is tissue culture adapted and can use heparin sulphate as a receptor allowing it to grow in BHK-21 cells.

## 2.2 Virus preparation and purification

Purified virus was required to study the interactions between FMDV and liposomes. Twenty roller bottles of BHK-21 cells were infected with virus and incubated at 37°C overnight to develop CPE. CPE of about 85 % was observed next day and the cells were scraped from the roller bottles and frozen in 500 mL disposable centrifuge tubes (Corning). The harvested cells were then thawed and the cellular debris removed by centrifuging the lysate at 3500 rpm for 10 min in a centrifuge (Beckman Allegra X12). The supernatant was decanted into clean 500 mL centrifuge tubes and protein was precipitated overnight in the fridge with the addition of 50 % (w/v) ammonium sulphate (Sigma-Aldrich). The precipitated protein was pelleted in the centrifuge at 4750 rpm for 1 hr. The supernatant was removed and the pellet was resuspended in 50 mL PBS with 1 % IGEPAL to aid resuspension of the pellet (Sigma-Aldrich). The resuspended pellet was divided between two SW32Ti ultracentrifuge tubes (Beckman) and a 2 mL 30 % (w/v) sucrose cushion was added under the sample. This was centrifuged at 28000 rpm at 12 °C for 2 and a half hours in the SW32Ti rotor. The supernatant was removed and the pellet was covered with 0.5 ml PBS and left in the fridge overnight. The pellets from the sucrose cushions were resuspended in a total volume of 2 mL PBS + 1 % IGEPAL. The resuspended pellet was clarified by centrifuging for 5 min at 4600 rpm under-bench centrifuge to pellet any remaining insoluble debris. The supernatant was then loaded onto a 15-45 % (w/v) sucrose gradient and centrifuged at 28000 rpm at 12 °C for 2 and a half hours in the SW32Ti rotor. The gradient was fractionated into 2 mL fractions from the top and the absorbance at 260 nm was measured for each fractions. The peak and shoulder fractions of the gradients were analysed by SDS-page to confirm the presence of viral proteins.

## 2.3 Preparation of liposomes

Lipids were used to prepare liposomes to be used in membrane permeability and FD release assays. Phosphatidylethanolamine with rhodamine conjugated (PE), phosphatidylcholine (PC) and phosphatidic acid (PA) (Avanti Polar Lipids) were mixed together in a 1:10:10 ratio respectively and 10 % cholesterol was added. Lipids were dried to form a film and rehydrated in 107 mM NaCl, 10 mM Hepes pH 7.5. The rehydrated lipids were extruded through a mini-extruder (Avanti Polar Lipids) using a 400 nm pore-size membrane (Whatman). Comparison of the rhodamine fluorescence in the liposome preparation and samples of rehydrated lipids with known lipid concentration was used to estimate the lipid concentration of the liposomes. Liposomes containing carboxyfluorescein (CF) were made by rehydrating lipids in 50 mM CF, 10 mM Hepes pH 7.5. Liposomes containing fluorescein isothiocyanate (FITC)-linked dextrans (FDs) of known molecular weights (4 kDa, 10 kDa, 70 kDa and 250 kDa) (Sigma) were made by rehydrating lipids in 25 mg/mL FD, 107 mM NaCl, 10 mM Hepes pH 7.5. Liposomes were separated from excess CF or FDs by ultracentrifugation in an SW55 rotor at 34000 rpm at 25°C three times. After purification liposomes were resuspended in 107 mM NaCl, 10 mM Hepes pH 7.5. CF is a fluorescent dye which remains quenched within the liposome and becomes unquenched when it is released. The fluorescence of released unquenched CF can be read at excitation 485 nm/ emission 520 nm wavelengths.

## 2.4 Membrane permeability assays

Membrane permeability assays were used to study the interaction between the peptides and the liposome membrane and the effect of antibodies against VP4 on virus and peptide induced membrane permeability.

### 2.4.1 CF release assays

Liposomes containing CF were used at a lipid concentration of approximately 50 µM. A baseline of CF-containing liposomes only was used as a control in the Plate Chameleon V plate reader (Hidex). Peptides or triton were added to the liposomes at the required concentrations and the fluorescence caused by unquenched CF was read in real time. The well-characterised pore forming peptide melittin was used as a control. Readings were taken at 485 nm/ 520 nm wavelengths every 30 seconds for 1 hr at room temperature for peptide CF release and 37°C for FMDV CF release.

The effect of antibodies against VP4 on virus and peptide induced membrane permeability was studied by incubating the antibodies with 1 µg of gradient purified FMDV and then using this in the membrane permeability assay described above. As controls virus only and heated virus were used.

### 2.4.2 FD release assays

FD release assays were used to study whether the membrane permeabilisation of liposomes by peptides was size selective. Liposomes were used at a lipid concentration of approximately 50 µM. Peptides and liposomes were incubated at room temperature for an hour and then centrifuged for 1 hr at 62000 rpm at 25 °C in the TLA100 rotor. The supernatant was removed and the fluorescence measured at 485 nm/ 520 nm wavelengths. Triton was then added and samples re-read to account for any change in the meniscus. Release was calculated as percentage of complete release where triton was taken as complete release.

## 2.5 Manipulation of DNA

### 2.5.1 Synthetic DNA

Plasmids from GeneArt were designed containing fragments of the N- and C-terminal sequence of FMDV VP4. These sequences were based on the sequence of the O1 Kaufbeuren strain of FMDV.

A linear synthetic DNA from GeneArt was ordered containing the native sequence of hepatitis B core protein and this was used to replace the FAGAS region of the CoHBc190 plasmid. This returns the sequence of the plasmid to the native sequence of the hepatitis B core.

### 2.5.2 TOPO blunt end cloning

The zero blunt TOPO PCR cloning kit (Invitrogen) allows one step cloning of blunt ended DNA fragments into a plasmid vector. The kit was used following the manufacturer's instructions. The linear DNA was mixed with the pCR™ II-blunt-TOPO vector and incubated for 5 min at room temperature to allow the topoisomerase reaction to occur. After the incubation the reaction mix was transformed into OneShot competent cells.

## 2.5.3 Restriction digests

All restriction digests were carried out using high-fidelity (HF) restriction enzymes from NEB. These enzymes had reduced star activity and can all be used in the same CutSmart buffer. For diagnostic digests 1 µg of plasmid DNA was incubated with 10 units of enzyme and CutSmart buffer and left at 37 °C for a minimum of 2 hours. For preparative digests 2 µg of plasmid DNA was mixed with 20 units of enzyme and CutSmart buffer and left at 37 °C for a minimum of 2 hours.

## 2.5.4 Dephosphorylation of plasmid backbone

The linearised backbones were dephosphorylated before ligation using rAPid alkaline phosphatase (Roche) and following the instructions provided with the reagent. Vector DNA was mixed with 1 unit of the rAPid alkaline phosphatase and the rAPid alkaline phosphatase buffer provided and incubated at 37 °C for 30 min. The alkaline phosphatase was then inactivated by heating the reaction mix at 75 °C for 30 min.

## 2.5.5 Agarose gel electrophoresis

Agarose was dissolved in 1x TBE buffer by gentle heating in the microwave. Once this was cooled ethidium bromide was added to a final concentration of 0.5 µg/mL (using a stock solution at 10 mg/mL) and mixed by gently swirling the flask. This was then poured into a gel tray and a comb with an appropriate number of wells placed into the warm agarose. Once set the gel was placed into a gel electrophoresis tank (Biorad) and filled with 1x TBE buffer. Samples were mixed with purple loading buffer (NEB) and loaded onto the gel. One kb, 100 bp or a low molecular weight marker (NEB) were included alongside samples. The gels were typically run at 90 V for 1 hr. Once finished the DNA bands were visualised using the ChemiDoc MP (Biorad). Frequently bands of the expected size were then cut out of the gel using a scalpel to purify the DNA.

## 2.5.6 Gel extraction

DNA from agarose gels was purified using the illustra GFX PCR DNA and gel band purification kit (GE healthcare) and following the manufacturer's instructions. Briefly agarose was dissolved in a buffer containing a chaotropic agent and high salt. The DNA is then bound to a silica membrane within a spin column. DNA binds tightly to silica in

the presence of high salt. The bound DNA was then washed with a wash buffer containing ethanol before eluting the DNA into the provided low-salt elution buffer. The DNA concentration was measured using spectrophotometry (Nanodrop 2000).

## 2.5.7 DNA ligations

Ligations were carried out using T4 ligase (NEB). Vector and insert were mixed at different ratios with T4 ligase and the provided T4 ligase buffer. This was then left on ice overnight to allow the temperature to gently come down ensuing effective ligation. The next day the ligation product was transformed into competent bacteria and any leftover reaction mix was stored in the freezer.

## 2.5.8 Transformation of chemically competent bacteria

Transformation of chemically competent bacteria was carried out according to the manufacturers' protocol. The same principle was used for all three bacterial strains. The bacteria were thawed on ice and incubated with 0.1-100 ng plasmid DNA or 2 µl of ligation mixture for 30 min. The bacteria were then heat shocked to allow the plasmid to enter the bacteria. After the heat shock the bacteria were once again briefly incubated on ice. NYZ+ or SOC broth was added and the bacteria were left to recover for 1 hr at 37°C in a shaking incubator. After recovering for an hour the bacteria were plated onto LB agar plates containing 50 µg/mL Kanamycin or 100 µg/mL Ampicillin. The plates were divided into two halves and 100 µl of the transformation product was plated onto one half. The rest of the transformation product was spun at 14000 RPM in the benchtop microfuge and then resuspended in 100 µl broth and plated onto the other half of the plate.

An additional step was included in the transformation of the XL-10 gold ultracompetent bacteria, prior to incubation with the plasmid DNA, the bacteria were pre-incubated on ice with β-mercaptoethanol to enhance the transformation efficiency. For all three types of bacteria between 0.1-50 ng of plasmid DNA or 2 µl of ligation mixture was added to the bacteria.

## 2.5.9 Bacterial cultures

Bacterial cultures were grown to generate plasmid DNA or for expression of recombinant protein. Minipreps and maxipreps were used for the purification of

plasmid DNA and bacterial cultures were grown as follows for these.

For obtaining small amounts of DNA minipreps were used and initially 10 mL Luria-Bertani (LB) broth containing 50 μg/mL of kanamycin was put into a 50 mL tube and a pipette tip was used to pick a single colony from a LB agar plate. This was then incubated overnight at 37 °C with shaking at 225-250 rpm. For a maxiprep culture a similar 2 mL start culture was grown through the day and then added to 500 mL of LB broth containing 50 μg/mL kanamycin and this was grown overnight at 37 °C shaking at 225-250 rpm.

For bacterial expression 10 mL LB broth containing 50 μg/mLof kanamycin was put into a 50 mL tube and a pipette tip was used to pick a single colony from a LB agar plate. This was then incubated overnight at 37 °C shaking at 225-250 rpm.

## 2.5.10 Purification of bacterial DNA

Bacterial plasmid DNA was purified using the QIAprep spin miniprep kit (Qiagen) for small volumes and diagnostic purposes or the plasmid maxi kit (Qiagen) for large volumes and to make a stock of plasmid. These kits were used following the manufacturer's instructions.

Bacterial cultures (detailed in 2.5.9) were centrifuged to pellet the bacteria and this was then resuspended. Once resuspended, lysis buffer was added to disrupt the bacteria membranes and release plasmid DNA, through alkaline lysis. The lysis buffer was neutralised and cellular debris was pelleted by centrifugation. The DNA from the supernatant was then bound to the column membrane. The bound DNA was washed with a wash buffer containing ethanol and then eluted in nuclease free water.

For the maxiprep kit the bound DNA was eluted into a buffer provided in the kit and the DNA was precipitated with isopropanol and washed with 70 % ethanol before resuspending the DNA in nuclease free water. These additional steps are required due to the high concentrations of DNA and isopropanol precipitation and ethanol wash that are required to provide a clean DNA sample. The DNA concentration for both was measured using spectrophotometry (Nanodrop 2000).

### 2.5.11 Quantification of DNA

The concentration of DNA obtained from mini preps and maxi preps was determined using spectrophotometry using the Nanodrop 2000 (Thermo Scientific). A 1 µl drop of the sample was placed onto the reader and then the absorbance 260 nm reading made. Based on this reading the Nanodrop software utilises a modified version of the Beer-Lambert equation to calculate the concentration of DNA present.

### 2.5.12 Sequencing for plasmids

Plasmids were sequenced by Source Bioscience using primers which bound T7 RNA polymerase promoter regions within the plasmid.

## 2.6 Protein biochemistry

### 2.6.1 SDS-PAGE

For SDS-PAGE 12 % Tris-glycine acrylamide gels were used to confirm the presence of proteins and for western blots. The 12 % acrylamide resolving gel was made using 8mL of 40 % (w/v) 29:1 acrylamide:bisacrylamide (Sigma) , 5 mL 1.5 M Tris-HCl pH 8.8, 1 % (w/v) SDS, 1 % (w/v) ammonium persulphate and made up to 20 ml with water and the 5 % acrylamide stacking gel was made using 1.7 mL of 40 % (w/v) 29:1 acrylamide:bisacrylamide (Sigma), 1.25 mL of 0.5 M Tris-HCl pH 6.8, 1 % (w/v) SDS, 1 % (w/v) ammonium persulphate and made up to 10 mL with water. Immediately prior to pouring the gels into the gel casting apparatus 0.001% N,N,N',N'-Tetramethylethylenediamine (TEMED) was added to polymerise the gel. The gels were placed in the gasket of the mini-PROTEAN (Biorad) gel electrophoresis cell filled with Tris-glycine running buffer (25 mM Tris-base, 190 mM glycine, 0.1 % (w/v) SDS). Samples were mixed in 3 x red SDS buffer (NEB). Precision plus dual colour marker (Biorad) was analysed alongside experimental samples to determine the approximate molecular weights of proteins. The samples were electrophoresed at 80 V for 10 min to allow the proteins to stack. The current was then increased to 120 V for around 1 hr.

### 2.6.2 Staining methods

SDS-PAGE gels were primarily stained using Coomassie blue stain (0.5 mM coomassie, 40 % absolute ethanol, 10 % acetic acid) to confirm the presence of

proteins. Coomassie stain works by binding to basic and hydrophobic residues, such as histidines, of proteins and staining the protein blue. SDS-PAGE gels were removed from the glass plates and put in enough Coomassie blue stain to cover the gel. This was left shaking for at least 1 hr before the Coomassie was poured off and destain (21 % absolute ethanol, 8 % acetic acid) was added. This was then left shaking and destain was changed regularly to ensure the gel was well destained. Stained SDS-PAGE gels were then imaged on the GelDoc (Biorad).

For samples with low protein concentrations the SDS-PAGE gels were stained using the Pierce Silver Stain Kit (Thermo Scientific). This was done following the protocol provided. Briefly after washing the gel in ultrapure water the gel was fixed using a solution containing 30 % ethanol and 10 % acetic acid and then treated with a sensitiser. Once fixed and sensitized, the staining solution containing silver ions was added. The silver ions bind certain function groups on amino acids, such as the carboxylic acid groups in glutamic acid and the imidazole group on histidine. The developer solution is then added and the silver ions are reduced to metallic silver, causing a colour change. This reaction is then stopped using dilute acetic acid.

### 2.6.3 Western blots

SDS-PAGE gels were prepared and samples were subjected to electrophoresis as described in 2.6.1. After electrophoresis the gel was put into transfer buffer (25 mM Tris-base, 190 mM glycine, 20 % methanol) and washed for 5 min to remove the SDS buffer. During this time a piece of nitrocellulose membrane was briefly soaked in ultrapure water before soaking in transfer buffer. The filter paper supports and pads were also soaked in transfer buffer. The gel was placed with the nitrocellulose membrane in a cassette for the Mini Trans-Blot Cell (Biorad) and the proteins were transferred for 1 hr at 90 V. After transfer the membrane was blocked in 1 % (w/v) fish skin gelatin (Sigma) in PBS-T (PBS + 0.05 % Tween 20) for 1 hr at RT or overnight at 4 °C. The block was then discarded and the membrane was washed twice with PBS-T. The primary antibody was then added to the membrane in a falcon tube and left rolling for 1 hr at RT or overnight at 4 °C. The primary antibody was removed and the membrane washed 5 times in PBS-T. The secondary antibody was then added to the membrane and left rolling for 1 hr at RT. The secondary antibody was then removed and the membrane was washed thoroughly 5 times in PBS-T. The Pierce ECL western blotting substrate (Thermo) interacts with the HRP group conjugated to the secondary, producing a luminescent signal. After

incubating the substrate on the membrane for 1 min the membrane was imaged using the ChemiDoc MP (Biorad).

### 2.6.4 Quantification of total protein concentrations

The protein concentration in expressed protein samples was determined using the Pierce Coomassie Plus (Bradford) Assay Kit (Thermo Scientific). Albumin standards from 2 mg/mL to 25 µg/mL were made up in the same buffer as the protein samples using albumin ampules from Thermo Scientific and these were used to produce a standard curve.

The assay was carried out in triplicate in a 96 well flat bottomed plate (Thermo Scientific). 10 µL of blank, standard or unknown sample was added to each well and 300 µL of Coomassie Plus reagent was added to each well and incubated for 10 min. The absorbance was then measured at 595 nm using the BioTek EL x808 plate reader. The average absorbance at 595 nm of the blank was removed from the average absorbance of each samples or standard. This was then plotted to make a standard curve and the protein concentration was calculated for each unknown sample.

## 2.7 Expression of HBc VLPs

After transformation of competent bacteria a 10 mL overnight bacterial culture was set up as previously described in section 2.5.9. 1 mL of starter culture was added for every 100 mL of expression culture grown and this was left to grow shaking at 225-250 rpm at 37 °C. The optical density (OD) at 600 nm (OD600) was measured before inoculation with starter culture and at regular intervals until the OD600 was between 0.6-0.8. Once this was reached a 1 mL uninduced sample was removed and spun down and the bacterial pellet frozen. At this point 1 mM IPTG was added to the remainder of the culture to induce expression and the bacteria were grown for 3 hrs at 37 °C shaking at 225-250 rpm.

After three hours of growth the OD600 was again measured and an equivalent amount of induced bacteria to the 1 mL uninduced bacteria was removed and the pellet frozen. The remaining culture was then pelleted by centrifugation in the Avanti J26S XP (Beckman) at 7000 x g for 20 min at 4°C in the JA 10 rotor and could be stored at -20 °C.

Lysis buffer was made up (20 mM Hepes, 250 mM NaCl, pH 7.5) and for every 10 mL

required 1 tablet Roche cOmplete mini EDTA-free protease inhibitor and 25 units of Benzonase nuclease was added (Merck Millipore). The cell pellet was then resuspended in lysis buffer. 4 mL of lysis buffer was added for every 100 mL of starter culture. The bacterial suspension was then sonicated 10 x 30 s on 30 s off at an amplitude between 5 and 10. This was repeated twice to ensure the bacteria were lysed. The lysed bacteria were then centrifuged at 7000 x g for 30 min to remove any insoluble cellular debris. The normalised samples of uninduced and induced were lysed first and the presence of expressed protein established using SDS-page before lysis of the remaining bacterial pellet was carried out.

After lysis the supernatant was centrifuged again at 7000 x g for 30 min to further clarify the supernatant. The soluble protein was then precipitated by adding 40 % (w/v) ammonium sulphate and storing in the fridge overnight. The precipitated protein was pelleted by centrifugation at 10000 rpm for 20 min at 4°C in the JA 10 rotor in the Avanti centrifuge. The supernatant was then removed and the pellet resuspended in capsid buffer (20 mM Hepes, 250 mM NaCl, 2 mM DTT, pH 7.5). This was then clarified further by centrifugation at 10000 rpm for 20 min at 4°C in the JA 10 rotor in the Avanti centrifuge.

## 2.8 Purification of HBc VLPs

A 20-60 % (w/v) sucrose gradient was formed using the Biocomp gradient maker and the clarified protein from section 2.7 was layered onto the gradient. The gradient was put in the ultracentrifuge and centrifuged for 3 hr at 151000 x g in the SW32Ti rotor at 4 °C. The gradient was then fractionated into 2 mL fractions and each fraction was analysed by SDS-page and by measuring the absorbance at 280 nm to determine which fractions contained the peak of the VLPs.

The peak fractions were then pooled and buffer exchanged into PBS (Gibco) and then layered onto a second 20-60 % (w/v) sucrose gradient to ensure the peak fractions were pure. The second gradient was made using the Biocomp gradient maker. The presence of purified VLPs was confirmed by western blot and EM.

## 2.9 Formation and purification of peptide-native HBc VLPs complexes

Peptides were resuspended in nuclease free water as described previously (section 2.1.6.2). Native hepatitis B core VLPs and synthetic peptides were mixed in a 1:4

molar ratio. These were incubated with shaking for a minimum of 1 hr at room temperature. After incubation the mixture was diluted to 15 mL and an amicon centrifugal desalting and concentrating device (Merck Millipore) with a molecular weight cut off of 100 kDa was used to remove unbound peptide. The sample was washed three times with PBS (Gibco) and the final concentrated sample was removed from the device and the concentration of the sample determined by Bradford assay.

## 2.10 Negative stain transmission electron microscopy

Electron microscopy was used to determine whether the purified HBc VLPs had self-assembled into particles. This was carried out by Dr Pippa Hawes at The Pirbright Institute. Purified samples were negatively stained using 2 % aqueous uranyl acetate. The prepared grids were visualised in the transmission electron microscope (FEI Tecnai 12 LaB6 TEM) and images were taken (Tietz F214 camera).

## 2.11 Inoculation of mice with VP4 constructs

Balb/c mice were used to study the immune response generated against the N-terminal 15 amino acids of VP4. The N-terminal 15 amino acids of VP4 were displayed using three different constructs. Six female mice of between 5-6 weeks of age were immunized with 10 µg of antigen in titermax adjuvant (Sigma) in a total volume of 250 µl. The adjuvant was mixed with immunogen at a 50:50 ratio. Three mice were immunized with a control VLP with no VP4. Two boosts were carried out with 10 µg of antigen at 2 and 4 weeks after the initial immunization. Before immunization and at days 10 and 24 blood samples were collected from the tail vein. At the end of the study the mice were euthanised and the terminal bleed was collected via cardiac puncture. The spleen was also dissected out to harvest splenocytes. Procedures requiring home office licences were carried out by Paul Smith (Animal Services) and Dr Rennos Fragkoudis (The Pirbright Institute)

## 2.12 Collection of serum from mouse blood

Blood samples collected from the pre-bleed, intermediate bleeds and terminal bleeds were all processed to obtain serum. Blood was left to coagulate and then centrifuged at 4000 rpm at 4 °C for 15 min to pellet the cellular debris. Serum was collected from the tube and stored at -20 °C.

## 2.13 Harvesting of splenocytes from mouse spleens

Splenocytes from the mice were harvested to be used for future monoclonal production. Spleens were dissected out of the mice in a cabinet and stored in sterile PBS. A 26 G needle was used to flush the spleen with PBS to remove some splenocytes and then the spleen was placed in a 100 µm cell strainer (VWR) and the spleen was forced through the strainer. This was then rinsed with more PBS to wash through any remaining splenocytes. The cells were then centrifuged for 5 min at 400 xg and resuspended in a 5 mL RPMI, Glutamax, 10 % FBS and stored on ice while the other spleens were processed. Once all spleens had been processed the cells were again centrifuged at 400 xg for 5 min and then resuspended in 3 mL of freeze down media (foetal bovine serum (FBS) + 10 % DMSO). This was then aliquoted into 1 mL cryovials and these were frozen in an isopropanol freezing unit in the -80 °C freezer. Once frozen these were transferred to liquid nitrogen.

The splenocytes from the mouse identified as having the best polyclonal response that recognises FMDV VP4N15 were then sent to The Roslin Institute for production of monoclonal antibodies.

## 2.14 Peptide ELISA to determine immune response against VP4

A peptide ELISA was used to evaluate the immune response of mice against FMDV VP4N15. This was done by coating a 96 well Nunc maxisorp plate (Thermo Scientific) with 1 µg/mL of VP4N15 peptide in coating buffer. The plate was then left overnight at 4 °C. The next day the coating buffer was washed off using PBS-T (PBS + 0.1 % Tween 20) and after washing 5 more times the plate blocked with 5 % fat free milk in PBS-T for 1 hr at 37 °C. After blocking the plate was again washed with PBS-T 5 times. The mouse serum was then used in a dilution series in triplicate. The mouse serum was diluted in 1 % fat free milk in PBS-T. This was incubated with gentle mixing for 1 hr at 37 °C. The mouse serum was then washed off and the plate was washed 5 times with PBS-T. The secondary HRP conjugated antibody was then added in 1 % fat free milk in PBS-T. This was incubated for 1 hr at 37 °C and then washed 5 times in PBS-T. A Sigmafast OPD table (Sigma) was diluted in 20 mL of water to a final concentration of 0.4 mg/mL OPD and 50 µl of OPD was added to each well. This was left for 10 min to allow colour to develop and then the reaction was stopped by adding 50 µl of 1 M sulphuric acid. The absorbance at 490 nm was then measured in the EMax plate reader (Molecular Devices).

The same protocol was used to evaluate the immune response of the commercial rabbit polyclonal serum to the KLH-conjugates. For this the plates were coated with 1 µg/mL of VP4C45 or myrVP4N45 peptide. The secondary antibody used was a goat anti-rabbit HRP conjugated antibody (Biorad) and this was used at 1:5000 dilution.

## 2.15 ELISA to determine immune response against homologous antigen

An ELISA was used to investigate mouse serum that did not seem to respond to VP4N15 to check the response to the original antigen. This was done by coating the plate with the original antigen at 1 µg/mL and then following the ELISA protocol for the peptide ELISA above.

## 2.16 Capture ELISA to determine immune response against FMDV

A capture ELISA using integrin as a capture was used to determine if the mouse serum recognised intact FMDV. A 96 well Nunc maxisorp plate (Thermo Scientific) was coated with 1 µg/mL of bovine integrin (kindly provided by Dr Alison Burman) in coating buffer and left at 4 °C overnight in the fridge. The next day the coating buffer was washed off using PBS-T (PBS + 0.1% Tween 20) and after washing 5 more times the plate blocked with 5 % fat free milk in PBS-T for 1 hr at 37 °C. After blocking the plate was again washed with PBS-T 5 times. FMDV O1M was diluted in 1 % fat free milk in PBS-T and added to the well. This was incubated with mixing for 1 hr at 37 °C. The virus was then washed off and the plate was washed 5 times again. The mouse serum was then used in a dilution series in triplicate. The mouse serum was diluted in 1 % fat free milk in PBS-T. This was incubated with gentle mixing for 1 hr at 37 °C. The mouse serum was then washed off and the plate was washed 5 time with PBS-T. The secondary HRP conjugated antibody was then added in 1% fat free milk in PBS-T. This was incubated for 1 hr at 37 °C and the washed 5 times in PBS-T. A Sigmafast OPD table (Sigma) was diluted in 20 mL of water to a final concentration of 0.4 mg/mL OPD and 50 µl of OPD was added to each well. This was left for 10 min to allow colour to develop and then the reaction was stopped by adding 50 µl of 1 M sulphuric acid. The absorbance at 490 nm was then measured in the Chameleon plate reader (Hidex).

## 2.17 Plaque reduction neutralisation assays

Plaque reduction neutralisation assays were used to determine if the mouse and rabbit serum was neutralising. To do this test serum, control neutralising serum or PBS were incubated with 12.5 µl of FMDV O1M for 1 hr at 37 °C. After the incubation the virus was diluted 1 in 10 in sterile PBS and then in a further tenfold dilution series was made.

Six well plates with BHKs at ~80 % confluency were used. The media was removed and the cells were washed with sterile PBS. After the PBS was removed 100 µl of virus dilution was added to the relevant well and this was incubated at 37 °C for 15 min. After incubation 4 mL of eagles overlay containing 0.6 g low melting point agarose (indubiose), 1 % FBS, 5 % tryptone phosphate broth, 100 units/ mL penicillin and 100 µg/ mL streptomycin was added on top of the cells. Once the overlay had set the plaque assay was incubated at 37 °C for two days. After two days incubation 4 mL of methylene blue stain was added to fix and stain the cells. This was left overnight before the plaques were removed.

The virus titre was calculated by counting the plaques in each well and taking into account the dilution factor in that well to establish the plaque forming units per ml (PFU/mL).

## 2.18 Purification of IgG from mouse and rabbit serum

Purified IgG was required for use in liposome assays as serum has too many contaminant proteins that have membrane activity. IgG was purified from the mouse serum using Pierce protein G magnetic beads (Thermo) and from the rabbit serum using Pierce protein A magnetic beads. The protocol provided was used for both with the following modifications. Magnetic beads were placed in a 1.5 mL microcentrifuge tube and 150 µl of wash/ binding buffer (TBS + 0.05 % Tween 20) was added. The beads were then collected using the magnetic stand and the wash buffer removed. The wash was repeated with 1 mL of wash/ binding buffer. 10 µl of serum was diluted in 490 µl of wash/ binding buffer and added to the beads. The beads were well mixed and then incubated with mixing at room temperature for 1 hr. The beads were then collected with the magnetic stand. 500 µl of wash/ binding buffer was added and the magnetic beads washed well. This was then removed and the wash repeated twice. 100 µl of elution buffer (50 mM glycine, 150 mM NaCl pH 1.9) was added to the beads. This was mixed well and incubated for 10 min at room

temperature with gentle mixing. The beads were collected and the eluted IgG removed. To neutralise the elution buffer 15 µl of neutralisation buffer (1 M Tris pH 8.5) were added. The purity of the eluted IgG was confirmed by SDS-PAGE.

# Chapter 3
# Characterisation of membrane permeability induced by FMDV VP4 peptides

# 3. Characterisation of membrane permeability induced by FMDV VP4 peptides

## 3.1 Introduction

One of the major hurdles in virus entry for picornaviruses is the movement of the viral genome from the endosome into the cytoplasm to enable replication of the genome and production of progeny virus particles. It is hypothesised that this is achieved through the formation of a pore in the endosomal membrane that allows the genome to transfer in a controlled and protected manner. Recently, work with PV has shown that the movement of the viral genome into receptor-decorated liposomes is not affected by the presence of RNase in the surrounding buffer (Groppelli *et al*., 2017). This suggests the formation of a pore that is attached to the virus particle and that protects the RNA during the transfer and follows on from previous work in PV that showed an umbilicus formed between PV bound to liposomes decorated with the natural receptor of poliovirus, CD155 or poliovirus receptor (PVr) (Strauss *et al*., 2013). Liposomes can be generated containing lipids with a nickel-charged nitrilotriacetic acid (NTA) head group which allows decoration with a recombinant PVr protein which contains a C-terminal His-tag (Tuthill *et al*., 2006).

During the entry process, VP4 is externalised from the virus capsid and it is hypothesised that VP4 then forms the pore required for genome transfer. In PV, VP4 has been shown to associate with membranes, as after incubating PV with PVr decorated liposomes VP4 remains associated with the liposome fraction of a floatation assay (Tuthill *et al*., 2006). There is also important evidence that VP4 plays a role specifically in entry, as the mutation of threonine-28 in PV VP4 does not prevent endocytosis of the virus into the cell but prevents genome movement into the cytoplasm (Moscufo *et al*., 1993). Recombinant RNA containing this T28G mutation was able to replicate and assemble virus particles when transfected into cells. These particles could associate with membranes during entry but were unable to initiate infection (Moscufo *et al*., 1993).The T28G particles were then shown to be unable to form an ion channel when compared to wild type and other viable mutants, which indicated the ability of VP4 to form a membrane channel is important for the virus lifecycle (Danthi *et al*., 2003) Previous work with HRV and other more distantly related viruses; HAV and the discistrovirus triatomavirus, have also shown that the VP4 from these viruses is able to interact with membranes

within a liposomes model system (Panjwani *et al*., 2014, Shukla *et al*., 2014, Sanchez-Eugenia *et al*., 2015). In these studies, this interaction has been shown to be size-selective using liposomes containing fluorescein isothiocyanate (FITC)-linked dextrans (FDs) of known molecular weights (Panjwani *et al*., 2014, Shukla *et al*., 2014, Sanchez-Eugenia *et al*., 2015). Recombinant VP4 from HRV has also been investigated using electron microscopy and has been shown to form ring-like structures consistent with pore formation containing 5 or 6 copies of VP4 (Panjwani *et al*., 2014). As the pore-forming ability seems to be a conserved feature of VP4 across a diverse range of picornaviruses and discistroviruses it seems likely the VP4 in FMDV may play a similar role.

Whilst FMDV entry must include the essential step of genome transfer FMDV does not remain in an altered particle like the enteroviruses but dissociates into 12 S pentamers after uptake in the cell (Baxt and Bachrach, 1980). Therefore, it is possible the mechanism of pore formation is subtly different. Work carried out in the group has shown that the induction of membrane permeability by FMDV increases as the pH lowers, which could be linked to the dissociation of the virus as the pH lowers. It has also been shown that the membrane permeability induced by FMDV is size-selective (Gold *et al*, manuscript in preparation).

Previous work within the laboratory had shown that is it possible to use synthetic peptides to further dissect the membrane permeability induced by HRV VP4. This work shows that the membrane permeability induced by HRV can be observed using a full length recombinant VP4 (Panjwani *et al*., 2014). The membrane permeability induced by the recombinant protein was then replicated using a synthetic peptide of the N-terminal amino acids of HRV VP4 (Panjwani *et al*., 2016). This work has demonstrated that it is possible to utilise peptides to understand the membrane permeability of HRV. This approach will be applied to FMDV VP4 in this chapter following previous work in the laboratory with FMDV (Gold *et al*, manuscript in preparation).

The N-terminus of FMDV VP4 is modified by the addition of the small 14-carbon saturated fatty acid myristic acid onto the N-terminal glycine by myristoyl-CoA:protein N-myristoyl transferase (Chow *et al*., 1987, Farazi *et al*., 2001). This process occurs both co-translationally and post-translationally depending on the target protein (Olson and Spizz, 1986, Zha *et al*., 2000). The presence of myristoylation is associated with membrane proteins or proteins that interact with membranes (Ray *et al*., 2017). Several other viral proteins are myristoylated and

these play a role in several different stages of the virus lifecycle. Some myristoylated viral proteins are involved in the entry of the virus, such as the µ1 protein in reovirus (discussed in section 1.7.2.3) (Chandran *et al*., 2002). Other myristoylated viral proteins are involved with the early stages of viral infection and the assembly of mature progeny virion, such as the Gag and Nef proteins of HIV (Veronese *et al*., 1988).

The Gag protein is a large polyprotein that is vital for the assembly of new virus particles (Göttlinger *et al*., 1989). It has been shown the presence of the myristate group, along with a membrane binding domain at the N-terminus of Gag allows the targeting of gag to the membrane (Zhou *et al*., 1994). Once Gag is associated with the membrane the myristate group has been shown to be essential for the multimerisation of Gag in cells (Li *et al*., 2007). Gag multimerisation is essential for the formation of progeny viruses and mutant viruses lacking the myristoylation site are unable to form new virus particles showing the myristoylation is essential for assembly (Göttlinger *et al*., 1989). While HIV Gag plays an essential role at the assembly step of the viral life cycle, the HIV protein Nef is expressed early in the virus lifecycle and interacts with several cellular pathways. Nef has been identified as an essential protein for viral replication and pathogenicity and is responsible for high viral titres and it is also associated with progression to acquired immunodeficiency syndrome (AIDS) (Kestler *et al*., 1991).

The work presented in this chapter has been carried out using liposomes as a model membrane system. Liposomes are synthetic lipid vesicles that mimic a lipid bilayer. There are several types of liposomes that can be made and these fall into two groups; multilamellar vesicles (MLV) and unilamellar vesicles. MLVs contain multiple lipid layers that are separated by buffer. Unilamellar vesicles can be further divided into small unilamellar vesicles (SUVs) and large unilamellar vesicles (LUVs). Both SUVs and LUVs are single lipid bilayers encapsulating the reagent within (as shown in the schematic in figure 3.1).

The method of preparation of SUVs and LUVs is different and results in the size differences. SUVs are formed through sonication of MLVs to produce vesicles of ~100nm (Akbarzadeh *et al*., 2013). LUVs are formed through a variety of methods including extrusion of the lipids through a membrane of a specific size (as detailed in section 2 .3) and are much larger going up to ~1000 nm in diameter.

Liposomes have been used for different purposes, including drug delivery vehicles

and as reagents to study membrane proteins and membrane interactions. Several viral proteins have been identified that can interact with membranes and specifically form pores in membranes to aid various stages in the viral lifecycle. In addition to the work mentioned previously in this section using picornaviruses, such as PV, HRV and HAV, liposomes have provided a useful model membrane system to study the interactions of viral proteins from other non-enveloped and enveloped viruses. Liposome studies have been important in understanding the function of viroporins, such as the human papillomavirus E5 protein and hepatitis C p7 protein (Wetherill *et al*., 2012, StGelais *et al*., 2007).

As discussed in section 1.7.2 several non-enveloped viruses have small capsid proteins or capsid-associated peptides that are produced as a result of cleavage of the major capsid protein, such as µ1 in reoviruses and infectious bursal disease virus (IBDV) pep46 (Chandran *et al*., 2002, Galloux *et al*., 2007). Liposomes have been a useful tool to determine how these small peptides interact with membranes and this has begun to shed light on some of the mechanisms utilised by non-enveloped viruses to penetrate host vesicles during entry.

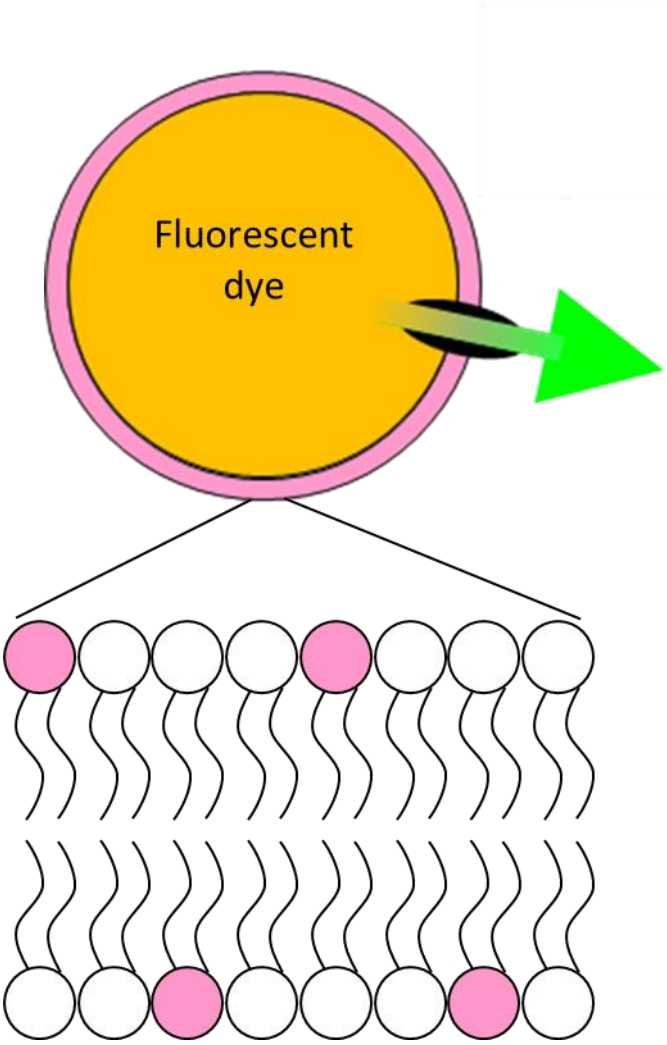


**Figure 3. 1**: **Schematic of a liposome.**

Liposomes composed of phosphatidic acid (PA), phosphatidylcholine (PC) and phosphatidylethanolamine with rhodamine conjugated (PE). The rhodamine group is indicated by the pink groups on the lipids. Liposomes were produced using extrusion through a 400 nm membrane.

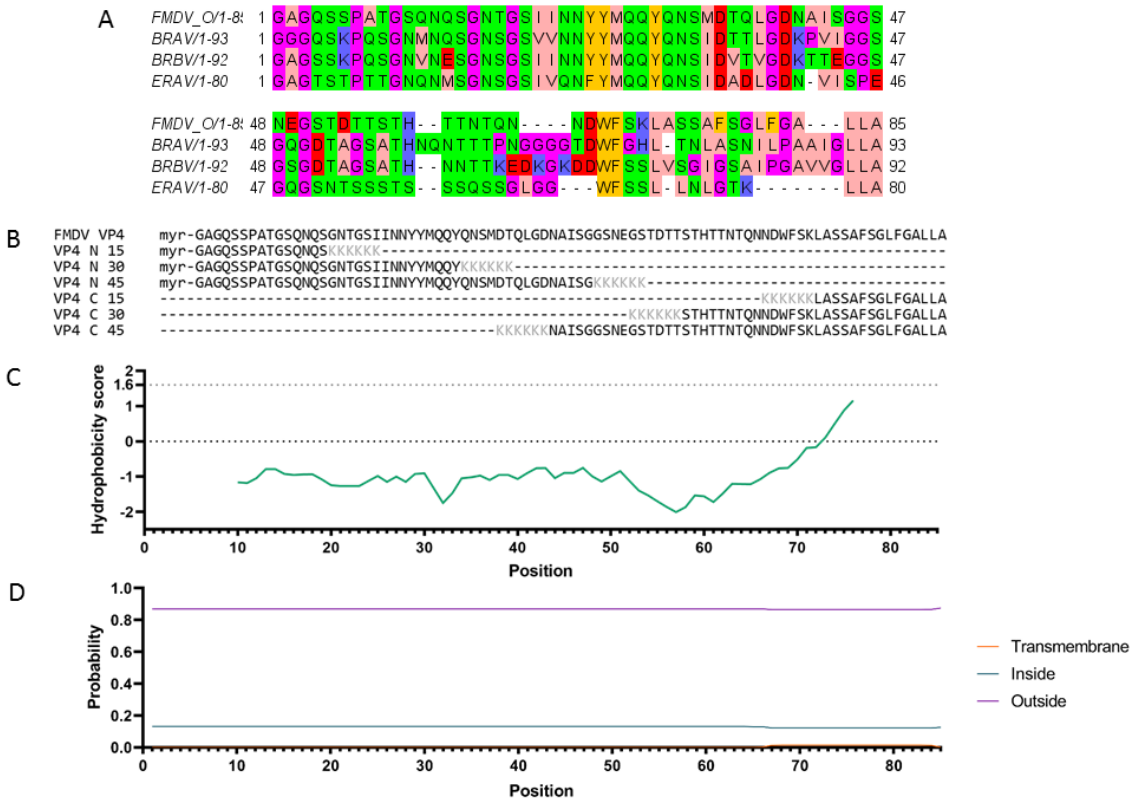


**Figure 3. 2 Analysis of FMDV VP4 sequence and sequence of the synthetic peptides used to study FMDV VP4 interactions with liposomes.**

(A) Alignment of the VP4 protein of 5 members of the aphthovirus genus aligned using the MUSCLE sequence alignment tool (Edgar, 2004). (B) Peptides designed based on the O Kaufbeuren sequence (top row). The name of each peptide is shown to the left in bold and the number refers to the number for amino acids from the FMDV VP4 sequence are in the peptide. Each peptide has 6 lysine residues added which are required to help with the solubility of the peptides (shown in grey) and N-terminal myristoylationis indicated by the myr at the beginning of the sequence. (C) Kyte Doolittle hydrophobicity plot for FMDV O Kaufbeuren VP4 generated using a sliding window of 19 (Kyte and Doolittle, 1982). Positions above 0 are hydrophobic and predicted transmembrane regions are identified by a score of greater than 1.6. Plot calculated using https://web.expasy.org/protscale/. (D) Transmembrane domain prediction calculated using TMHMM (Krogh et al., 2001). The plot shows the probability of each position to be found on the outside or inside of a membrane and the probability that a position is transmembrane. Plot calculated using http://www.cbs.dtu.dk/services/TMHMM/.

## 3.2 Both the N- and C-terminus of FMDV VP4 independently induce membrane permeability

Previous studies with HRV16 have shown that it is exclusively the N-terminus of HRV16 VP4 that is able to induce size-selective membrane permeability. These studies used liposomes as a model membrane system and investigated the membrane permeability induced by peptides representing both termini (Panjwani *et al*., 2016). FMDV has been shown to interact with membranes, inducing a size-selective membrane permeability similar to that observed in HRV (Gold *et al*, manuscript in preparation). As VP4 has been identified as the capsid protein responsible for membrane permeabilisation in several picornaviruses, it is likely this is the case for FMDV. However, it is not known for FMDV VP4 whether the N-terminus of VP4 is the membrane permeabilising region (as for HRV).

Peptides have been used to characterise the membrane permeability induced by viral proteins such as HRV VP4 and the γ-peptide of flock house virus (Bong *et al*., 1999, Panjwani *et al*., 2016). Following the recent work in HRV (which has shown that a peptide of the N-terminus of HRV VP4 induce membrane permeability consistent with the membrane permeability induced by full length recombinant VP4) a panel of synthetic peptides based on the O Kaufbeuren stain of FMDV were designed to study the interaction of FMDV VP4 with membranes. Each peptide contained six lysine residues to improve the solubility of the peptides and the N-terminal peptides were myristoylated at the N-terminus as the presence of the myristate group has been shown to be important in VP4 membrane interaction (shown on figure 3.2 B) (Panjwani *et al*., 2016).

Analysis of the sequence of FMDV VP4 indicates that the C-terminus contains several positions with a high hydrophobicity score (figure 3.2 C). However, the hydrophobicity scores in these positions does not reach the threshold of 1.6 that is used to predict a transmembrane region (figure 3.2 C). When the VP4 sequence is analysed for the presence of transmembrane regions there are no regions with a high probability for a transmembrane domain (figure 3.2 D). There is a small increase in probability at the C-terminus but this is has a probability of less than 0.1 (figure 3.2 D).

The membrane permeability induced by both the N- and C- terminus of FMDV VP4 was studied by mixing CF-containing liposomes with peptides representing the 45 amino acids at the N- and C-terminus of FMDV VP4 at room temperature and detecting the resulting fluorescence in real-time, indicating peptide-induced

membrane permeability.

Melittin is a well characterised pore forming peptide found in bee venom, which has been shown to form pores with a diameter of 7-8 nm (Park *et al*., 2006). Therefore, melittin was used as a positive control. Melittin was used at a lower concentration than the FMDV peptides as it gives very abrupt release at higher concentrations in the liposomes used here. This is consist with work by Park *et al* which shows that depending on the composition of the liposomes, melittin can induce near complete release of the fluorescent dye calcein at concentrations of about 1 μM. For the data presented here melittin was used at 0.1 μM to ensure it did not induce complete release of the fluorescent dye.

Both the N- and C-terminal 45 amino acid peptides (myrVP4N45 and VP4C45) induced the release of the fluorescent dye from the liposomes (figure 3.3). This release was not as abrupt as observed with the detergent triton, which was considered to induce complete dye release as triton has been shown to induce complete release of CF from small unilamellar vesicles (Sila *et al*., 1986). The dye release by both myrVP4N45 and VP4C45 followed similar kinetics to the well-characterised pore-forming peptide melittin, suggesting this membrane permeability could be due to the formation of a pore in the membrane (Vogel and Jähnig, 1986). Therefore both the N- and C-terminus of FMDV VP4 appeared to induce membrane permeability. These data are different from previous observations with HRV, suggesting FMDV VP4 may function in a subtly different way from HRV VP4.

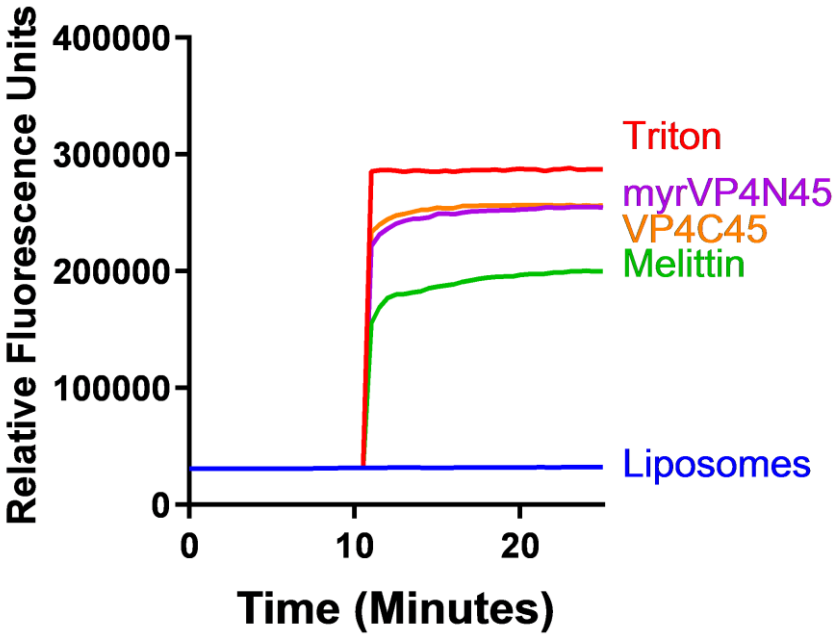


**Figure 3. 3: Both the N- and C-termini of FMDV VP4 induce membrane permeability.**

Liposomes containing carboxyfluorescein (CF) at self-quenching concentrations were mixed with Melittin at 0.1 µM, myristoylated VP4 N 45 at 0.5 µM, VP4 C 45 at 0.5 µM and triton. Membrane permeability resulting in leakage and dequenching of CF was detected by fluorescence measurements (excitation 492 nm/ emission 512 nm) recorded every 30 seconds. Data shown represents multiple experiments (n>3).

## 3.3 Membrane permeability induced by both the N- and C-terminus of FMDV VP4 is dependent on both the concentration and the length of the peptide

It is hypothesised that during virus entry, one of the VP4 termini would preferentially emerge from the virus particle and engage with the membrane, initiating pore formation. In HRV the N-terminus of VP4 has been shown to interact with membranes (Panjwani *et al*., 2016). However, the work carried out in section 3.2 has shown that both the N- and C- terminal 45 amino acids are able to induce membrane permeability in the case of FMDV VP4. It is not known how much of the termini of VP4 would need to be externalised in order to induce the membrane permeability and as such peptides were designed in increasing lengths from the N- and C-termini i.e. 15, 30 and 45 amino acids (figure 3.2). These peptides are intended to mimic the short sequences of the N- or C-terminus of VP4 that may be externalised from the virus during the entry process.

Alongside this, the membrane permeability induced by the peptides was compared at different concentrations. A concentration-dependent membrane permeability would suggest the peptides could be multimerising as this would require a concentration threshold to form the multimeric structures within the membrane.

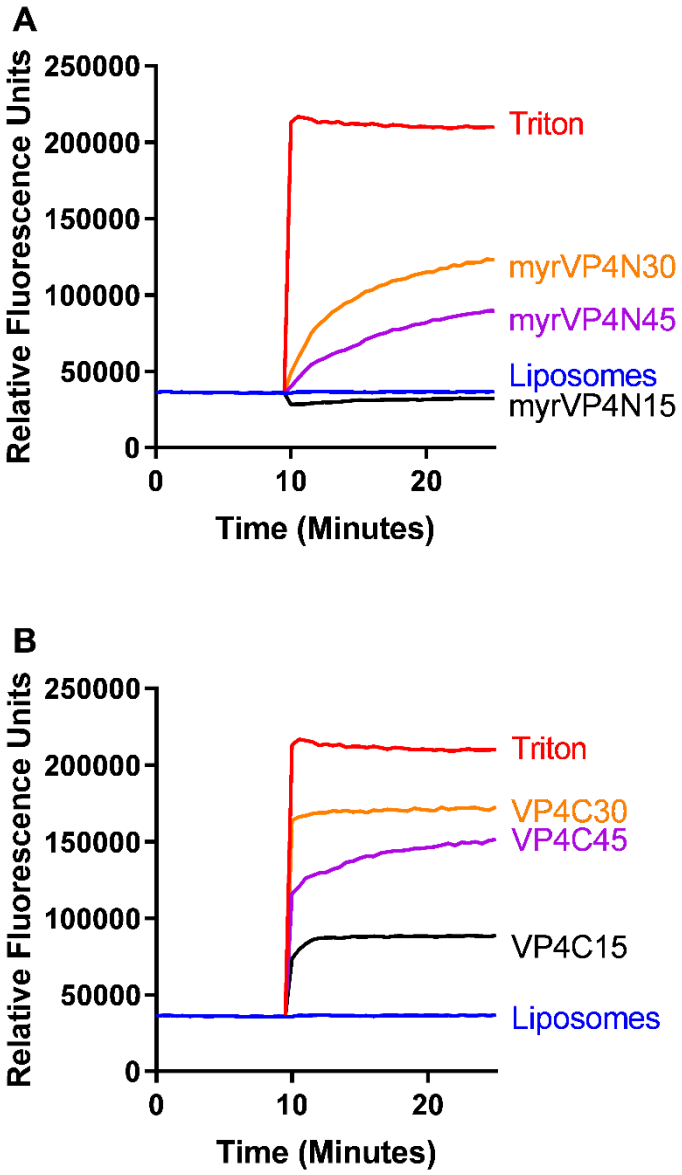


**Figure 3. 4: Membrane permeability induced by FMDV VP4 N- and C-terminal peptides varies with peptide length.**

Liposomes containing carboxyfluorescein (CF) at self-quenching concentrations were mixed with (A) myristoylated VP4 N or (B) VP4 C 45 peptides of lengths 45, 30 or 15 at 1 µM. Membrane permeability resulting in leakage and dequenching of CF was detected by fluorescence measurements (excitation 492 nm/ emission 512 nm) recorded every 30 seconds. Data shown represents multiple experiments (n>3).

Both the 30 and 45 amino acid VP4 N peptides (termed myrVP4N30 and myrVP4N45 respectively) were able to induce membrane permeability, whereas the 15 amino acid peptide myrVP4N45 was not. This could indicate that the N-terminal 15 amino acids is not where a pore-forming sequence is located in FDMV VP4, or that a peptide of greater length is required to induce pore formation. All of the lengths of the VP4 C peptides (termed VP4C15, VP4C30 and VP4C45) were able to induce release of the CF dye. The release of the CF by VP4C30 and VP4C45 was similar, but experiments with VP4C15 showed reduced membrane permeability (figure 3.5).

When peptides previously identified as able to induce membrane permeability were compared at different concentrations (1 μM, 0.5 μM and 0.1 μM) all three concentrations were able to release the CF dye to different degrees (fig. 3.6 A, B, C, D and F). Furthermore, as the concentration decreased the peptide induced less membrane permeability (figure 3.6 A-D and F). As expected following the results in figure 3.5, the VP4N15 peptide induced no membrane permeability at any of the concentrations tested (figure 3.6 E). These results indicated the dye release induced by most of the VP4 peptides is concentration dependent. This could indicate that all of the peptides that induce membrane permeability require a concentration of peptide above a threshold, possibly indicating the peptides are multimerising to induce the membrane permeability.

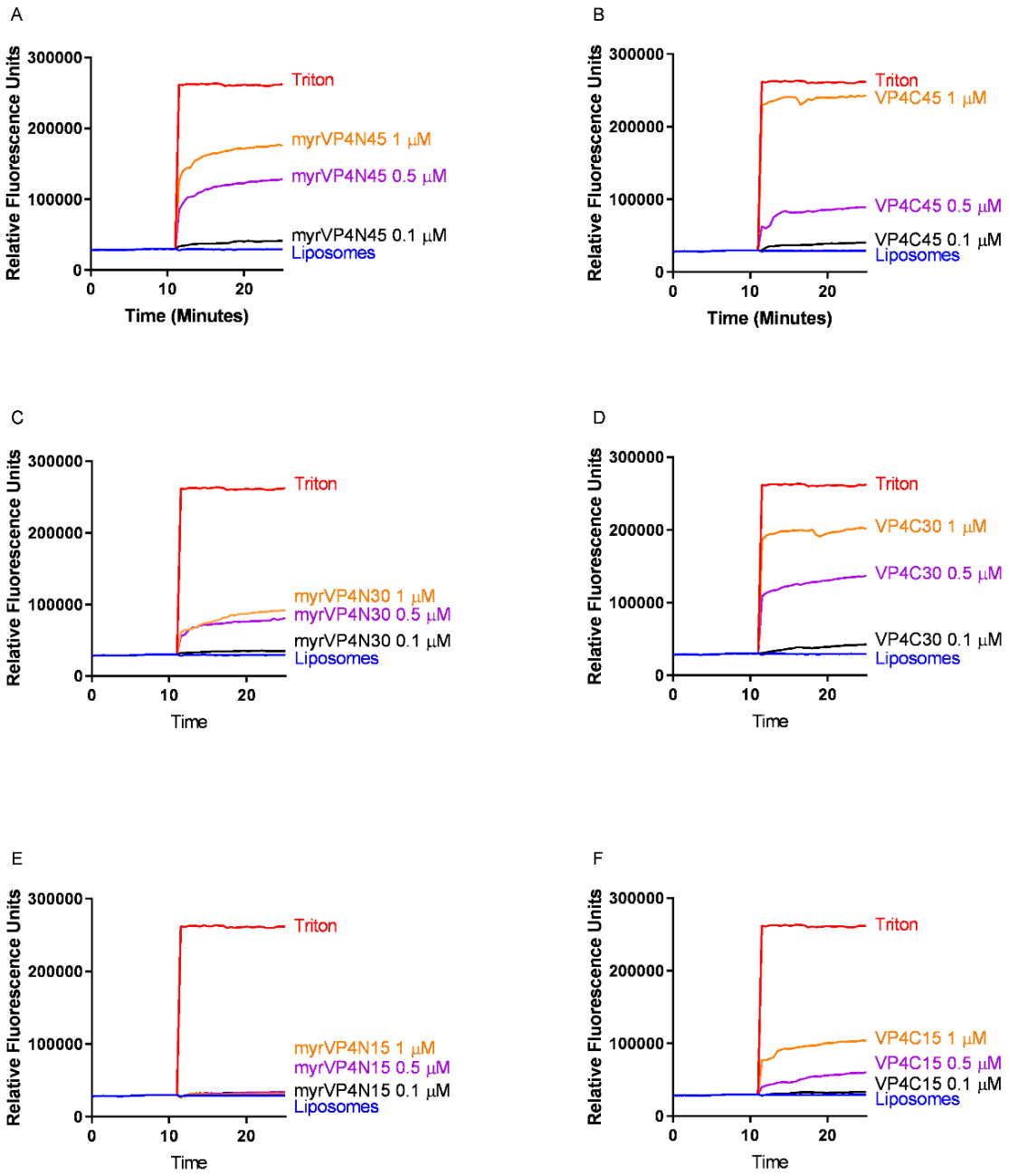


**Figure 3. 5: Membrane permeability induced by FMDV VP4 N- and C-terminal peptides is concentration dependent.**

Liposomes containing carboxyfluorescein (CF) at self-quenching concentrations were mixed with (A) myrVP4N45, (B) VP4C45, (C) myrVP4C30, (D) VP4C30, (E) myrVP4N15 and (F) VP4C15 at 1 µM, 0.5 µM and 0.1 µM. Membrane permeability resulting in leakage and dequenching of CF was detected by fluorescence measurements (excitation 492 nm/ emission 512 nm) recorded every 30 seconds. Data shown represents multiple experiments (n>3).

## 3.4 Membrane permeability induced by N- and C-terminal peptides is size selective

The membrane permeability induced by HRV VP4 has been shown to be size-selective and is consistent with a pore of sufficient size to allow movement of the unfolded RNA genome to the cytosol (Panjwani *et al*., 2014). To characterise the size-selective nature of the permeability induced by FMDV VP4, the N- and C-terminal peptides of 45 and 15 amino acids were used in a FD release assay to determine if either terminus would induce size selective membrane permeability. Comparing the 45 and 15 amino acid peptides could help to indicate if there is a minimum sequence required for pore formation or if it is a result of the hydrophobic sequence in this region disrupting the membrane. This may help to understand which terminus of FMDV VP4 is biologically relevant in pore-formation and allowing genome transfer.

The FD release assay uses liposomes containing fluorescein isothiocyanate (FITC)-linked dextrans (FDs) of known molecular weights. The FD-containing liposomes are then mixed with the membrane permeabilising peptide of choice and the release of FD from the liposomes is measured. As the FDs are of a known molecular weight and have a known diameter, it is possible to estimate the size of an opening in the membrane induced by the test peptide. The restricted movement of larger FDs indicates that there is an opening in the membrane that is of a diameter less than the diameter of the restricted FD. If the liposome was completely disrupted there would be no restriction of larger FDs. In the experiments described in this section the FDs used have dextrans of 4, 10, 70 and 250 kDa.

VP4 peptides were incubated with the FD containing liposomes for 1 hour to allow membrane permeability to occur. After incubation intact liposomes were collected by ultracentrifugation and the fluorescence in the supernatant was measured. The release from the liposomes was then normalised for any background fluorescence and displayed as a percentage of total release induced by triton.

Both 45 amino acid peptides (myrVP4N45 and VP4C45) exhibited size-selective FD release, allowing the movement of both the FD4 and FD10 but limiting the movement of FD70 and FD250 (fig. 3.7). There was a small increase in the FD70 release by VP4C45 compared to myrVP4N45 but this release was not as high as FD4 or FD10. There was no release of FDs by myrVP4N15 (fig. 3.7), which is expected as this did not induce CF release (fig 3.5). The VP4C15 peptide was able to induce size-selective membrane permeability (fig. 3.7). The extent of VP4C15-induced

permeability was lower than that induced by the VP4C45 peptide, which fits with the CF results as this peptide induced reduced levels of CF release. This could suggest the C-terminal 15 amino acids is a minimal sequence for C-terminal membrane permeability but as the longer peptide induces more FD release it could be that a longer peptide has enhanced permeability due to the additional sequences. Overall, the key unexpected result that both termini of FMDV VP4 were able to induce size-selective membrane permeability is further discussed in section 3.7.

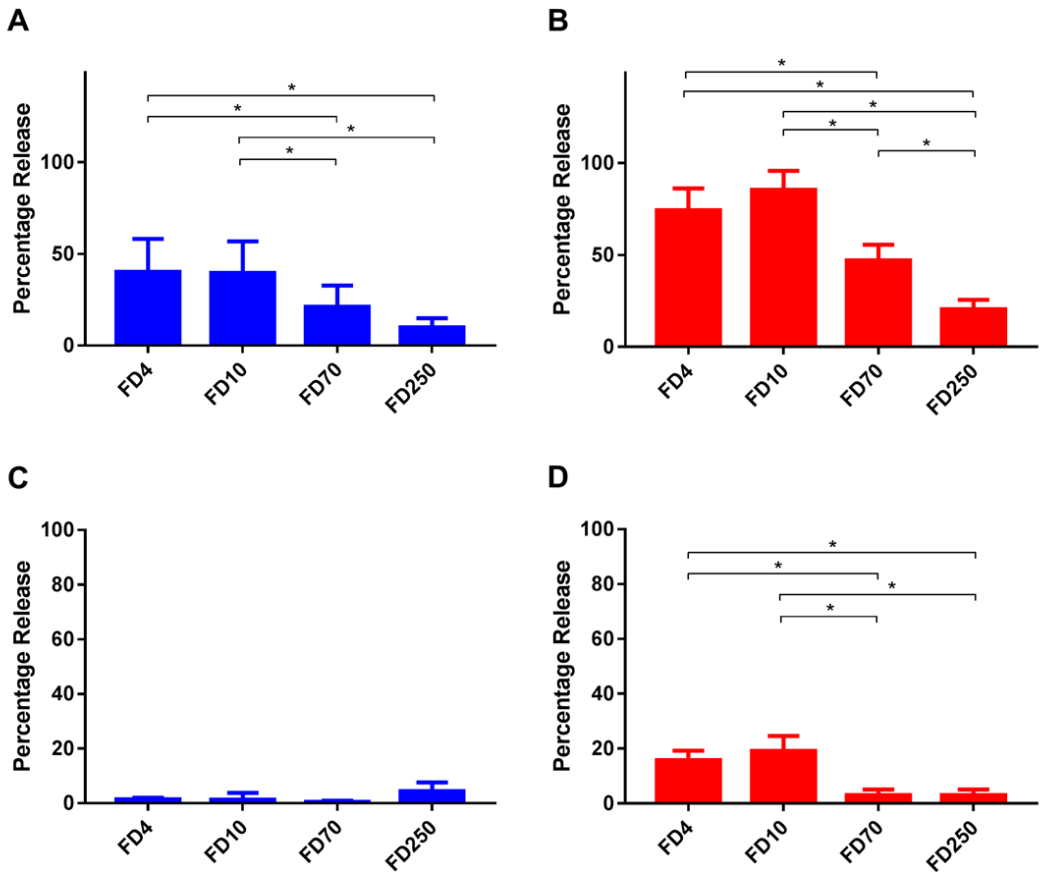


**Figure 3. 6: Membrane permeability induced by both 45 length peptides and VP4 C 15 is size-selective.**

Liposomes containing FITC-linked dextrans (FDs) were mixed with (A) myristoylated VP4 N 45, (B) VP4 C 45, (C) myristoylated VP4 N 15 or (D) VP4 C 15 at 1 µM. Membrane permeability results in leakage of the FDs and fluorescence was measured in the supernatant after pelleting the liposomes. Data is presented as percentage of total release when detergent is added to the liposomes. Data shown is the mean of multiple experiments (n>3) and error bars shown standard deviation. Asterisk indicates statistical significance by one-way ANOVA (* P<0.05).

## 3.5 Effect of myristoylation on the membrane permeability induced by the N-terminus of FMDV VP4

As detailed in the section 3.1 the addition of a myristic acid to an N-terminal glycine is associated with membrane proteins and it has been shown for HRV VP4 that the presence of the myristate group enhances the membrane permeability of the N-terminus of VP4 (Panjwani *et al*., 2016). As the N-terminus of FMDV VP4 is myristoylated, the studies shown above included myristoylated peptides representing the N-terminus of VP4. Here, the effect of myristoylation was explored to confirm whether myristoylation plays a similar role in enhancing membrane permeability in FMDV VP4. This was done by comparing the membrane permeability induced by the myristoylated VP4N45 peptide (figure 3.3) with that of an unmyristoylated VP4N45 peptide.

Dye release assays showed that the presence of the myristate group enhanced the membrane permeability induced by the N-terminal 45 amino acids of FMDV VP4 (fig 3.8).The unmyristoylated VP4N45 peptide was able to induce membrane permeability indicating the pore formation by the myristoylated peptide (termed myrVP4N45) was not solely due to the presence of the myristate group. These results show that the N-terminus of FMDV VP4 may be working in a similar way to previously published work with HRV VP4 (Panjwani *et al*., 2016).

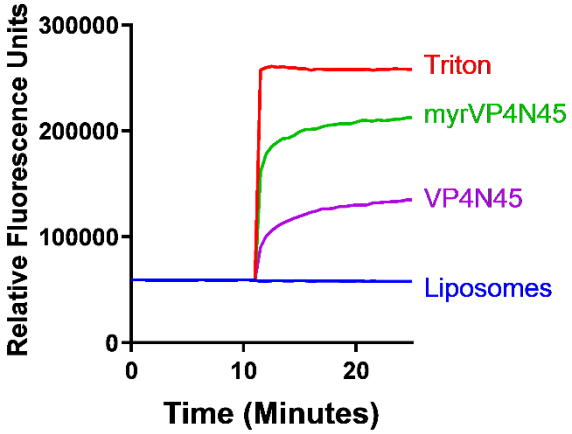


**Figure 3. 7: Membrane permeability induced by VP4N45 is enhanced by the presence of myristoylation.**

Liposomes containing carboxyfluorescein (CF) at self-quenching concentrations were mixed with myrVP4N45 or VP4N45 at 0.5 µM. Membrane permeability resulting in leakage and dequenching of CF was detected by fluorescence measurements (excitation 492 nm/ emission 512 nm) recorded every 30 seconds. Data shown represents multiple experiments (n>3).

## 3.6 Scrambled sequences do not induce membrane permeability

It is possible that the peptides for the N- and C-terminus of FMDV VP4 are able to induce membrane permeability due to the hydrophobic nature of these sequences as free peptide and not due to a specific interaction found in the full length FMDV VP4 sequence. To test this scrambled peptide sequences for the N- and C-terminal 45 amino acid peptides were generated using the shuffle protein software to generate random shuffled peptide sequences (software found at http://www.bioinformatics.org/sms2/shuffle_protein.html). The only amino acid that was kept the same was the N-terminal glycine to allow the generation of a myristoylated scrambled peptide. The scrambled peptides were then compared to the native VP4 peptides in membrane permeability assays.

When the scrambled peptides for the unmyristoylated N- terminus and C-terminus of FMDV VP4 (termed Scr VP4N45 and Scr VP4C45) were compared to the original VP4 peptides (VP4N45 and VP4C45 respectively) the membrane permeability was reduced to baseline levels (fig. 3.9). The myrVP4N45 scrambled peptide (Src myrVP4N45) induced a low level of membrane permeability, which was likely due to the presences of the myristate group as the unmyristoylated VP4N45 scrambled peptide has an identical sequence and does not induce any membrane permeability. This is likely to be due to the role in targeting proteins to membranes associated with myristoylation. Overall, the data shows that the membrane permeability induced by the N- and C-terminal 45 amino acids of FMDV VP4 was sequence specific and was not due to the hydrophobic amino acids present in the sequence.

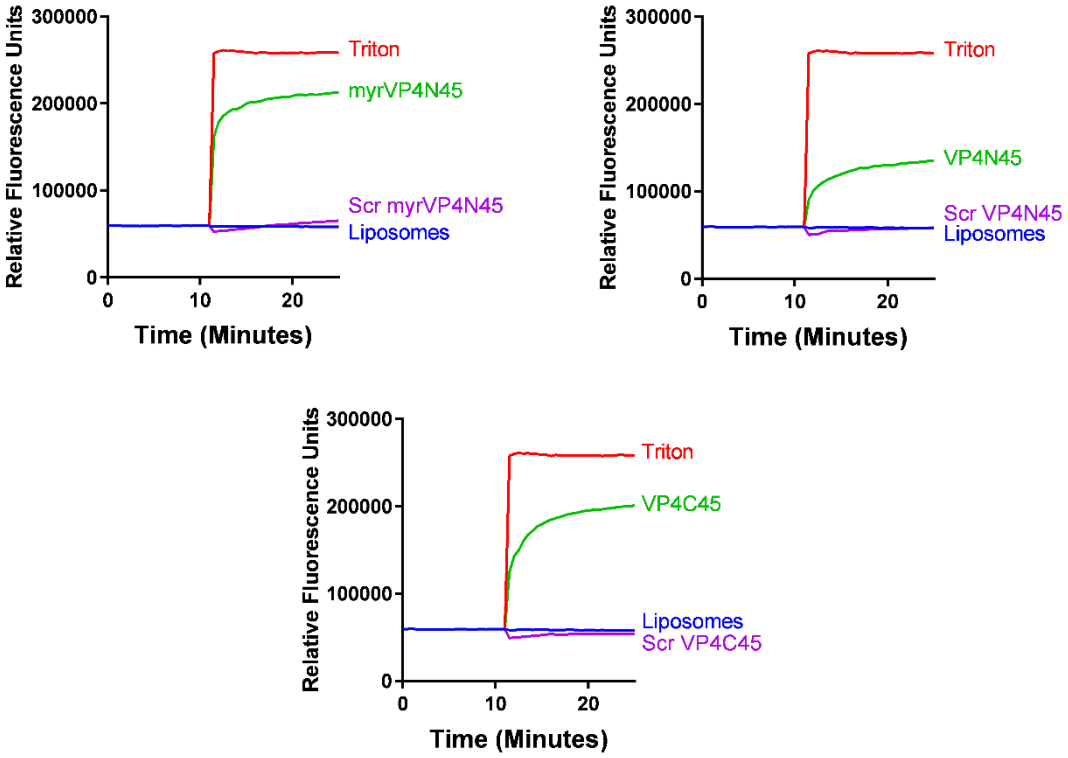


**Figure 3. 8: Membrane permeability induced by FMDV VP4 N- and C-terminal peptides is concentration dependent.**

Liposomes containing carboxyfluorescein (CF) at self-quenching concentrations were mixed with myrVP4N45, VP4N45, VP4C45 and the equivalent scrambled peptides at 0.5 µM. Original peptide is shown in green and the scrambled version is shown in purple. Membrane permeability resulting in leakage and dequenching of CF was detected by fluorescence measurements (excitation 492 nm/ emission 512 nm) recorded every 30 seconds. Data shown is representative for multiple experiments (n>3).

## 3.7 Discussion and future work

Previous studies using PV VP4 have shown that VP4 associates with membranes and plays a role in the movement of the genome from the endosome to the cytoplasm (Moscufo *et al*., 1993, Tuthill *et al*., 2006). Recently, recombinant VP4 has also been shown to form pores in model membrane systems (Davis *et al*., 2008, Panjwani *et al*., 2014, Shukla *et al*., 2014), suggesting this could be the mechanism of facilitation of genome movement by VP4. Most of the studies of VP4 have been carried out in enteroviruses so the mechanism of aphthovirus VP4 membrane permeabilisation is not understood. The work described here has shown that peptides encoding both the N- and C-terminus of FMDV VP4 are able to induce membrane permeability in model membranes and has started to examine which regions of the protein could be involved.

The induction of membrane permeability by both N- and C-terminal FMDV VP4 peptides shows that like other picornavirus VP4 proteins, FMDV VP4 is also able to induce membrane permeability. This suggests that FMDV VP4 is likely to play a similar role to VP4 in enteroviruses, facilitating the movement of the viral genome from the endosome to the cytoplasm. The induction of membrane permeability induced by both termini of FMDV VP4 was different from the result seen in HRV16 as only the N-terminus of HRV VP4 has been shown to induce membrane permeability, consistent with that of HRV and the full length recombinant protein (Panjwani *et al*., 2016). The difference in VP4 peptide induced membrane permeability induced by FMDV VP4 peptides compared to HRV VP4 peptides could indicate that there is a difference in the mechanism of membrane permeability, possibly with the C-terminus playing a role. FMDV VP4 is 16 amino acids longer than HRV VP4 and this additional length could be responsible for an alternative mechanism of membrane permeability and whether this plays a role in entry warrants further investigation.

Our hypothesis is that the membrane permeability induced by the N-terminus of FMDV VP4 is similar to that seen for the VP4 protein of other picornaviruses. The membrane permeability induced by the C-terminus may represent an additional step in virus entry and uncoating found exclusively in aphthoviruses. The aphthovirus ERAV dissociates at low pH via the formation of an intermediate particle (Tuthill *et al*., 2009). This is different from the conformational changes seen in the entry of enteroviruses such as PV, as enteroviruses produce an altered particle rather than fully dissociating. During PV entry the virus undergoes a conformational change induced by receptor binding. This results in the formation of an altered particle, known

as the 135S particle, before releasing the genome and forming the empty capsid known as the 80S particle (Tuthill *et al*., 2006). In FMDV it could be envisaged that the N-terminus membrane permeability is linked to the intermediate step and the formation of a pore linking FMDV to the membrane, allowing the transfer of the RNA genome from the intermediate particle into the cytoplasm, and the C-terminus permeability could be linked to the complete dissociation of FMDV under low pH conditions. This would allow FMDV to ensure controlled genome release into the host cell but may require this two-step process to ensure rapid release before or in conjunction with full dissociation. To shed further light on this, polyclonal serum against the N- or C-terminal 45 amino acids has been generated and the effect of these on virus-induced membrane permeability and virus infectivity are discussed in chapter 5.

In addition to VP4, other capsid proteins have been identified that may contribute to the process of membrane permeability and facilitate genome transfer. In the case of PV the N-terminus of VP1 has been identified as being externalised during the formation of the altered particle and the removal of this sequence prevents poliovirus 135S particles from interacting with liposomes (Fricks and Hogle, 1990). Mutations to the N-terminus of VP1 have been shown to reduce the rate of RNA release from the virus (Kirkegaard, 1990). This shows that the VP1 proteins of enteroviruses may play a role in the permeabilisation of endosomal membranes to allow genome transfer. The N-terminus of VP1 has been studied previously utilising the liposome system used here but it has been shown that the N-terminus of VP1 lacks the ability to induce membrane permeability (Panjwani *et al*., 2016). The lack of membrane permeability induced by HRV VP1, in spite of its requirement in poliovirus-liposome interactions, suggest it may play a role in maintaining or stabilising the pore formed in enteroviruses. The VP1 capsid protein in FMDV lacks the homologous N-terminal sequence which indicates FMDV may induce membrane permeability through a subtly different mechanism compared to the enteroviruses (Acharya *et al*., 1989). There is evidence from an intermediate structure of ERAV that the N-terminus of VP2 becomes disordered under low pH and this could be playing a similar role to PV VP1 during aphthovirus entry (Tuthill *et al*., 2009).

Using sets of peptides of 3 different lengths for both the N- and C-termini, it has been possible to start to dissect which regions of FMDV VP4 are able to induce membrane permeability. The length of peptide seems to be important for the N-terminal sequences as only peptides of 30 and 45 amino acids could induce membrane permeability, whereas all 3 of the C-terminal peptides could permeabilise

membranes, albeit at a lower efficiency in the shortest peptide. As the N-terminal 15 amino acids of FMDV are not sufficient to induce membrane permeability, a longer peptide is needed possibly due to the truncation of a membrane permeabilising region rendering it non-functional. Alternatively, if the N-terminal myristoylation is key to membrane interaction then removing amino acids 16 onwards may prevent the complete membrane function of VP4. The presence of a N-terminal myristate group does enhance the membrane permeability induced by the N-terminal 45 amino acids of FMDV VP4 so could play a role in FMDV VP4 membrane permeability during virus entry.

Bioinformatic analysis of the hydrophobicity of FMDV VP4 and prediction of transmembrane domains within FMDV VP4 did not highlight any potential transmembrane domains. The C-terminus was observed to have a high hydrophobicity score but there was low probability that this region would form a transmembrane domain. Based on the experimental data presented here, the prediction of the hydrophobic region at the C-terminus may explain the observed C-terminal membrane permeabilisation and could indicate this region is a transmembrane domain. Future work to investigate the structure of the C-terminus within a membrane through techniques such a molecular dynamic simulations would further explore this.

In contrast to the C-terminus the N-terminus lacked any predicted transmembrane domains and the hydrophobicity plot indicated no regions with a hydrophobic nature. This analysis contradicts the liposome membrane permeability data presented here, which demonstrates some of the N-terminus of FMDV VP4 is able to induce membrane permeability. The analysis software is based on the hydrophobicity of several characterised proteins and it is possible that the N-terminus of FMDV VP4 contains membrane penetrating sequences that are sufficiently diverse that any transmembrane regions are not recognised. Alternatively, it is possible that the membrane permeabilisation induced by the N-terminus of FMDV VP4 is caused by an unknown mechanism.

The membrane permeability induced by FMDV has been characterised in our group and other work in the laboratory has shown that FMDV is able to induce size-selective membrane permeability similar to that observed for HRV (Gold *et al*, manuscript in preparation). The membrane permeability induced was compared at decreasing pH and it was observed that as the pH lowered to pH 6.6-6.5 there was an increase in FMDV-induced CF release compared to neutral pH. The CF release

induced by FMDV at a pH below 6.4 was very rapid and at pH 6.2 was complete (Gold *et al*, manuscript in preparation). This could be related to capsid instability as the pH in the endosome reduces, resulting in complete VP4 release and therefore increasing membrane permeabilisation. It is interesting to consider that as the pH lowers there could be an increase in the exposure of the C-terminus of VP4, which has been shown to induce membrane permeability in this chapter, and this could have an additive effect to the total virus membrane permeabilisation induced.

Despite their short length, the FMDV VP4 peptides could be long enough to induce the formation of some kind of pore in membranes and therefore be biologically relevant in the context of FMDV entry. Structures of membrane proteins have been studied computationally and this has revealed the average length of a hydrophobic helix that spans the lipid bilayer is predicted to be 17.3 residues in length, which means that all peptides in this study would be sufficient to form a transmembrane helix (Hildebrand *et al*., 2004).

Alternatively the FMDV VP4 sequences could be interacting with the membrane through another mechanism such as the membrane permeability induced by antimicrobial peptides (AMPs). There are two main models predicted for pore formation by AMPs: the barrel-stave model and the toroidal pore model. AMPs that interact through the barrel-stave model insert multiple copies of the peptide into the membrane forming a pore, such as the pore formed by alamethicin, and illustrated in figure 3.9A (Baumann and Mueller, 1974, Qian *et al*., 2008). Melittin has been shown to form toroidal pores (Yang *et al*., 2001, Irudayam and Berkowitz, 2011). This type of pore is formed when the peptides insert and cause the lipid membrane to curve over and forms a pore lined with the peptide and the lipid head groups from the membrane and is illustrated in figure 3.9B. Toroidal pores have been identified as the mechanism of other viral proteins, such as the unrelated VP4 of the well-studied polyomavirus simian vacuolating virus 40 (SV40) so it may be possible FMDV VP4 is forming a similar pore (Raghava *et al*., 2013).

Membrane permeabilising proteins from a range of organisms have been studied to characterise their interactions with membranes. A common technique is to determine if membrane permeability observed is size-selective using FITC-linked dextrans (FDs). If smaller FDs are released significantly more than the larger FDs, this indicates the membrane permeability that is induced is controlled in some manner, as the movement of the larger FDs is restricted. The selective release of FDs cannot be due to the complete disruption of the membrane as that would result in equal

movement of all FDs so it is likely movement across the membrane is being controlled through the formation of a pore. This technique has been used to evaluate the size-selective membrane permeability of the VP4 proteins from HRV and HAV. For both of these it has been shown that the membrane permeability that was induced predominantly resulted in the release of the smallest FDs (up to 10 kDa) but larger FDs were restricted (FD 70 and FD 40 in HRV and HAV respectively) (Shukla *et al*., 2014, Panjwani *et al*., 2014). This indicates that these VP4 molecules can form a pore. In the case of HRV VP4 a pore formed of recombinant GST-tagged VP4 has been identified by TEM, showing the size-selective permeability associated with VP4 is indeed pore formation (Panjwani *et al*., 2014).

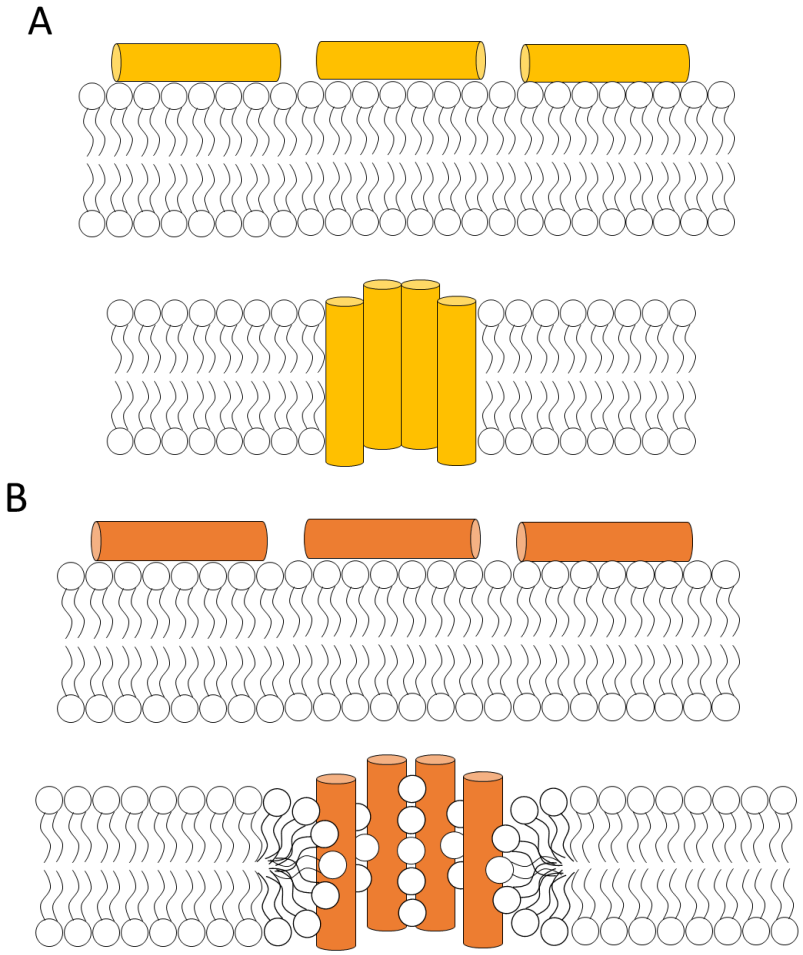


**Figure 3.9: Schematic showing the model of pore formation by antimicrobial peptides.**

Two models of pore formation by antimicrobial peptides. (A) Pore formation through the barrel-stave model results in the formation of a pore lined with the antimicrobial peptide as the hydrophobic peptides insert into the target membrane. (B) The model for toroidal pore formation differs as during peptide insertion into the membrane the lipid bilayer curve and the resulting pore is lined with both the antimicrobial peptide and the lipid head groups.

The N-terminus of FMDV VP4 induces size-selective membrane permeability, predominantly allowing the movement of small FDs (FD 4 and FD 10), which supports the model that the N-terminus of FMDV VP4 induces a pore that allows genome transfer. This result is similar to previous work with HRV which showed high levels of release of FD4 and FD10 but minimal release of FD70 (Panjwani *et al*., 2016). The smaller FDs have stokes radii of 14 Å and 23 Å whereas the restricted FD70 has a stokes radius of 60 Å. This would indicate a pore formed with a diameter greater than 4.6 nm but smaller than 12 nm. A pore of this diameter would be sufficient to allow the movement of single-stranded, unfolded viral RNA (1-1.5 nm in diameter) and agrees with previous work in HRV, supporting a conserved N-terminal role in membrane permeabilisation (Kienberger *et al*., 2004, Panjwani *et al*., 2014).

Both the C-terminal peptides used were able to induce size-selective membrane permeability but there are differences in which FDs are able to pass through. The 45 amino acid length C-terminal peptide allows more of the FD70 (stokes radius 60 Å) to move through the membrane than the N-terminal 45 amino acid length peptide but continues to restrict the FD250. Based on the stokes radii mentioned previously this could indicate this peptide makes a pore with a diameter of >12 nm. The small C-terminal 15 amino acid length peptide is able to induce size selective membrane permeability but this is restricted to FD4 and FD10 (stokes radius 14 Å and 23 Å respectively) indicating a pore with a diameter in the same range as the longer N-terminal peptide. The size-selective membrane permeability observed for the C-terminus of FMDV VP4 would be of an appropriate size to suggest it can also form a pore of a sufficient size to allow RNA movement.

Alternatively, the release of FD70 by the longer C-terminal peptide could indicate this peptide initially makes pores of a similar size to N-terminal peptide but punctures multiple pores in the liposomes which combine to form larger holes allowing movement of the larger FD. This could fit with the more abrupt CF release seen with this peptide. The release of only FD4 and FD10 by the shorter C-terminal peptide supports the hypothesis that the longer C-terminal peptide is overloading the membrane and inducing larger pores than it would in the context of entry as it could be the minimal sequence required for C-terminal membrane permeability. This could be explored further using native VP4 purified from virus as this might help make clear how VP4 would act when released from the FMDV particle following virus disassembly.

It is important to consider how the concentration of peptide used in these permeabilisation events compares to the concentration of VP4 that would be present when all 60 copies of VP4 are released from the FMDV virion. In the case of HRV16 it has been calculated this would result in a concentration of 14 μM in a 350 nm diameter endosome (Davis *et al*., 2008). Thus, the molar concentration for FMDV VP4 would be at a similar concentration. Therefore, the concentrations used in this work are biologically relevant and are similar to those used in other studies.

FMDV VP4 presents an interesting potential novel target for the control of FMDV. Currently our understanding of the role of VP4 in entry is limited to studies carried out in other branches of the picornavirus family, such as enteroviruses. Whilst it is likely there is a conserved mechanism by which VP4 proteins facilitate the movement of the picornavirus genome from the endosome to the cytosol the data presented here shows a difference between the FMDV and HRV16 VP4 proteins. This is the first study into the interaction between FMDV VP4 and membranes and could highlight an essential role for FMDV VP4 in virus entry.

# Chapter 4 Presentation of FMDV peptides on HBcAg VLPs

# 4. Presentation of FMDV peptides on HBcAg VLPs

## 4.1 Introduction

Antibodies against FMDV VP4 could be useful to understand the role of FMDV VP4 in membrane interactions and due to the high level of conservation across all 7 serotypes they have the potential to recognise multiple serotypes if they affect FMDV infectivity. Virus-like particles (VLPs) are excellent scaffolds for presenting a protein sequence of interest as they have a large regular structure which induces a strong immune response. The VLP chosen for this work was the highly immunogenic and well-characterised hepatitis B core (HBc) VLP. Several strategies for displaying antigens on the HBc VLP have been published including expressing a recombinant protein HBcAg containing the epitope of choice and strategies for attaching protein to the top of the spikes of the HBcAg to maintain the native confirmation of the antigen (Blokhina *et al*., 2013, Zhao *et al*., 2013).

This chapter introduces the approaches taken to display small sequences from FMDV VP4 on the HBc VLPs. These VLPs were generated by mutating an existing HBc expression construct and purifying the recombinant VLPs. An alternative strategy involved decoration of a purified native HBc VLP with short VP4 peptides. These VLPs were then used to immunise mice (detailed in chapter 5).

Previous work on human rhinovirus (HRV) has shown that antibodies against the N-terminal 15 amino acids of VP4 were able to interfere with the membrane interactions of HRV and also reduced the infectivity of HRV (Panjwani *et al*., 2016). It is currently unknown if antibodies against a similar region of FMDV VP4 would have similar properties. As it is not confirmed which of the termini of FMDV VP4 are exposed during the process of virus breathing (detailed in section 1.6.3), initially both the N- and C-terminal 15 amino acids of FMDV VP4 were cloned into the VLP.

Producing recombinant HBc VLPs displaying an epitope of choice can be achieved through cloning the sequence of the antigen into one of three locations on the HBc VLP. The possible insertion sites are at either terminus or in the major immunodominant region (MIR). The most common insertion site is the MIR at the top of the spike of the HBcAg protein and this is tolerant of the largest insertions (figure 4.1). The HBc VLP forms two types of capsids, containing either 240 or 180

copies of the HBcAg protein which form capsids of either 34 nm or 30 nm in diameter and have triangulation numbers of T=4 and T=3 respectively (Pumpens and Grens, 2001).

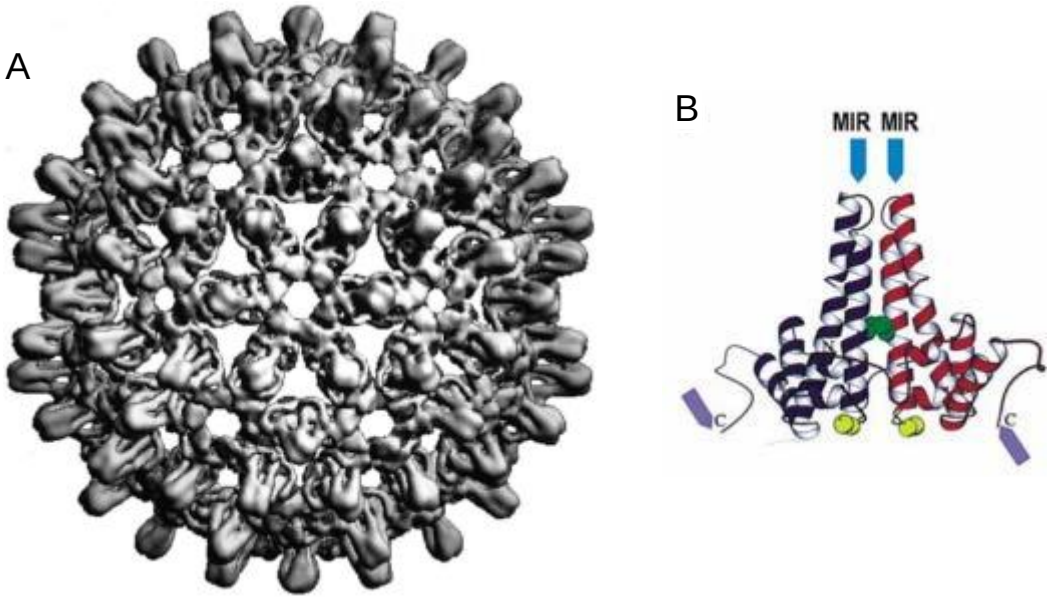


**Figure 4. 1: Structure of the HBc VLP and dimer subunit of the VLP.**

(A) Three-dimensional structure of the HBc VLP showing the protruding spike structures. Each of the spikes is formed from a dimer subunit. (B) Structure of the dimer subunits which form the VLP. The major immunodominant region (MIR) is highlighted on the dimer and this would be located at the tip of the spike. Figure adapted from (Pumpens and Grens, 1999) and (Pumpens and Grens, 2001).

Previous work has shown that the sequence of the 238 amino acid GFP has been successfully inserted into the VLP at the MIR (Kratz *et al*., 1999). Several pathogen antigens have been displayed on the HBc including the FMDV VP1 protein and a region of the circumsporozoite protein from *Plasmodium falciparum*, a causative agent of malaria (Chambers *et al*., 1996, Gregson *et al*., 2008).

An alternative approach is to attach peptides to the top of the spike region and there are two approaches to this previously described in the literature. Firstly, peptides can be attached at random by chemical cross-linking. This has been described as a successful approach for presenting peptides but it is not possible to predict the orientation of the peptides on the VLP (Jegerlehner *et al*., 2002). Secondly, it is possible to utilise an interaction between the HBcAg proteins and a short peptide

sequence (Bottcher *et al*., 1998). This interaction relies on opposing charges between the peptide and the top of the spike and this protein-protein interaction holds the peptide antigen onto the VLP. Previous work has shown that this sequence can be used as a specific HBc tag can attach peptides containing this spike tag onto the MIR of the HBc VLP. This has successfully allowed the display of an influenza A M2e peptide on the HBc VLP and induce a neutralising immune response (Blokhina *et al*., 2013).

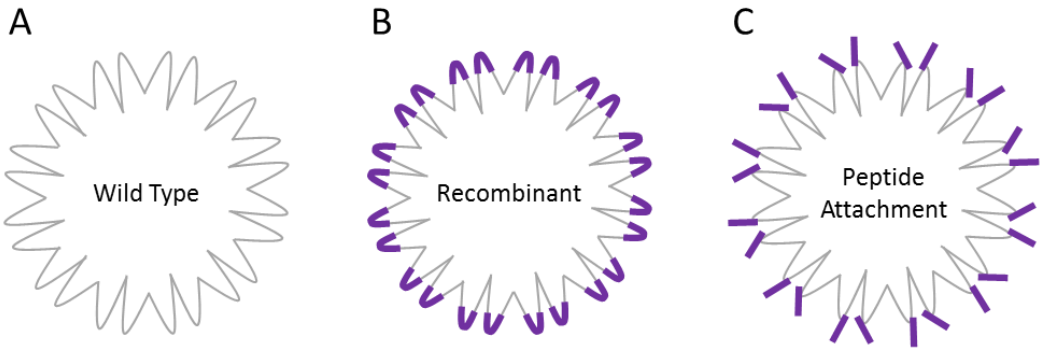


**Figure 4. 2**: **Schematic showing the antigen presentation approaches used with the hepatitis B core.**

The native core (A) will have the N-terminal 15 amino acids of FMDV VP4 inserted, allowing this sequence to be presented on the major immunodominant region (B). Alternatively, tagged peptides will be used to attach the VP4N15 peptides to the native core (C).

Based on the different approaches to display antigens on the HBc VLP, a recombinant VLP with a FMDV VP4 sequence displayed in the MIR (termed HBcN15) and a VLP decorated with a FMDV VP4 peptide attached by the specific peptide sequence (termed HBc PepN15) were constructed (schematic of approaches is shown in figure 4.2). As previous evidence has suggested that the N-terminal 15 amino acids of HRV VP4 and the N-terminal 20 amino acids of EV71 are able to elicit neutralising immune responses it was decided to start with generating recombinant VLPs displaying the N- and C-terminal 15 amino acids of FMDV VP4. The short terminal sequences from both the N- and C-termini were chosen as it is likely one of the termini would be exposed during the process of virus breathing (described in section 1.6.3). Therefore, these amino acids were deemed as good targets for antibody recognition of virus.

## 4.2 Expression and purification of recombinant HBc VLPs

### 4.2.1 Cloning of recombinant HBc VLPs displaying the N- and C- terminal 15 amino acids of FMDV VP4

As previous work has shown that a recombinant HBc VLP displaying the N-terminal 20 amino acids of EVA71 VP4 successfully induces a protective cross-serotypic antibody response a similar approach was used for displaying the N- and C-terminal 15 amino acids of FMDV VP4. A plasmid encoding the full length HBcAg in the pET28b backbone (CoHBc190) was kindly provided by the Dr Sam Stephen, University of Leeds. This construct encodes the full length protein with restriction sites flanking the MIR in a region called the FAGAS region, allowing easy insertion of sequences of interest into the MIR, and has the C61A mutation which prevents disulphide bonds forming between the dimers.

The nucleotide sequences encoding FMDV VP4 N- or C-terminal 15 amino acids flanked by *EcoR*I and *Nhe*I sites were designed and ordered as GeneArt gene synthesis plasmids (see table 4.1). Once received the GeneArt plasmids were digested with *EcoR*I and *Nhe*I restriction enzymes and the released bands were identified by agarose gel electrophoresis and purified from the gel. The CoHBc190 backbone was also digested with *EcoR*I and *Nhe*I and the backbone separated on an agarose gel and purified. The VP4 insert was then ligated into the CoHBc190 backbone. The ligated plasmid was transformed into XL-10 gold *E. coli*. Colonies were picked, grown overnight in LB media and plasmid DNA purified by miniprep. Successful clones were identified by diagnostic restriction digest (shown in figure 4.4) and Sanger sequencing. The sequencing showed the nucleotide sequence of the plasmid was as intended. The diagnostic digest using *EcoR*I and *Eag*I sites (indicated on fig 4.3) showed inserts of the correct size (fig 4.3). This confirmed that expression plasmids termed CoHBc190 FMDV VP4N15 and CoHBc190 FMDV VP4C15 were correctly constructed.

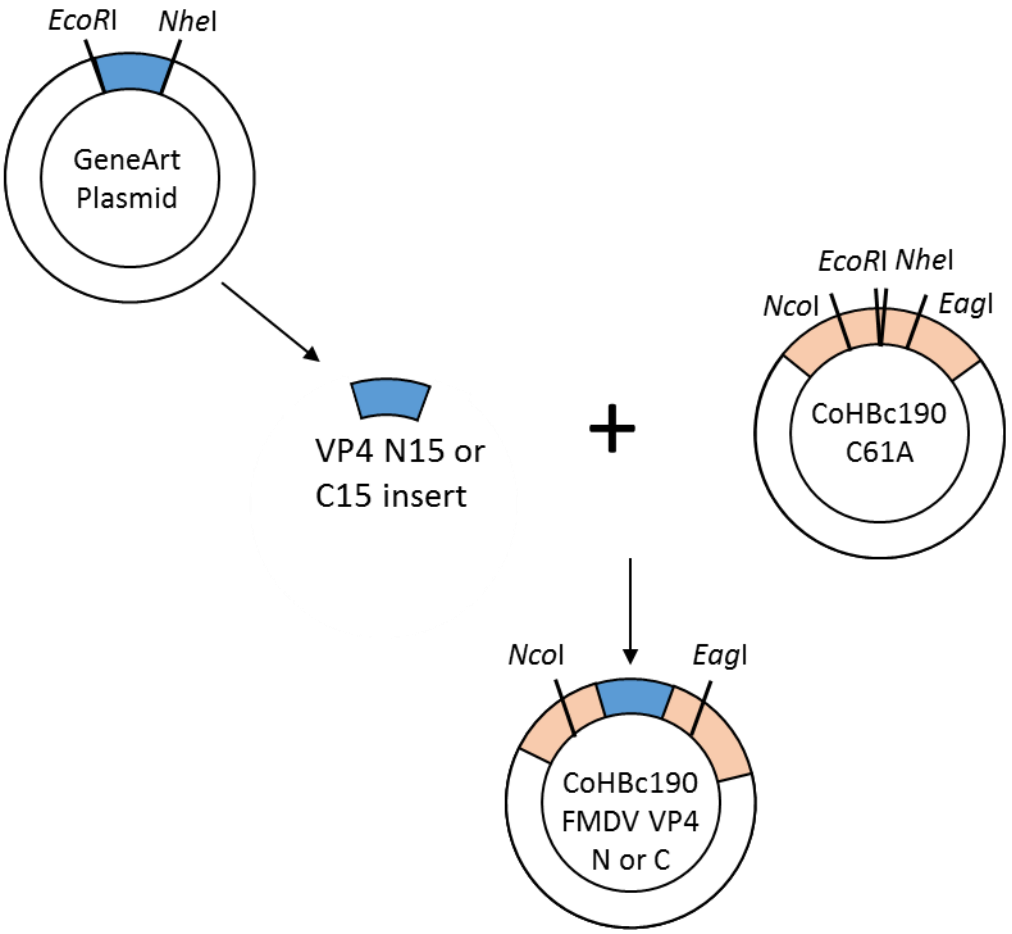


**Figure 4. 3: Schematic of cloning strategy using the GeneArt gene synthesis plasmids.**

GeneArt gene synthesis plasmids were designed to contain the 15 N- and C-terminal amino acids of FMDV VP4. These were then flanked by *EcoR*I and *Nhe*I restriction sites. This allowed easy insertion into the FAGAS region of the CoHBc190 plasmid. *Nco*I and *Eag*I sites used for diagnostic digests shown.

| Construct name | Sequence | Layout | Information |
|---|---|---|---|
| FMDV VP4N15 | ATATCGACCCATATAAAGAATTTGGCGCGACGGTTGA GCTGCTGAGCTTTCTGCCAAGCGATTTCTTTCCGAGC GTCCGCGACCTGCTGGATAAATCTGGAATTCGGGGC TGGACAATCCAGTCCAGCGACCGGCTCGCAGAACCA ATCTGCTAGCCTCGAGATATCGACCCATATAAAGAAT TTGGCGCGACGGTTGAGCTGCTGAGCTTTCTGCCAA GCGATTTCTTTCCGAGCGTCCGCGACCTGCTGGATA | Spacer, *EcoR*I, FMDV VP4N15, *Nhe*I, Spacer | GeneArt gene synthesis to insert the FMDV VP4N15 sequence into the MIR of the HBc. (4.2.1) |
| FMDV VP4C15 | ATATCGACCCATATAAAGAATTTGGCGCGACGGTTGA GCTGCTGAGCTTTCTGCCAAGCGATTTCTTTCCGAGC GTCCGCGACCTGCTGGATAAATCTGGAATTCCTTGCC AGCTCTGCTTTCAGCGGTCTTTTCGGCGCTCTTCTCG CCGCTAGCCTCGAGATATCGACCCATATAAAGAATTT GGCGCGACGGTTGAGCTGCTGAGCTTTCTGCCAAGC GATTTCTTTCCGAGCGTCCGCGACCTGCTGGATA | Spacer, *EcoR*I, FMDV VP4C15, *Nhe*I, Spacer | GeneArt gene synthesis to insert the FMDV VP4C15 sequence into the MIR of the HBc. (4.2.1) |
| Native HBc | GTATACCCCA***ATG***GATATCGACCCATATAAAGAATTTG GCGCGACGGTTGAGCTGCTGAGCTTTCTGCCAAGCG ATTTCTTTCCGAGCGTCCGCGACCTGCTGGATACCG CCAGCGCACTGTATCGTGAAGCCCTGGAGAGCCCGG AACATTGCAGCCCGCATCATACGGCCCTGCGTCAGG CAATCCTGTGCTGGGGCGAACTGATGACCCTGGCAA CCTGGGTCGGCAATAATCTGGAAGACCCAGCAAGCC GTGATCTGGTTGTTAATTACGTGAACACCAACATGGG CCTGAAGATCCGCCAACTGCTGTGGTTTCATATCAGC TGTCTGACGTTTGGCCGCGAGACGGTGCTGGAATAC CTGGTTAGCTTTGGCGTTTGGATTCGTACGCCACCG GCCTACCGCCCACCAAACGCACCGATTCTGAGCACG CTGCCGGAAACGACGGTTGTTCGTCGCCGTGATCGC GGCCGTAGCCCA | Spacer, *Nco*I, ***ATG start*** (within *Nco*I site), HBc Protein (including C61), *Eag*I, Spacer | GeneArt DNA string to replace the mutated region of the HBc with the native HBcAg sequence. (4.3.1) |

**Table 4. 1: Sequences of inserts in GeneArt gene synthesis plasmids or ordered GeneArt strings.**

The coding sequence is shown in blue and restriction sites are shown underlined. The start codon in the Native HBc is highlighted in bold.

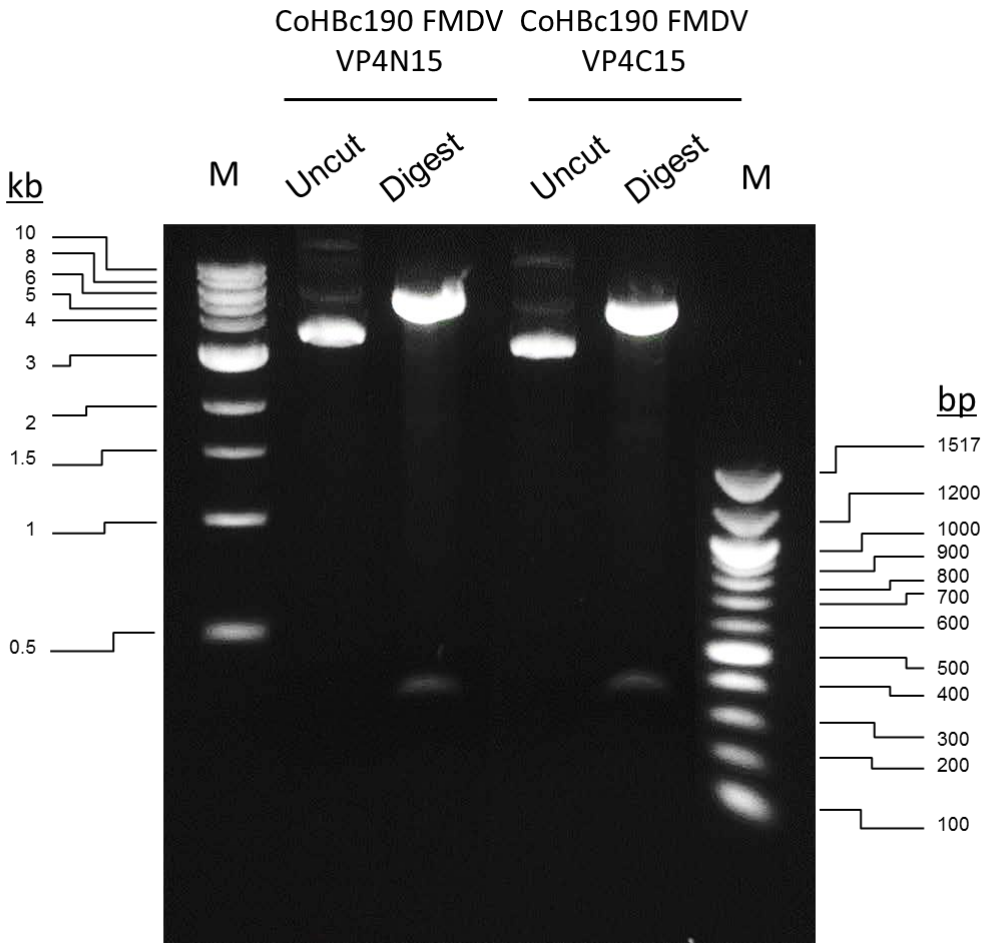


**Figure 4. 4: Both CoHBc190 FMDV VP4N15 and CoHBc190 FMDV VP4C15 were confirmed by diagnostic digest.**

CoHBc190 FMDV VP4N15 and CoHBc190 FMDV VP4C15 were digested with *EcoRI* and *EagI* to release an insert of approximately 500 bp. The uncut vector for CoHBc190 FMDV VP4N15 and CoHBc190 FMDV VP4C15 were analysed alongside the digests on a 1 % agarose gel. A 1 kb ladder is shown to the left and a 100 bp ladder is shown to the right.

## 4.2.2 Expression of recombinant HBc VLPs displaying the N- and C-terminal 15 amino acids of FMDV VP4

Once the CoHBc190 FMDV VP4N15 and CoHBc190 FMDV VP4C15 plasmids were produced and validated, expression trials with these plasmids were carried out. The method for this is described in section 2.7.

The plasmids were transformed into BL21 DE3 bacteria and single colonies were picked for each construct. The starting colony was grown overnight in LB media and then inoculated into a larger volume expression culture. This culture was grown until

an OD600 reading of as close as possible to 0.8 was obtained. At this point expression was initiated by the addition of IPTG, an analogue of lactose, which drives expression as this is controlled by the *LacZ* operon. After 3 hours of growth, the OD of the culture was recorded and the bacteria were pelleted. Before induction of expression a sample of the bacterial culture was removed to allow comparison of the levels of expression before and after induction with IPTG. The before and after induction samples were lysed by sonication and the presence of the HBcAg proteins was established by Coomassie-stained SDS-PAGE.

On induction of expression in the CoHBc190 transformed culture, there was an increase in signal intensity for a band of protein of approximately 21.8 kDa, the expected size of the HBc monomer, consistent with expression of this protein (figure 4.5).

On induction of expression in the CoHBc190 VP4N15 transformed culture, there was a similar increase for a band of approximately 23 kDa, the expected size of the HBc monomer engineered to contain the 15 amino acids from FMDV VP4 (figure 4.5).

In both cases when this material was sonicated and separated into soluble and insoluble fractions, the expressed protein was predominantly found to be in the former, with only a small amount in the insoluble fraction (figure 4.5).

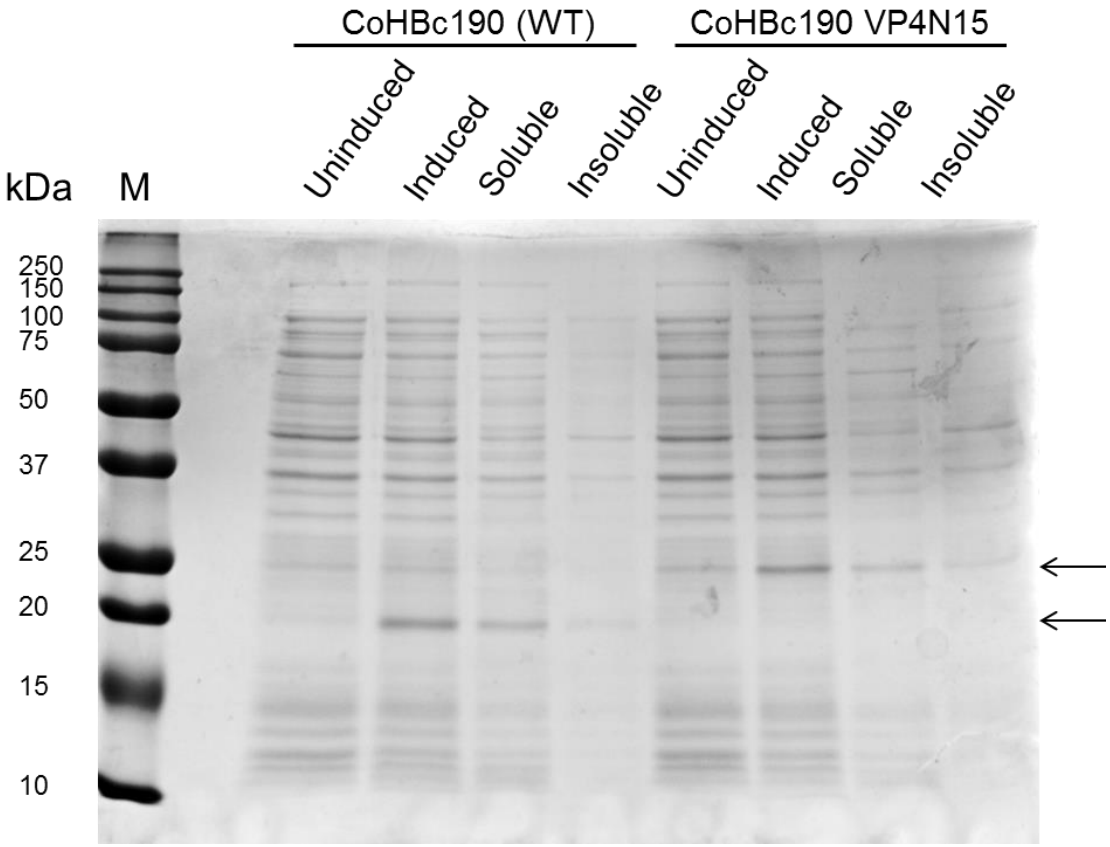


**Figure 4. 5: Soluble CoHBc190 (WT) and CoHBc190 FMDV VP4N15 were expressed in *E.coli.***

The expression of CoHBc190 (WT) and CoHBc190 FMDV VP4N15 was confirmed using Coomassie stained SDS-PAGE. Lanes show uninduced bacteria, induced bacteria and the soluble and insoluble fractions after lysis of the bacteria. Arrows to the right indicate the expected sizes of CoHBc190 and CoHBc190 FMDV VP4N15 (expected molecular weights 21 kDa and 23 kDa respectively). Molecular weight marker (M) shown to the left.

Expression of the CoHBc190 FMDV VP4C15 resulted in a band of a molecular weight approximately 21 kDa (indicated in figure 4.6 A by the black arrow) which was much lower than expected. There is no difference in the number of charged amino acids between the two. The predicted molecular weight was around 23 kDa and is indicated by the green arrow on figure 4.6. Furthermore, expressed protein was found to be insoluble (figure 4.6 A). After repeating the cloning of this construct, the expression was repeated and the same result was observed. The expressed insoluble protein was then confirmed to be the HBcAg protein by western blot (figure 4.6 B). The expression was repeated at a lower temperature to encourage correct folding of the expressed protein but this had no effect on the solubility of the protein. The insoluble protein expressed from the CoHBc190

FMDV VP4C15 was unexpected as this was a small insertion and will be discussed further in section 4.5.

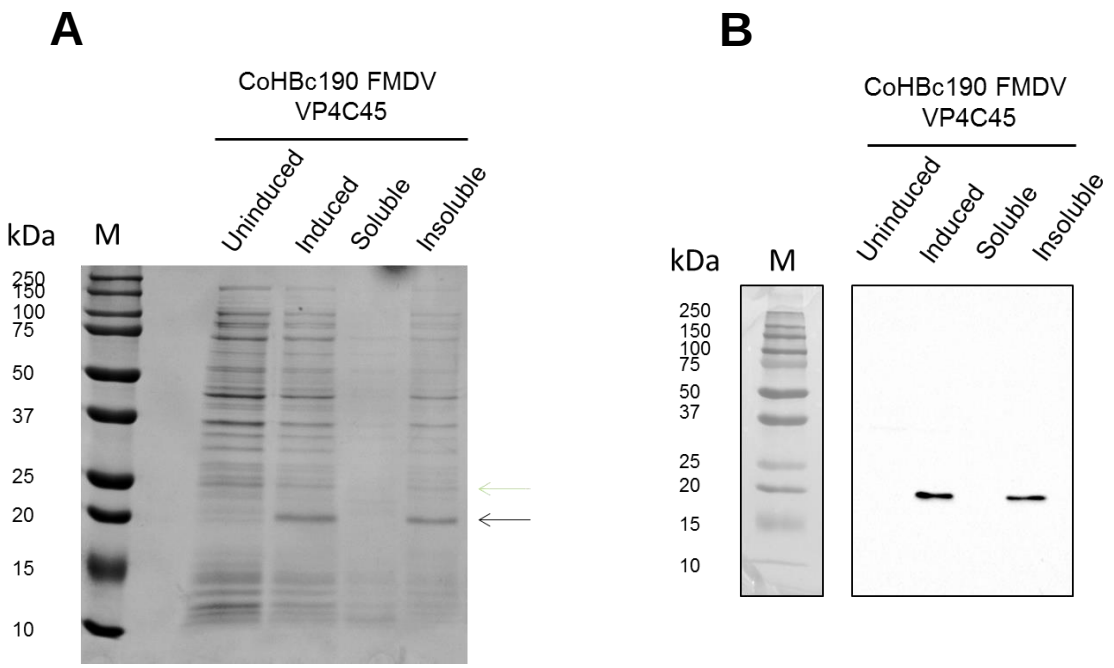


**Figure 4. 6: CoHBc190 FMDV VP4C15 is an insoluble protein of the incorrect molecular weight.**

The expression of CoHBc190 FMDV VP4C15 was studied using (A) Coomassie stained SDS-PAGE and (B) Western blot using the 10E11 monoclonal antibody which recognises the N-terminus of the HBcAg protein. Lane 1-4 bacteria expressing CoHBc190 FMDV VP4C15. Lane 1: Uninduced; Lane 2: Induced; Lane 3: Soluble protein from lysed bacteria; Lane 4: Insoluble protein from lysed bacteria. The black arrow indicates the protein that has been expressed when expression is induced by IPTG and the orange arrow indicated the expected molecular weight of the HBcAg with FMDV VP4C15 present. Molecular weight markers in kilodaltons are shown to the left.

### 4.2.3 Purification of recombinant HBc VLPs displaying the N-15 amino acids of FMDV

Having shown that no soluble protein was made with the CoHBc190 FMDV VP4C15 construct the work was carried forward with the protein expressed from the CoHBc190 FMDV VP4N15 plasmid. As this should spontaneously form VLPs, sucrose gradients were used to purify the VLPs and they were identified by western blot and visualised by EM.

Protein was precipitated from the soluble fraction of the bacterial lysate using ammonium sulphate and pelleted by centrifugation. The pellet was then resuspended, clarified and layered onto a 20-60 % sucrose gradient. The gradient was subjected to ultracentrifugation and fractionated from the top of the gradient down. Peak fractions for protein were identified by measuring the absorbance 280. The presence of the expressed protein in the peak fractions was confirmed by coomassie stained SDS-PAGE (figure 4.7). After the initial gradient several contaminant proteins remained present in the peak fractions so the peak fractions were pooled, desalted and layered onto a second gradient. The peak fractions were once again confirmed by measuring the absorbance 280 and the purity of these assessed by SDS-PAGE. After the second purification, the products were buffer exchanged into PBS.

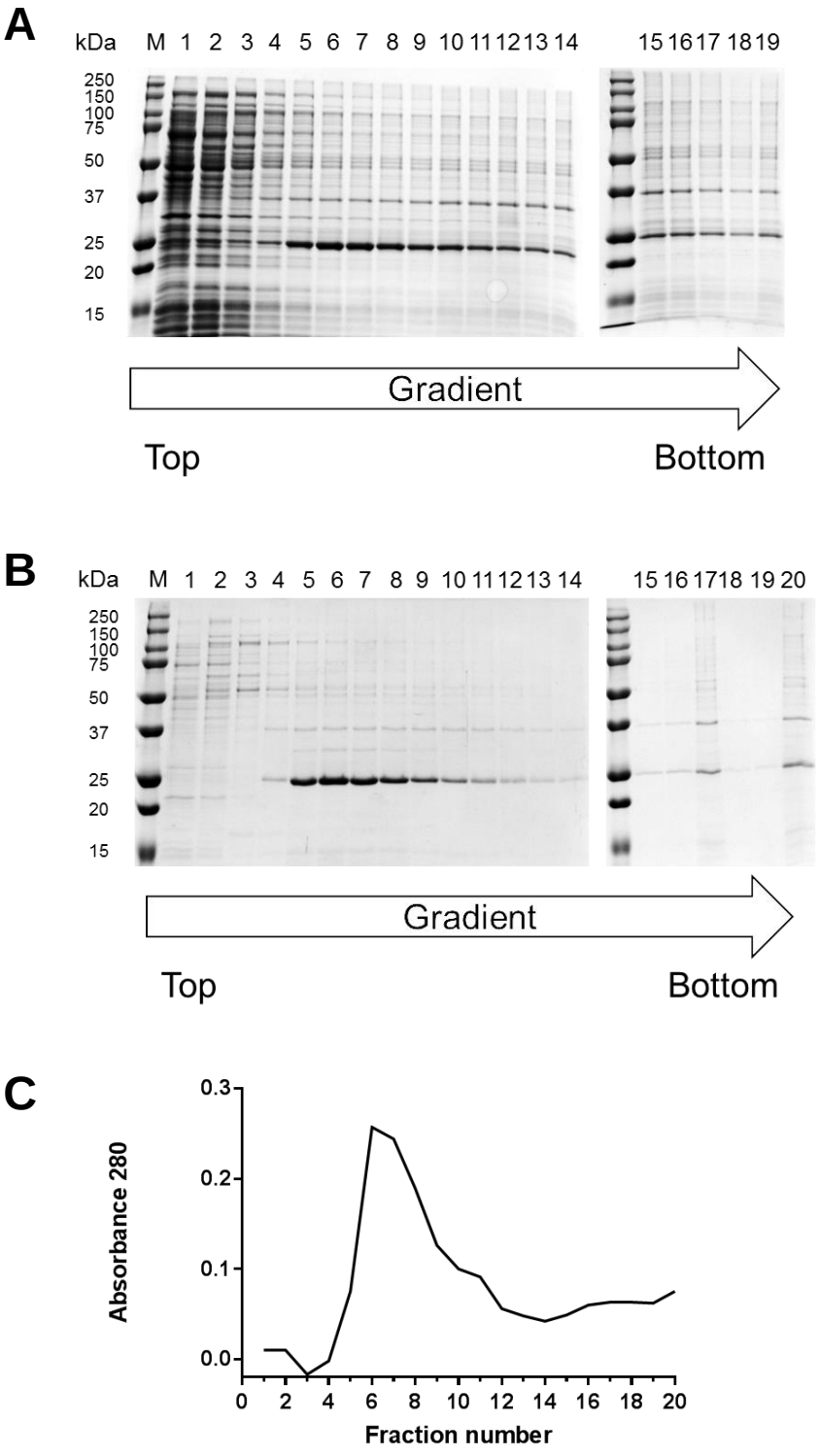


**Figure 4. 7: Expressed recombinant HBcAg protein can be purified by sucrose gradient and sediments as expected for HBc VLPs.**

Soluble protein precipitated from expression bacterial lysates were layered onto a 20-60 % sucrose gradient. (A) Fractions were analysed by coomassie stained SDS-PAGE. Peak fractions were pooled, desalted and layered onto a second gradient. Fractions from the second gradient were then analysed by Coomassie stained (B) SDS-PAGE and (C) measuring the absorbance at 280. Arrows indicate orientation of the gradient.

The peak fractions of both the CoHBc190 VLPs and the HBcN15 VLPs were confirmed by western blot for the HBcAg protein (figure 4.8C). Following this the VLPs were visualised by negative stain TEM to ensure the insertion of the VP4N15 sequence had not altered the structure. The TEM images in figure 4.8 A&B show no difference between the WT VLPs and the VP4N15 particles. This shows that HBc VLPs displaying the N-terminal 15 amino acids of FMDV VP4 were successfully generated.

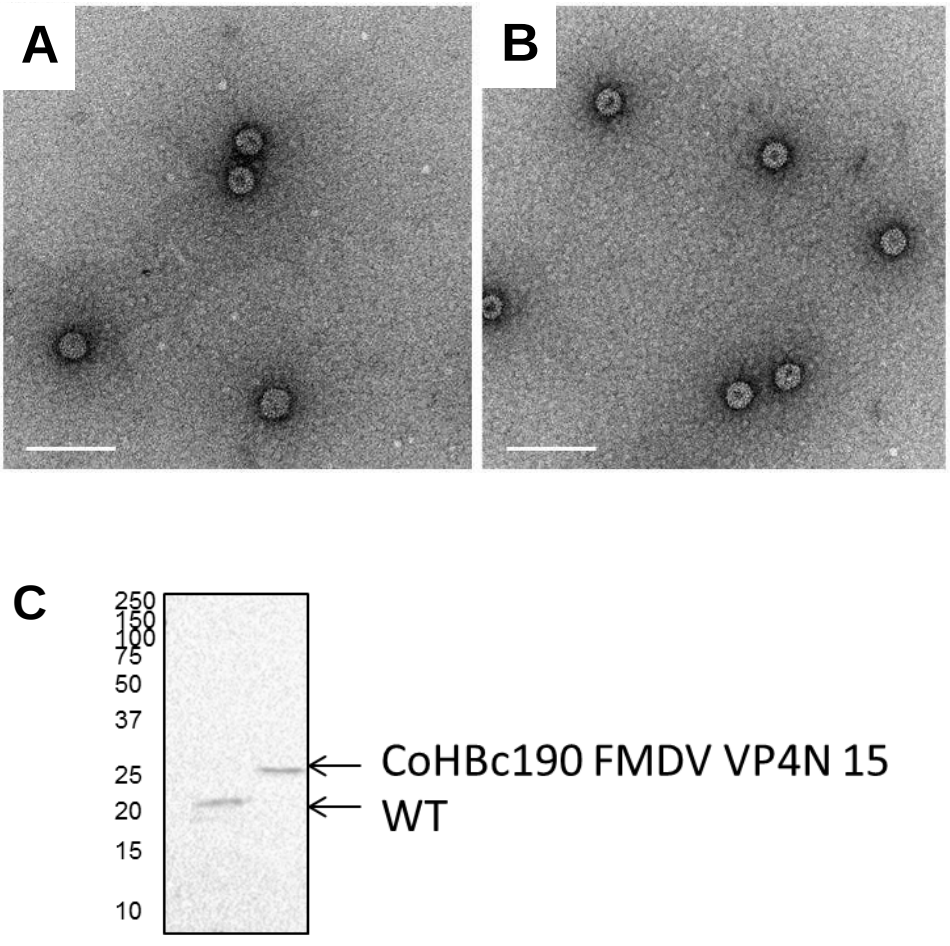


**Figure 4. 8**: **Expressed and purified recombinant hepatitis B core protein forms virus-like particles.**

Samples of expressed (A) CoHBc190 (WT) and (B) HBcN15 were given to Dr Pippa Hawes (The Pirbright Institute) and she kindly prepared the samples by negative staining and visualised them by TEM. The scale bar denotes 100 nm. These were also confirmed by western blot using the 10E11 monoclonal antibody that recognises the N-terminus of the hepatitis B core protein (C). Molecular weight in kilodaltons indicated to the left.

## 4.3 Production of native HBc VLP

### 4.3.1 Cloning of native HBc VLPs

As introduced in section 4.2.1, the CoHBc190 plasmid encodes the full length HBcAg protein with mutations in the MIR allowing easy insertion of antigens of interest. According to work by Bottcher *et al*, this mutated region coincides with the charged amino acids in the native HBcAg sequence involved in the attachment of the spike tag. Therefore to ensure our tagged peptides would be able to bind to the spike the CoHBc190 plasmid was reverted back to the native sequence. The cloning strategy is shown in the schematic in figure 4.9.

The nucleotide sequence encoding 158 amino acids of the native HBcAg sequence flanked by *Nco*I and *Eag*I sites was designed and ordered as GeneArt gene string (see table 4.1). Once received the GeneArt string was inserted into the TOPO blunt end vector and transformed into TOPO10 *E. coli*. Colonies were picked, grown overnight in LB media and plasmid DNA purified by miniprep. Successful clones were identified by diagnostic restriction digest. These were then confirmed to be the correct intermediate plasmid by Sanger sequencing. Once the native TOPO construct was confirmed a restriction digest was performed with *Nco*I and *Eag*I to release the native string insert. The CoHBc190 backbone was also digested with *Nco*I and *Eag*I and the backbone was separated by agarose gel electrophoresis and purified. The native insert was then ligated into the CoHBc190 backbone. The ligated plasmid was transformed into XL-10 gold *E.coli*. Colonies were picked, grown overnight in LB broth and plasmid DNA purified by miniprep. Successful clones were identified by diagnostic restriction digest using *Nco*I and *Eag*I (figure 4.10) and Sanger sequencing. The sequencing of the plasmid confirmed that the nucleotide sequence of the plasmid was as intended. This confirmed that an expression plasmid for the native HBc construct had been successfully produced.

**A**

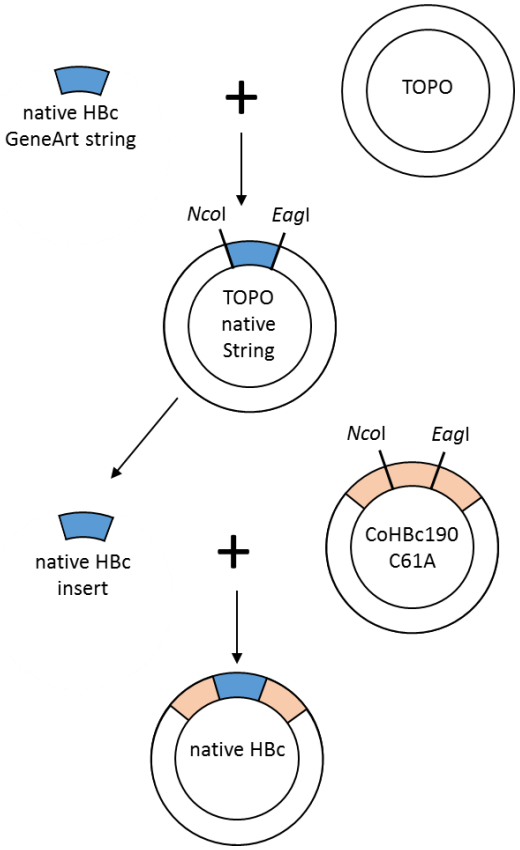


**B**

```
CoHBc190        MDIDPYKEFGATVELLSFLPSDFFPSVRDLLDTASALYREALESPEHCSPHHTALRQAIL      60
Native          MDIDPYKEFGATVELLSFLPSDFFPSVRDLLDTASALYREALESPEHCSPHHTALRQAIL      60
                ************************************************************

CoHBc190        AWGELMTLATWVGNNLEFAGASDPASRDLVVNYVNTNMGLKIRQLLWFHISCLTFGRETV      120
Native          CWGELMTLATWVGNNLE-----DPASRDLVVNYVNTNMGLKIRQLLWFHISCLTFGRETV      115
                .***************     ************************************

CoHBc190        LEYLVSFGVWIRTPPAYRPPNAPILSTLPETTVVRRRDRGRSPRRRTPSPRRRRSQSPRR      180
Native          LEYLVSFGVWIRTPPAYRPPNAPILSTLPETTVVRRRDRGRSPRRRTPSPRRRRSQSPRR      175
                ************************************************************

CoHBc190        RRSQSRESQC        190
Native          RRSQSRESQC        185
                **********
```

**Figure 4. 9**: **Schematic of cloning strategy for native HBc expression plasmid and comparison of the CoHBc190 and Native HBc sequences.**

(A) Schematic showing the insertion of the ordered GeneArt string into TOPO and subsequent cloning into the CoHBc190 construct to produce the native HBc construct. (B) Alignment of CoHBc190 and Native HBc sequences created using Clustal Omega. This shows the native HBc lacks the FAGAS sequence from amino acids 78-82 and has had C61 replaced.

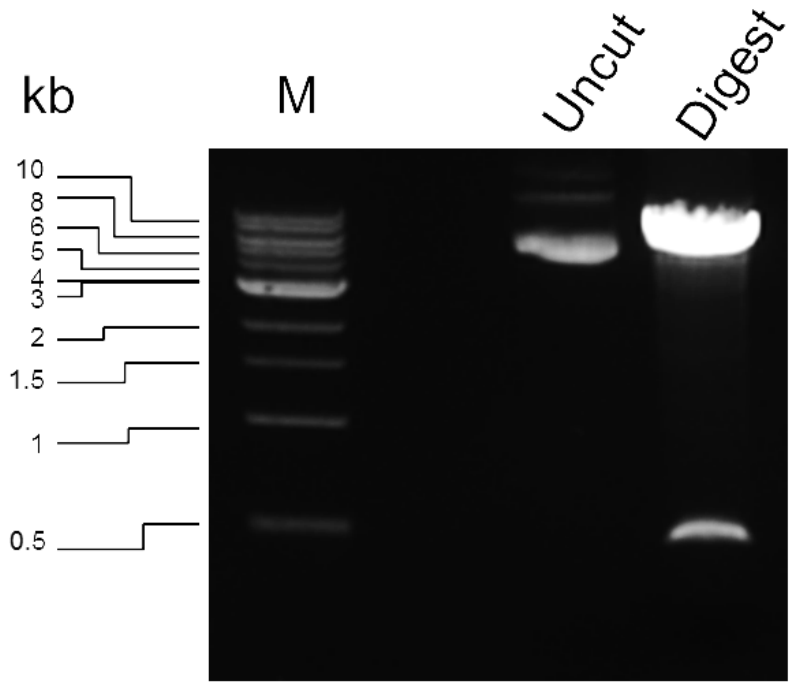


**Figure 4. 10**: **CoHBc190 native was confirmed by diagnostic digest.**

CoHBc190 native was digested with *Nco*I and *Eag*I to release an insert of approximately 500 bp. The uncut plasmid was analysed alongside the digests on a 1 % agarose gel. A 1 kb ladder is shown to the left.

## 4.3.2 Expression of native HBc

Once the plasmid encoding native HBc was generated, expression was tested to determine if the VLPs would assemble correctly (detailed in section 4.2.2).

The expression of the native HBc protein was successfully induced by the addition of IPTG and following sonication was found to be predominantly in the soluble fraction of the bacterial lysate. The expressed protein has a smaller molecular weight than the predicted molecular weight of the native HBc monomer (21.4 kDa). This is approximately 0.4 kDa smaller than CoHBc190 C61A and this reduction in size is due to the removal of 5 amino acids. The actual size of the native HBc monomer on the SDS-page appears to be below 20 kDa which is much smaller than expected and this reduction appears to be more than that caused by removing 5 amino acids. This could be due to the change in sequence causing the protein to migrate differently.

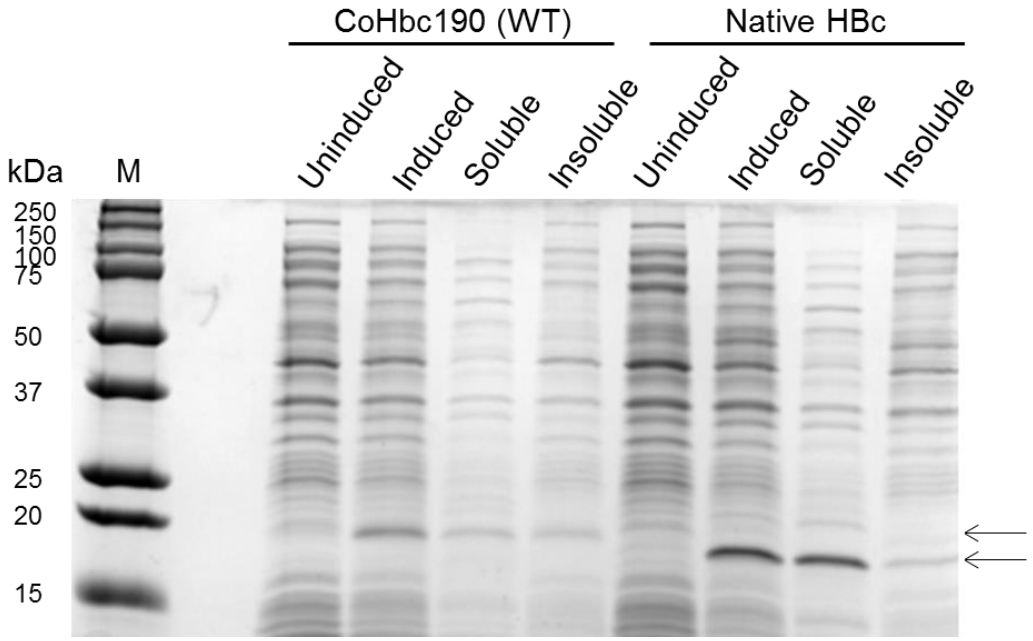


**Figure 4. 11: Soluble CoHBc190 (WT) and native HBc were expressed in *E.coli.***

The expression of CoHBc190 (WT) and native HBc was confirmed using coomassie stained SDS-page (A) Lane 1-4 bacteria expressing CoHBc190. Arrows to the right indicate the presence of CoHBc190 and native HBc. Molecular weight markers (M) in kilodaltons are shown to the left.

## 4.3.3 Purification of native HBc

Following the evidence that the expressed native HBc protein was both soluble and approximately the correct molecular weight, VLPs were purified as described in 4.2.3.

Protein from the soluble fraction of the expression bacterial lysate was precipitated and layered over a 20-60 % sucrose gradient. This was then fractionated and the protein content analysed by absorbance 280 nm and coomassie stained SDS-page. The peak fractions were pooled and after buffer exchange to remove the sucrose the VLPs were layered onto a second gradient. The peak fractions were pooled and buffer exchanged into PBS.

After the first gradient, contaminant proteins remained present in peak gradient fractions (figure 4.12 A) but this was removed by passing the VLPs through the second gradient (figure 4.12 B) and the absorbance 280 of this gradient gave a robust peak of protein in the corresponding fractions (figure 4.12 C). The pooled

peak fractions were then desalted and concentrated using an Amicon concentrating and desalting device with a 100 kDa molecular weight cut off. The purified VLPs were then examined by negative stain electron microscopy and the particles found to have correctly formed, with capsids of around 30 nm in diameter (figure 4.13 A). These were also confirmed to be HBc VLPs by western blot (figure 4.13 B).

The native HBc VLPs sediment to a similar position to the CoHBc190 FMDV VP4N15 VLPs, with the VLP containing fractions occurring from fraction 5 (figures 4.7 and 4.12).

**A**

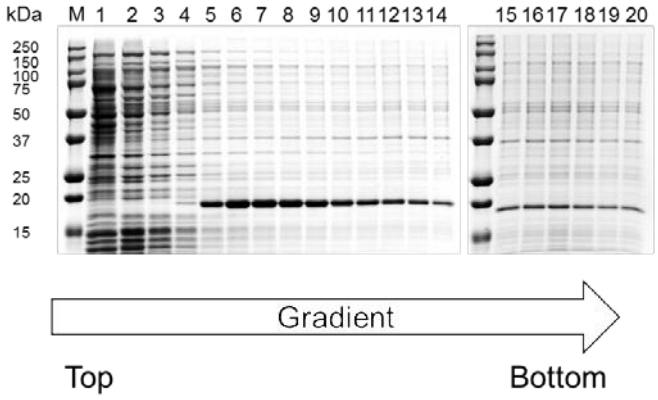


**B**

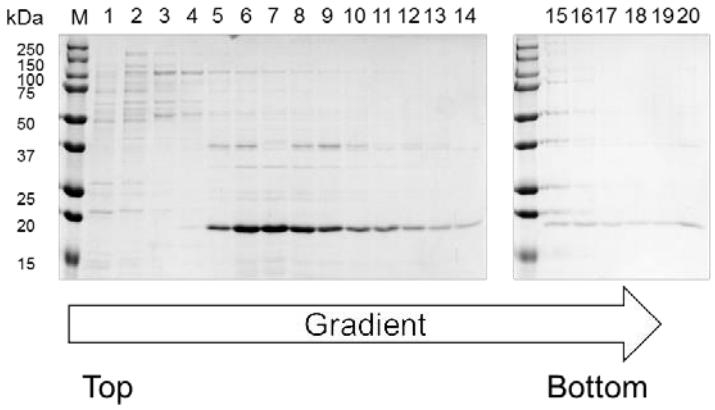


**C**

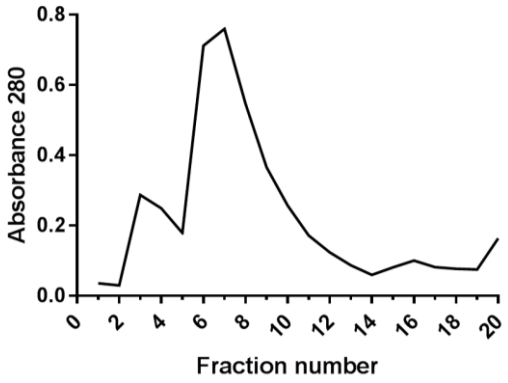


**Figure 4. 12**: **Expressed native HBc protein can be purified by sucrose gradient and sediments as expected for HBc VLPs.**

Soluble protein precipitated from expression bacterial lysates were layered onto a 20-60 % sucrose gradient. (A) Fractions were analysed by coomassie stained SDS-PAGE. Peak fractions were pooled, desalted and layered onto a second gradient. Fractions from the second gradient were then analysed by coomassie stained (B) SDS-PAGE and (C) measuring the absorbance at 280 nm. Arrows indicate orientation of the gradient.

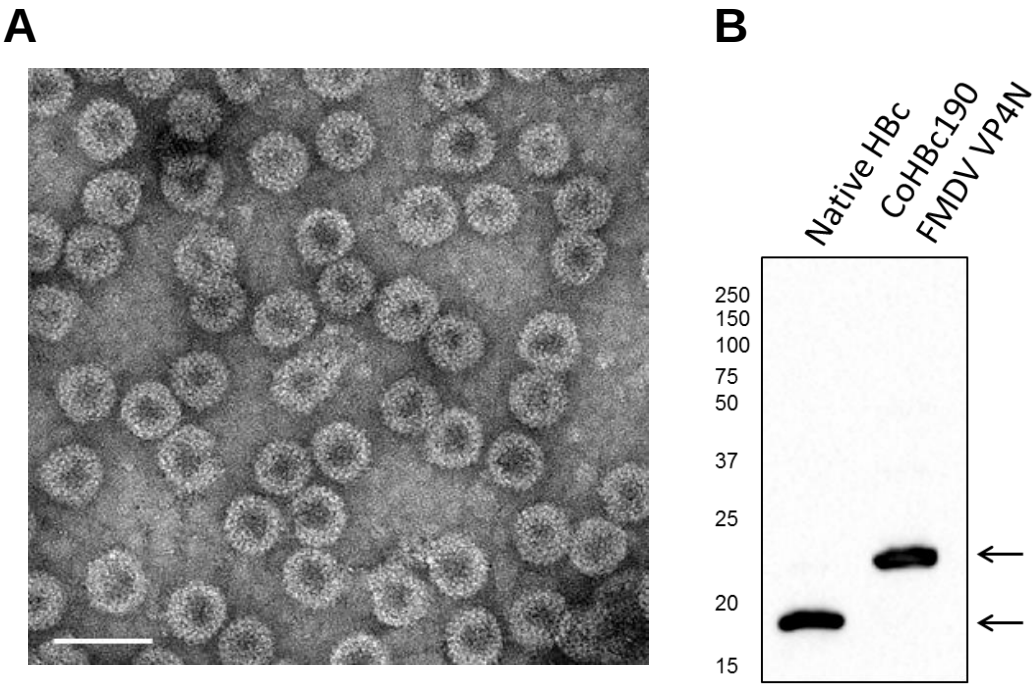


**Figure 4. 13: Expressed and purified native hepatitis B core protein forms virus-like particles.**

(A) Expressed native HBc VLPs were negatively stained and visualised by TEM by Dr Pippa Hawes. The scale bar denotes 50 nm. The native HBc protein (B, lane 1) were confirmed by western blot alongside the CoHBc190 FMDV VP4N15 protein described previously (B, lane 2). The expected molecular weight of the native HBc protein is 21 kDa and the CoHBc190 FMDV VP4N15 is 23 kDa. These were calculated using the protparm Expasy software (Wilkins *et al*., 1999). These were detected using the 10E11 monoclonal antibody that recognises HBcAg.

## 4.4 Attachment of FMDV VP4N 15 peptide to the Native core

An alternative strategy for antigen display on the HBc VLP is to decorate the spikes of the VLP with peptides of the VP4N sequences. This has several advantages over the recombinant protein. Firstly, the structure of the peptide is not altered by inclusion in the HBcAg structure as it is a free peptide bound to the VLP. Secondly, this presentation method has a specific advantage for the presentation of VP4 as this allows the myristoylated N-terminus to freely protrude from the VLP, mimicking the externalisation of the N-terminus of VP4 during virus breathing. This may therefore yield antibodies that are better at recognising FMDV as this undergoes breathing. The peptide was designed to contain the VP4N15 amino acid sequence and the spike tag at the C-terminus (sequence shown in table 2.1).

The interaction between the peptide and native HBc VLPs was formed by incubating native HBc and excess peptide at a 1:4 molar ratio with gentle mixing (described in section 2.10). The unbound peptide was washed away through a centrifugal concentrator device. This used a 100 kDa molecular weight cut off device to allow the VLP and VLP-peptide complex to be retained but the free peptide was washed through the filter. To ensure the free peptide was removed the VP4N15 peptide only was processed alongside the VLP-peptide mixture and a VLP only control.

At the end of multiple washes, samples of VLP were retained in the device but the N15 peptide washed through completely (Figure 4.14). In contrast, the peptide-VLP mixture showed bands for both the VLP and peptide. This indicates the peptide was in complex with the VLP forming the VLP immunogen, termed HBc PepN15.

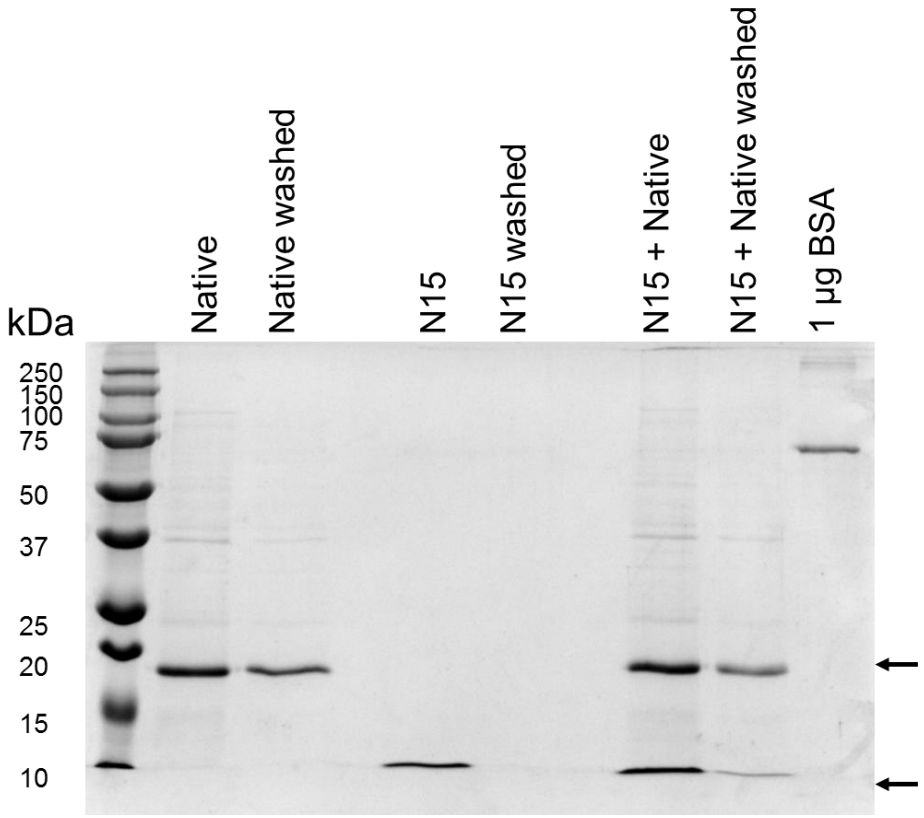


**Figure 4. 14**: **Hepatitis B core VLP and FMDV VP4N15 peptides form complexes that remain after free peptide is removed.**

VLP only (native), VP4N15 peptide only (N15) or VLPs + VP4N15 peptide (N15 +native) were incubated and unbound peptide was removed using a 100 kDa molecular weight cut off centrifugal desalting and concentrating device. The reaction mix and the washed mix were compared by coomassie stained SDS-page. The ladder and molecular weight is shown to the left. Arrows on the right indicate the expected sizes of HBc protein and the peptide (21 kDa and 4 kDa).

## 4.5 Discussion

FMDV VP4 is thought to play an essential role in the entry pathway of FMDV and it is hypothesized this would be in a similar role to the VP4 protein of other picornaviruses such as HRV and PV. The overall aim of this project was to characterise the pore-forming ability of FMDV VP4 and the effect of antibodies against FMDV VP4 on virus infectivity. In order to generate antibodies specific to FMDV VP4, the well-established bacterially expressed HBc VLP system was utilised to generate two variations of the HBc VLP to present sequences from FMDV VP4 to the immune system. The work detailed in this chapter confirms it was possible to generate two versions of the HBc VLP displaying the N-terminal 15 amino acids of FMDV VP4.

Previous work by other groups has shown it is possible to display other peptide sequences from the capsids of picornaviruses, such as FMDV VP1 and EVA71 VP4, on the MIR of the HBcAg and this can assemble into VLPs (Chambers *et al*., 1996, Zhao *et al*., 2013). Following a similar design, recombinant VLPs have successfully been expressed and purified that have the N-terminal 15 amino acids of FMDV VP4 inserted into the MIR.

In addition to the recombinant VLPs another approach was used in parallel. This involved generating VLPs decorated with a VP4N15 peptide through a previously described tag that bound the top of the spike (Blokhina *et al*., 2013).The VP4N15 was used for this to allow comparison between the recombinant display and the peptide attachment display.

The insertion of the nucleotide sequence encoding the N- or C-terminal 15 amino acids in the CoHBc190 expression plasmid was successful. Both recombinant proteins were expressed but the CoHBc190 FMDV VP4C15 did not express as a soluble protein as expected and therefore was not taken forward. This could be due to the hydrophobic nature of this sequence and the impact this could have had on the structure of the HBcAg monomers. An alteration in the structure of HBcAg monomers could have resulted in incorrect dimerisation and therefore no VLP formation. A possible solution to this would be to insert short linker regions to allow more flexibility into the structure and prevent the VP4C15 sequence interfering with the VLP formation.

An alternative reason for the failure to obtain soluble VLPs from the protein expressed from CoHBc190 FMDV VP4C15 plasmid could be linked to the previously

described ability of the VP4C15 sequence to induce membrane permeability. It is likely that in order to induce the size-selective membrane permeability described in section3.3, this sequence would need to multimerise and it could be this feature of the peptide that is disrupting the VLP formation. There is evidence that the insertion of dimeric or tetrameric fluorescence protein reduces or completely abolishes the ability of HBc VLPs to assemble (Vogel *et al*., 2005). That study showed that while monomeric GFP is readily inserted into the HBc VLP the insertion of multimeric red fluorescent proteins has a detrimental effect on the structure. Modified red fluorescent protein that is no longer able to make dimers or tetramers is able to rescue the formation of the tagged VLPs (Vogel *et al*., 2005). Taking this into account, it seems that it is important to consider not just the impact of a foreign insert on the folding of the monomeric subunit and its subsequent dimerisation but also that the impact on the quaternary structure is essential as it is possible the insert will preferentially form multimers over the formation of the VLP.

The VP4N15 VLPs described here (termed HBcN15 and HBc PepN15) have been immunised into mice to generate serum against the N-terminus of VP4 (detailed in chapter 5). This allowed the generation of key reagents to further understand the interactions of FMDV VP4 with membranes and offered the opportunity to investigate the antibodies ability to neutralise virus infectivity.

# Chapter 5
# Characterisation of antibodies against VP4 reveals evidence of FMDV capsid breathing

# 5. Characterisation of antibodies against VP4 reveals evidence of FMDV capsid breathing

## 5.1 Introduction

The FMDV capsid protein VP4 is highly conserved between serotypes (as shown in figure 5.1) and is hypothesised to play an essential role in the entry of FMDV into host cells (discussed in section 1.8). The highly conserved nature of FMDV VP4 makes it an interesting novel target for antibodies and therapeutic strategies. Due to its location in atomic models, FMDV VP4 is considered to be an internal capsid protein and therefore not considered an important epitope for FMDV. Consistent with this, to date very few antibodies against VP4 have been identified and investigated. However, there has been a neutralising conformational monoclonal antibody identified that contains VP4 residue S19 as part of the epitope, as determined by sequencing monoclonal antibody neutralising resistant viruses (Mahapatra *et al*., 2011), indicating VP4 must be externalised for this antibody to neutralise virus infection.

Neutralising antibodies against VP4 have been generated against the VP4 sequence of several enteroviruses, including HRV and EVA71 (Panjwani *et al*., 2016, Katpally *et al*., 2009, Zhao *et al*., 2013). These have been generated using both peptide display using keyhole limpet haemocyanin (KLH)-peptide conjugates and display of a short VP4 sequence on the HBc VLP (Katpally *et al*., 2009, Zhao *et al*., 2013, Panjwani *et al*., 2016). Both methods of presentation produced antibodies that showed cross-serotypical neutralising ability. Recently, it has been shown that antibodies against the N-terminus of HRV VP4 are also able to reduce the pore forming ability of HRV (Panjwani *et al*., 2016).

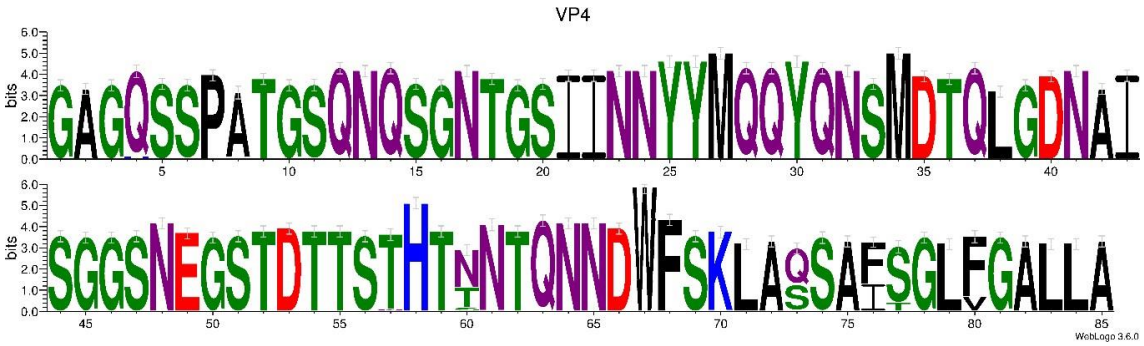


**Figure 5. 1: FMDV VP4 is highly conserved across serotypes.**

VP4 sequences representing the variation in FMDV sequences were compared for sequence conservation. Amino acids are coloured based on their chemical properties as follows; polar amino acids (green), basic amino acids (blue), acidic amino acids (red) and hydrophobic amino acids (black). The conservation of the amino acid is indicated by the number of bits at each position and the higher the value the more conserved the amino acid is. The data set was kindly provided by Dr Lidia Lasecka (The Pirbright Institute). The data set was compiled to represent the diversity in sequence across the FMDV serotypes was generated by forming a tree based on the VP1 sequence of viruses across all serotypes and then FMDV sequences representing the variation were used as a representative set of sequences. WebLogo 3 was used to generate the plot (Crooks *et al*., 2004).

In this chapter two sets of antibodies have been raised against FMDV VP4 and these have been characterised for their ability to detect FMDV and to neutralise virus infection. The first group of polyclonal antibodies were produced in mice using the VLP display methods (described in chapter 4) to display the N-terminal 15 amino acids of VP4. The second set of polyclonal antibodies were produced by displaying the N- and C-terminal 45 amino acids of VP4 on keyhole limpet haemocyanin (KLH) to compare the antibodies against both termini and evaluate the recognition and neutralisation of FMDV by these antibodies, as has been undertaken previously for HRV (Panjwani *et al*., 2016).

In addition to the characterisation of the two groups of antibodies, these antibodies were used here to investigate whether FMDV capsids undergo a similar breathing process as has been described for enteroviruses. In the case of the enteroviruses both the N-terminus of VP4 and the N-terminus of VP1 have been identified as being transiently externalised due to subtle short-lived conformational changes that occur to the capsid proteins (Li *et al*., 1994). While it is likely that FMDV undergoes a

similar process, this has not been documented. Therefore, the panel of VP4-specific antibodies generated here aims to help the exploration of whether the internal capsid protein of FMDV is also exposed due to virus breathing.

## 5.2 Comparison of epitope display methods to display the N-terminal 15 amino acids of FMDV VP4 and evaluation of VP4N15-specific antibodies

### 5.2.1 Immunisation of mice with VLPs displaying the VP4N15 peptide

Previous work has shown that immunisation of mice with the N-terminal 20 amino acids of EVA71 VP4 displayed on the HBc VLP elicits a neutralising immune response and these antibodies predominantly bound to the N-terminal 15 amino acids (Zhao *et al*., 2013). Therefore immunogens utilising the well characterised HBc VLP system were used to investigate if a neutralising immune response could be generated against the N-terminus of FMDV VP4, in a similar way to the experiments described in section 5.1.

The HBc VLPs displaying the N-terminal 15 amino acids within the major immunodominant region (MIR) of the HBc VLP (termed HBcN15) and HBc VLPs with the VP4N15 peptide attached (termed HBc PepN15) (described in chapter 4) were used in an immunisation study. Alongside the experimental VLPs an N-terminal 15 amino acid peptide conjugated to a keyhole limpet haemocyanin carrier protein (termed KLHN15) was used to compare the response against the VLPs with a common peptide display methon. The native HBc VLP were used as a negative control.

The polyclonal serum was generated by immunising experimental groups of 6 Balb/c mice with 10 µg of either HBcN15, HBc PepN15 or KLHN15 immunogen three times and blood samples were collected periodically throughout the experiment (timeline shown in figure 5.2). Alongside this 3 control Balb/c mice were immunised with 10 µg of native HBc VLP. The immunisation schedule was designed based on a literature search of other HBc immunisations studies and this found that theamount of immunogen used was most commonly between 10-50 µg and the protocol used either 2 or 3 immunisations. The protocol used by the previous peptide attachment study was 10 µg per immunisation with two immunisations (Blokhina *et al*., 2013). It was decided to include a second boost as this was commonly done in other studies and to ensure the best response possible had been obtained as this pilot experiment

would be used to inform the planning of future experiments. At the end of the experiment terminal bleeds were obtained and splenocytes were harvested. Serum and splenocytes were obtained for all mice. All work requiring personal home office licences was carried out by Dr Rennos Fragkoudis and Paul Smith at The Pirbright Institute under the project licence held by Dr Bryan Charleston for the production of mouse monoclonal antibodies.

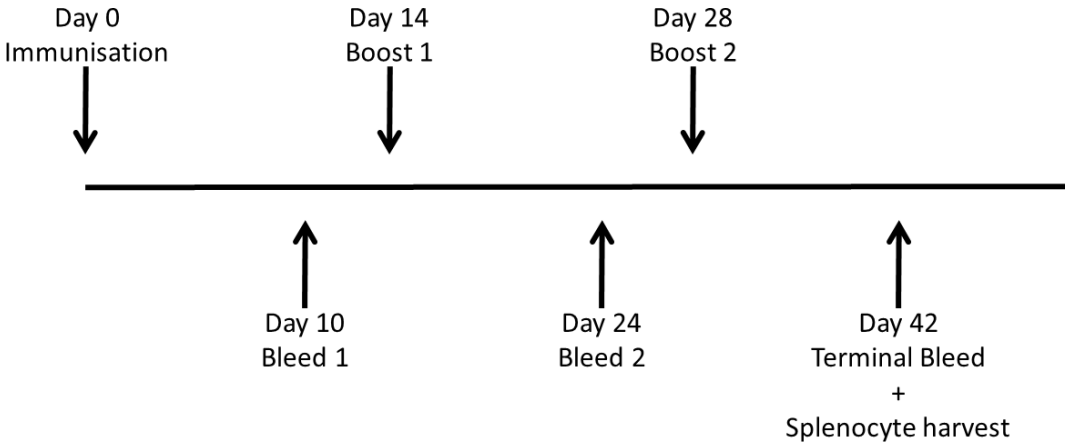


**Figure 5. 2: Timeline of mouse experiment.**

Six mice per experimental group and 3 mice in the control group were immunised with 10 µg of antigen three times. Bleeds were collected periodically and at the end of the experiment splenocytes were harvested.

## 5.2.2 Comparison of responses to VP4N15 by different antigen presentation methods

Pooled serum collected from each group of mice was evaluated for the ability to recognise a VP4N15 peptide (sequence in table 2.1 in chapter 2). This was carried out using a peptide ELISA to determine which groups of mice had produced an antibody response against the displayed VP4N15 sequence. In addition this technique was used to gain some insight into why the animals in some groups did not generate antibodies.

The serum from each group was pooled due to the small volumes obtained and the pooled serum was used in an ELISA to determine if the groups had generated a response to the FMDV VP4N15 peptide. When the groups were compared, the only group to have produced antibodies that recognise the FMDV VP4N15 peptide was the HBcN15 group (figure 5.3).The other two VP4N15 groups (HBc PepN15 and KLHN15) unexpectedly did not generate any detectable immune response to the VP4N15 peptide (figure 5.3). The native HBc VLP did not elicit a response, as

expected (figure 5.3).

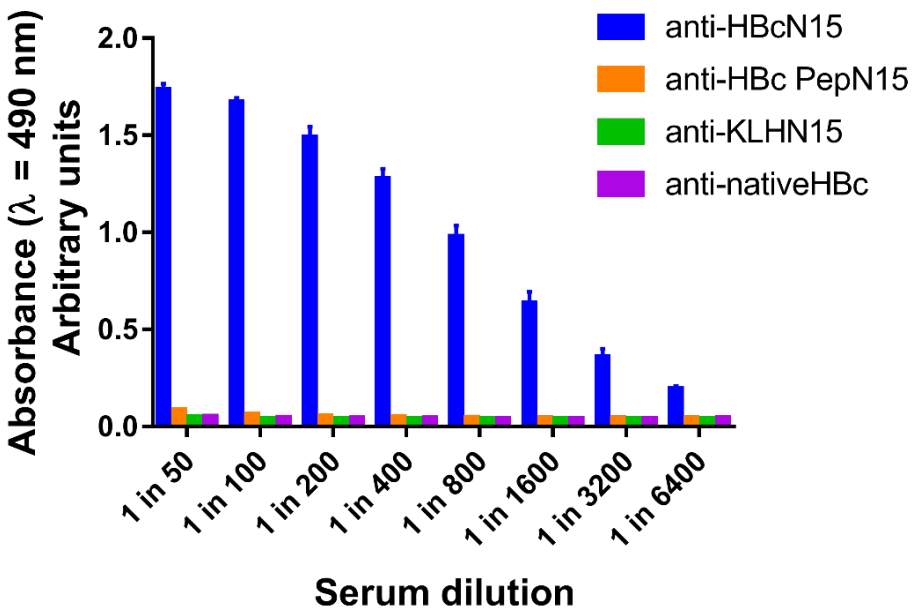


**Figure 5. 3**: **Immunisation of mice with HBcN15 induces a VP4N15-specific immune response.**

Peptide ELISAs were used to detect antibodies against VP4N15. Plates were coated with 1 µg/mL VP4N15 peptide and pooled serum from the HBcN15, HBc PepN15, KLHN15 or native groups was added at the dilutions indicated. After addition of the anti-mouse HRP antibody 0.4 mg/mL OPD substrate was added and the absorbance at 490 nm was measured. Data plotted represent mean of triplicate wells ± SD and are representative of multiple experiments.

The immune response in the HBcN15 group was further characterised by looking at the individual responses of each mouse in the group at the different bleeds throughout the experiment (days detailed in figure 5.2). As the experiment progressed, four of the mice began generating VP4N15 antibodies after the first boost, whereas mice 1 and 6 did not start to produce antibodies until after the second boost (figure 5.4). After the second boost all 6 mice generated antibodies against VP4N15 (figure 5.4).

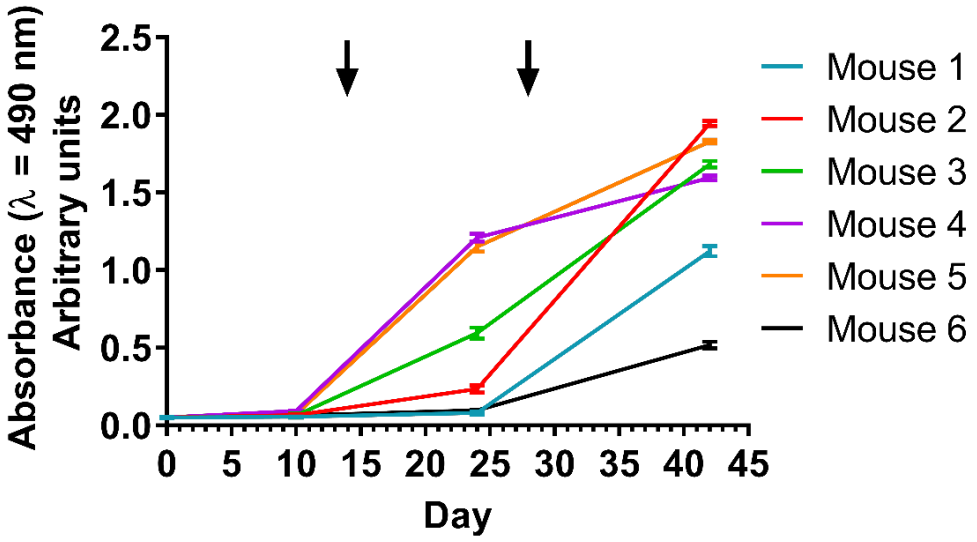


**Figure 5. 4**: **All mice in the HBcN15 group produced an immune response against VP4N15 after three immunisations.**

Peptide ELISAs were used to detect antibodies against VP4N15 to provide information about the kinetics of the immune response. Plates were coated with 1 µg/mL VP4N15 peptide and serum from each mouse in the HBcN15 group was added at 1:100 dilution. After addition of the anti-mouse HRP antibody 0.4 mg/mL OPD substrate was added and the absorbance at 490 nm was measured. The arrows indicate the days on which the boost immunisations were carried out. Data plotted represent mean of triplicate wells ± SD.

The groups that unexpectedly did not elicit a VP4N15-specific antibody response were investigated to understand why these mice had not produced these antibodies. It is possible that the presentation of VP4N15 in these groups was not sufficient to generate a response and this was tested for by assessing the ability of the serum to recognise the non-VP4 component of the original immunogen. To do this the ELISA plates were coated with the original immunogen, except for the analysis of the response to HBc PepN15, where the plate was coated with the native HBc (as the native VLP is the backbone VLP in this immunogen).

Sera from both the HBc PepN15 and native groups recognised the original HBc VLPs immunogen, indicating there was no issue with the immunisations of these groups (figure 5.5). This suggests the lack of response to the HBc PepN15 is due to the peptide display not being sufficient to elicit the response and this will be discussed in more details in section 5.4.

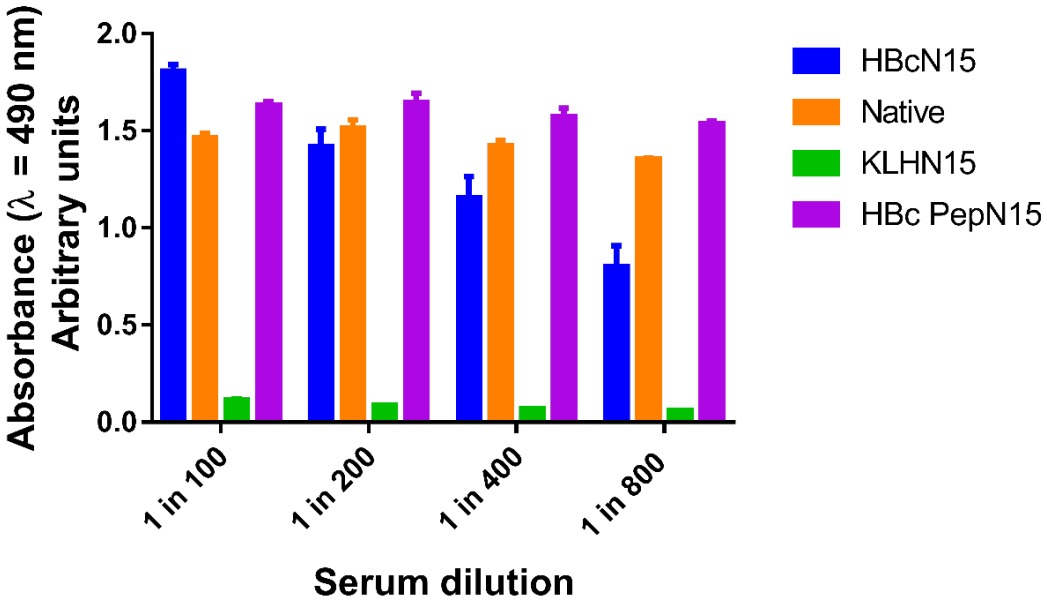


**Figure 5. 5: Serum from native and HBc PepN15 groups recognise homologous immunogen.**

ELISAs were used to detect antibodies against the homologous immunogen in the serum from the native, KLHN15 and HBc PepN15 groups. Plates were coated with 1 µg/mL native HBc VLPs or KLH-peptide conjugate and pooled serum from the homologous group was added at the dilutions indicated. Alongside this wells were coated with 1 µg/mL VP4N15 peptide and the anti-HBcN15 serum used to detect this as a positive control. After addition of the anti-mouse HRP-conjugated antibody 0.4 mg/mL OPD substrate was added and the absorbance at 490 nm was measured. Data plotted represent mean of triplicate wells ± SD and are representative of multiple experiments.

In contrast to the situation with the HBc VLPs the KLHN15 pooled serum was not able to recognise the original KLHN15 immunogen (figure 5.5). There are three potential steps in the process carried out which could have caused the lack of response. Firstly, the lack of immune response could be due to experimental error. This seems unlikely as all other groups were successfully immunised and the immunisations were carried out by the same people on the same day. Secondly, there may have been some problems relating to the mixing of the immunogen and adjuvant. Thirdly, the KLH-VP4N15 conjugate was produced commercially and not characterised in house.

To characterise the KLHN15 conjugate, positive serum against the VP4N15 peptides from the HBcN15 group generated in this study was used to confirm the presence of the VP4N15 sequence conjugated to KLH by ELISA (figure 5.6). This showed that the KLHN15 does have the VP4N15 peptide accessible and the immunogen had VP4N15 conjugated as expected. Together the results in figures 5.5 and 5.6 suggested that a problem had occurred in the formulation of the KLHN15 in the adjuvant.

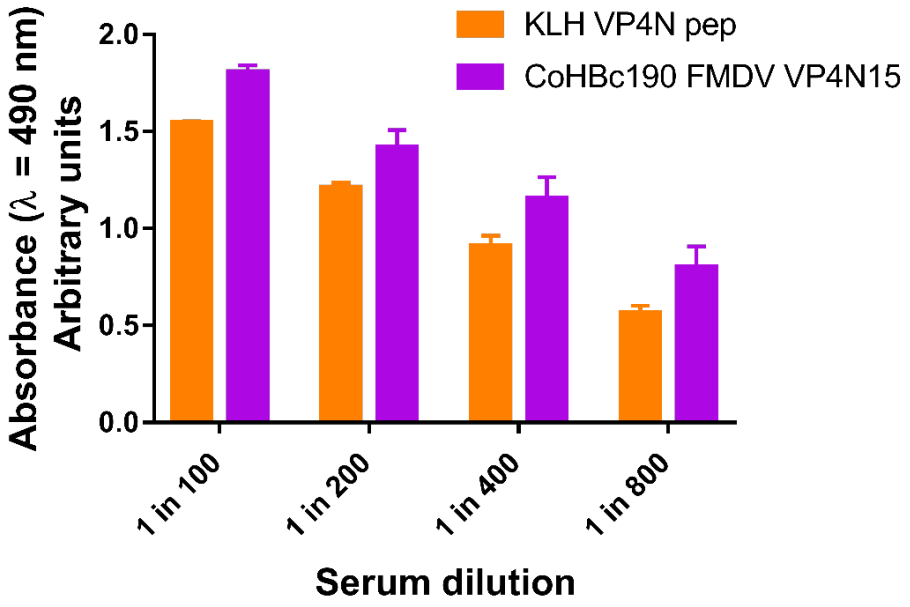


**Figure 5. 6: KLH-VP4N15 conjugate does have accessible VP4N15 peptides.**

Peptide ELISAs were used to confirm the commercially obtained KLH-VP4N15 conjugate behaved as expected. Plates were coated with 1 µg/mL VP4N15 (red bars) or KLH-peptide conjugate (purple bars) and pooled serum from the HBcN15 group was added at the dilutions indicated. After addition of the anti-mouse HRP antibody 0.4 mg/mL OPD substrate was added and the absorbance at 490 nm was measured. Data plotted representmean of triplicate wells ± SD and are representative of multiple experiments.

### 5.2.3 Antibodies against FMDV VP4N15 recognise FMDV providing evidence for capsid breathing in FMDV

Despite the view that VP4 is the internal capsid protein of FMDV it is also hypothesised that FMDV VP4 would be externalised due to the process of capsid breathing. This process has been demonstrated for enteroviruses but to date no

direct evidence of this process in FMDV has been described. As such the VP4N15-specific serum was tested for its ability to detect FMDV capsids, both to investigate the process of breathing in FMDV and to confirm the VP4N15 antibodies recognise VP4 in a biologically relevant confirmation, should VP4 be externalised. This was investigated by using a sandwich ELISA to see if the pooled serum would recognise FMDV. The virus was captured using bovine αvβ6 integrin, the natural receptor of FMDV (discussed in section 1.8.1), and the ability of the pooled serum from the anti-HBcN15 group to detect the capsids was determined.

The pooled serum was able to detect FMDV, which provides new evidence for capsid breathing (figure 5.7). This suggests that capsid breathing could be a conserved feature across picornaviruses. Furthermore, these data show that the display of the VP4N15 sequence on the HBc VLP was sufficient to generate antibodies that recognise VP4 in a biologically relevant confirmation.

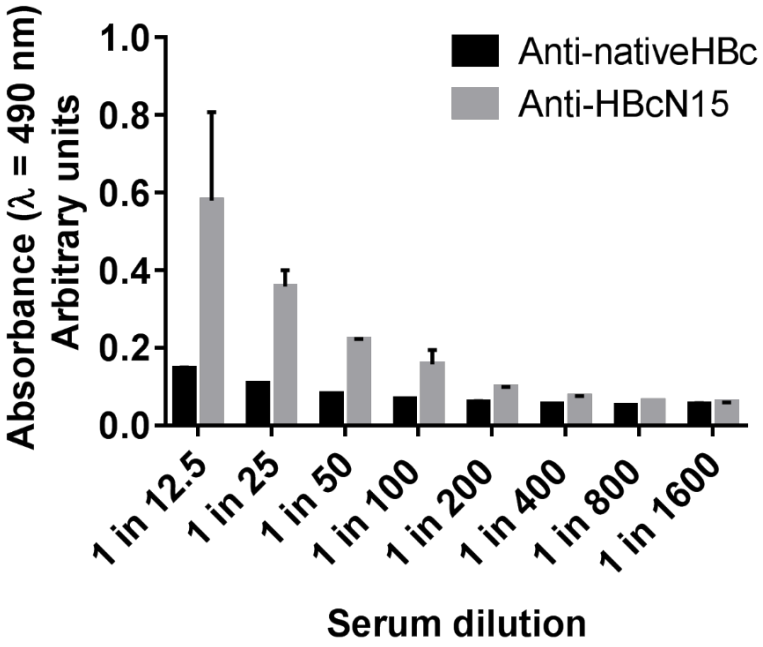


**Figure 5. 7: Anti-HBcN15 serum recognises FMDV.**

Sandwich ELISAs using bovine αvβ6 integrin as the capture were used to confirm that serum against HBcN15 recognised FMDV virus particles. Plates were coated with 1 µg/mL of bovine αvβ6 integrin. FMDV O1M was captured by integrin and serum was used in two-fold dilutions and detected using 1:1000 anti-mouse HRP antibody. Following this 0.4 mg/mL OPD substrate was added and the absorbance at 490 nm was measured. Data plotted represent mean of triplicate wells ± SD and are representative of multiple experiments.

### 5.2.4 Neutralising ability of antibodies against FMDV N15

Previous studies have shown that antibodies against the N-terminus of EVA-71 or HRV VP4 were able to neutralise virus infection and offered some neutralisation against viruses from other serotypes (Katpally *et al*., 2009, Zhao *et al*., 2013, Panjwani *et al*., 2016). The possibility of cross-serotypic antibodies against FMDV is particularly interesting as there are 7 serotypes. The ability of antibodies against the N-terminal 15 amino acids of FMDV VP4 were first evaluated for their ability to neutralise a homologous virus by plaque reduction neutralisation assay.

The plaque reduction assay was used to determine if pre-incubation of FMDV with the anti-HBcN15 serum would cause a reduction in virus titre. FMDV was incubated with serum at 37°C for 1 hr. The incubation at 37°C was included to allow the virus to undergo the process of breathing, as evidence from enteroviruses indicates breathing is a temperature dependent phenomenon and evidence from section 5.2.3 suggests breathing is occurring in FMDV (Li *et al*., 1994). The anti-native HBc serum was used as a negative control as this does not contain FMDV or VP4N15 specific antibodies (figures 5.3 and 5.7). A neutralising bovine polyclonal serum against the O1M strain was used as a positive control.

After incubation with the serum against O1M, there was a 2.5 log difference in virus titre, showing the O1M serum could neutralise virus infectivity. After pre-incubation of FMDV with either the anti-HBcN15 or anti-nativeHBc serum there was no change in the virus titre which shows there is no neutralisation of FMDV by antibodies against the N-terminal 15 amino acids (figure 5.8). This is quite unexpected since neutralising antibodies against VP4 have been found for enteroviruses. This will be discussed further in section 5.4.

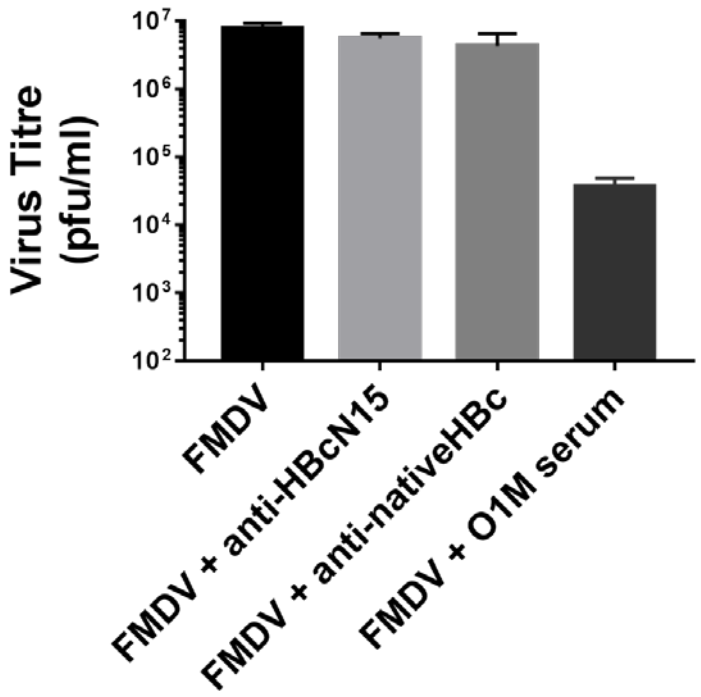


**Figure 5. 8: Antibodies that recognise FMDV VP4N15 have no effect on virus infectivity.**

Plaque reduction neutralisation assays were carried out to assess the effect of the anti-HBcN15 serum on virus infectivity. FMDV O1M was incubated with either anti-HBcN15 serum, anti-nativeHBc serum or anti-O1M serum for 1 hr at 37 °C and titrated by plaque assay. Data plotted represent mean of triplicate wells and error bars indicate the standard deviation.

## 5.2.5 Effect of VP4N15-specific antibodies on FMDV-induced membrane permeability

Previous work has shown that antibodies against the N-terminus of HRV VP4 reduce HRV-induced membrane permeability, showing these neutralising antibodies also affect the pore-forming ability of HRV VP4 (Panjwani *et al*., 2016). Despite the lack of neutralising ability in the VP4N15-specific serum it is possible the VP4-specific antibodies could shed some light on the role of the N-terminus of VP4 in membrane permeability. This could be particularly informative as the results in chapter 3 indicate that either termini of FMDV VP4 has the potential to induce size-selective membrane permeability as a peptide but it is not clear how this relates to the FMDV-induced size-selective membrane permeability previously identified by Dr Sarah Gold (Gold *et al*, manuscript in preparation).

As serum contains an abundance of proteins as well as VP4-specific antibodies, IgG was purified from the mouse serum to prevent background membrane permeation by serum proteins. FMDV O1M was incubated for 1 hr at 37 °C in the presence of purified IgG from the pooled anti-HBcN15 and anti-nativeHBc serum. This temperature was chosen to promote externalisation of VP4 through capsid breathing as this phenomenon is likely to be temperature sensitive, as seen in enteroviruses (Li *et al*., 1994). Following incubation the virus was mixed with carboxyfluorescein (CF) liposomes to investigate the membrane permeability induced.

Due to time constraints, this experiment was only repeated twice and therefore the data presented below is preliminary.

However, incubation with anti-HBcN15 IgG had no effect on FMDV-induced membrane premeabilisation as both FMDV and FMDV incubated with anti-HBcN15 produced similar dye release curves (figure 5.9). Incubation with antibodies with no specificity to FMDV (anti- nativeHBc IgG) may induce a small decrease but it seems unlikely this is due to a non-specific effect on FMDV as results in sections 5.2.2, 5.2.3 and 5.2.4 indicate that these antibodies have no VP4 specificity and do not recognise FMDV. Therefore the slight reduction in membrane permeability induced in the presence of these antibodies requires further investigation.

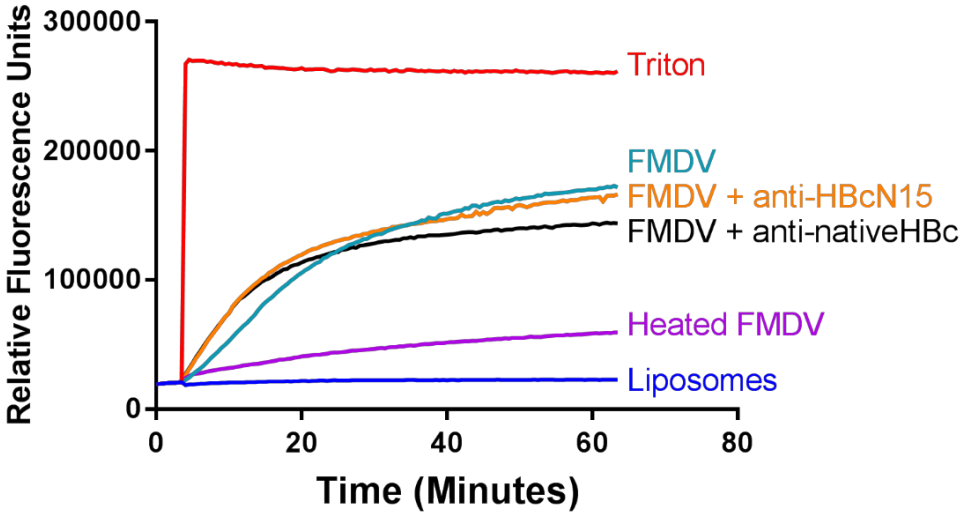


**Figure 5. 9: Antibodies that recognise FMDV VP4N15 have no effect on virus-induced membrane permeability.**

Liposomes containing carboxyfluorescein (CF) at self-quenching concentrations were mixed with 1 µg of FMDV O1M that had been preincubated with 0.1 µg of IgG purified from the anti-HBcN15 or anti-nativeHBc serum for at 37 °C 1 hr. FMDV only was incubated for 1 hr with liposome buffer and as a negative control FMDV was heated at 60°C to dissociate the virus. Membrane permeability resulting in leakage and dequenching of CF was detected by fluorescence measurements (excitation 492 nm/ emission 512 nm) recorded every 30 seconds. Data shown are representative of two experiments.

## 5.2.6 Production of monoclonal antibodies against FMDV VP4N15

Monoclonal antibodies are useful tools to study viruses and the functions of viral proteins but there are very few available that target FMDV VP4. Due to its conserved nature, such antibodies could be cross serotypically neutralising and could provide useful tools for the further study of several key lifecycle stages of FMDV including entry and assembly.

The spleens of the immunised mice were harvested and the splenocytes isolated at the end of the animal experiment. The immune response of the individual mice were compared. As shown before in figure 5.4 there was variation in the immune response against VP4N15 between the mice in the group. Four mice had a lower response than the pooled serum control and two mice had a response higher than or similar to the pooled serum (Figure 5.10). Mouse 4 had the highest response and the splenocytes from this mouse were sent to the Roslin Institute. From the hybridomas, 28 clones

have been identified that strongly recognise the VP4N15 peptide. Supernatants from the 28 clones have been pooled into 7 groups and the ability of these pools to neutralise FMDV infection has been investigated by Dr Joseph Newman and they do not seem to have any neutralisation ability against FMDV (table 5.1). Regardless of the neutralisation ability of these monoclonal antibody they will be useful reagents for studying FMDV.

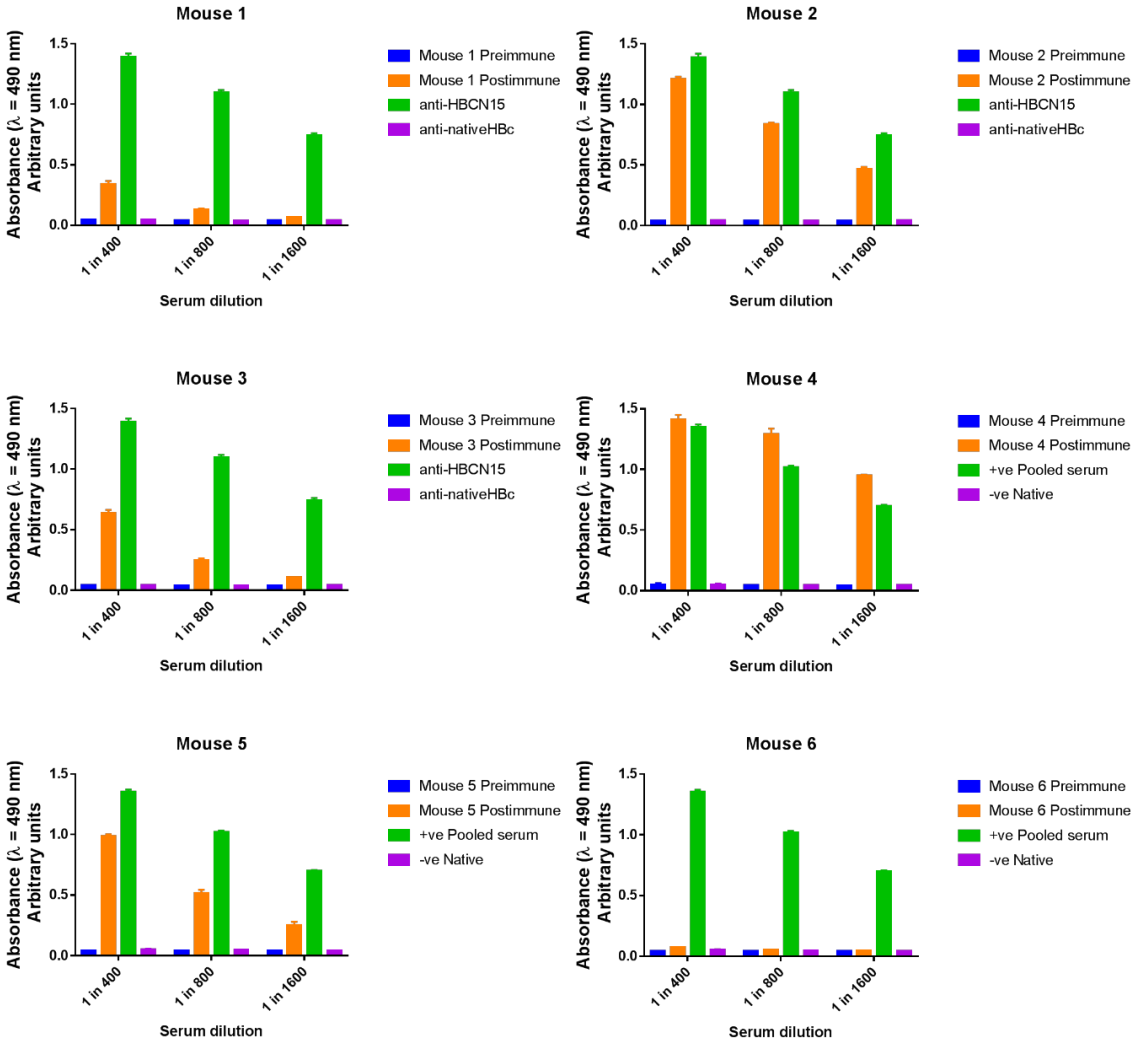


**Figure 5. 10: Selection of the best responding mouse for monoclonal production.**

Peptide ELISAs were used to confirm which mouse from the HBcN15 produced the best immune response to the VP4N15 peptide to determine which splenocytes to take forward. Plates were coated with 1 µg/mL VP4N15 and preimmune and postimmune serum from each mouse in the HBcN15 group was added at the dilutions indicated. After addition of the anti-mouse HRP secondary 0.4 mg/mL OPD substrate was added and the absorbance at 490 nm was measured. Data plotted represent mean of triplicate wells ± SD and are representative of multiple experiments.

| Antibody | Virus neutralisation test result |
|---|---|
| Pool 1 | <0.6 |
| Pool 2 | <0.6 |
| Pool 3 | <0.6 |
| Pool 4 | <0.6 |
| Pool 5 | <0.6 |
| Pool 6 | <0.6 |
| Pool 7 | <0.6 |
| Control O1M serum | 2.4 |

**Table 5. 1: Neutralisation of FMDV by mouse monoclonal antibodies.**

Following screening of hybridoma supernatants for reactivity with the VP4N15 peptide 28 supernatants were pooled into 7 groups and tested by virus neutralisation test (VNT) by Dr Joseph Newman (The Pirbright Institute). The resulting value is the $\log_{10}$ antibody dilution required to neutralise 100 $TCID_{50}$ of O1M FMDV. Data are representative of duplicate wells in multiple experiments.

## 5.3 Characterisation of antibodies against the N- and C-terminus of FMDV reveals more details about VP4 function and virus breathing

### 5.3.1 Antibodies against the N- and C-terminus of FMDV VP4 recognise the peptide immunogen and FMDV

Neutralising antibodies against the N-terminus of HRV VP4 reduce HRV-induced membrane permeability but antibodies against the C-terminus of HRV VP4 do not, this fits with the N- terminus being able to induce membrane permeability whilst the C-terminus has no activity. As discussed in chapter 3, both termini of FMDV VP4 are able to induce size-selective membrane permeability which would be of an appropriate size to allow the movement of the viral genome across the endosomal membrane. This result is different from previous studies on HRV VP4, suggesting there could be differences in the mechanism of membrane permeability between HRV and FMDV. Taking this difference in membrane permeability into consideration, polyclonal antibodies were raised against the N- and C-terminal 45 amino acids of FMDV VP4 as the immune response to these could further elucidate the mechanism of membrane permeability induced by FMDV VP4.

Rabbits were immunised with peptides of the N- or C-terminal 45 amino acids of FMDV conjugated to a KLH carrier. KLH conjugated with myrVP4N45 or VP4C45 peptides were synthesised by Peptide Synthetics and sent to Envigo, where rabbits were immunised to produce the polyclonal serum. Once the final bleeds were received, serum from each rabbit was assessed for its ability to recognise the VP4N45 or VP4C45 peptide.

As expected all the rabbits immunised with KLH-peptide conjugate produced an immune response that recognised the peptide they were immunised with (figure 5.11). In both groups one rabbit produced a stronger response than the other, rabbit 2 and rabbit 4 (figure 5.11). This showed that whilst there were differences in the responses between rabbits the immunisations had been successful and specific antibodies for either VP4 terminus had been generated.

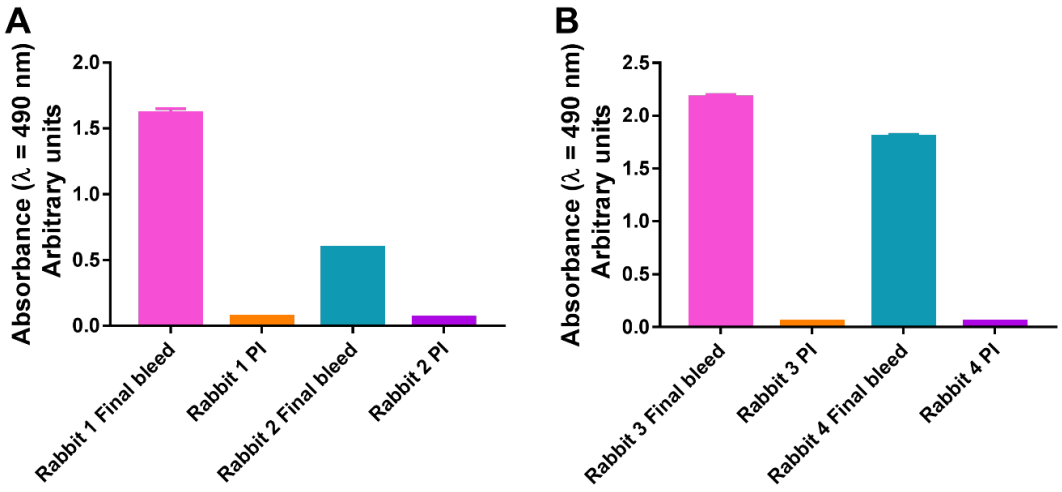


**Figure 5. 11: Serum from all rabbits immunised generated a VP4 peptide specific immune response.**

Peptide ELISAs were used to confirm the immunised rabbits had generated an immune response against the VP4 peptides. Plates were coated with 1 µg/mL (A) VP4N45 or (B) VP4C45 and preimmune (PI) and final bleed sera from each rabbit in the two groups added at a 1 in 100 dilution. After addition of the anti-rabbit HRP secondary at 1 in 5000 dilution 0.4 mg/mL OPD substrate was added. The absorbance at 490 nm was measured. Data plotted represent mean of triplicate wells ± SD and are representative of multiple experiments.

Following the result in section 5.2.3 that suggest FMDV may undergo the process of capsid breathing, the anti-KLHN45 and anti-KLHC45 serum were tested in the same ELISA. The results of the sandwich ELISA demonstrated that serum generated against either the N- or C-terminus of FMDV VP4 was able to detect FMDV (figure 5.12). This result is interesting for two reasons. Firstly, the detection of FMDV by antibodies specific for the N-terminus of VP4 supports the results in section 5.2.3 adding to the evidence that the N-terminus of FMDV VP4 is externalised during the process of virus breathing, as shown for the enteroviruses. Secondly, the unexpected detection of FMDV by antibodies specific for the C-terminus of VP4 suggests that, in contrast to the process of virus breathing in enteroviruses, the C-terminus of FMDV VP4 is also externalised from the capsid at physiological temperatures. This will be discussed further in section 5.4.

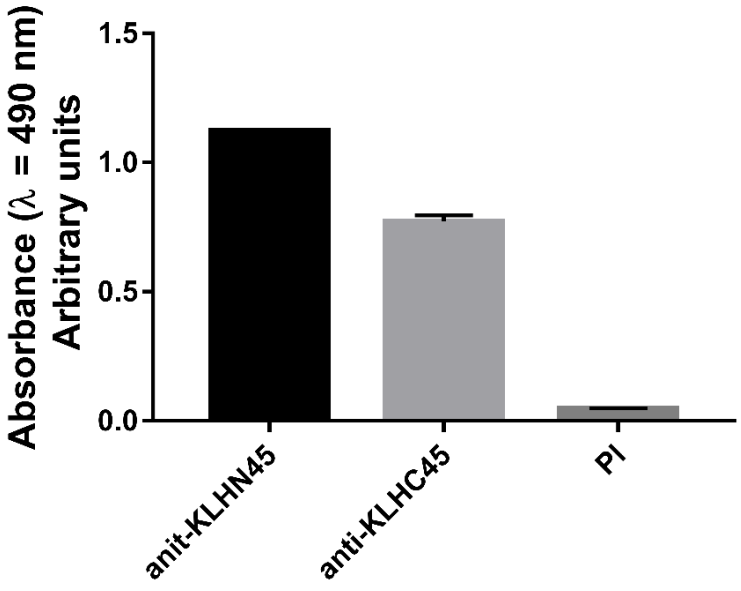


**Figure 5. 12: Figure 5.12: Serum against the N- or C-terminal 45 amino acids of VP4 recognise FMDV.**

Sandwich ELISAs using bovine αvβ6 integrin as the capture were used to confirm that serum against KLHN45 or KLHC45 recognised FMDV virus particles. Plates were coated with 1 µg/mL of bovine αvβ6 integrin. FMDV O1M was captured by integrin and serum was used at a 1:50 dilution and detected using 1:5000 anti-rabbit HRP. 0.4 mg/mL OPD substrate was added and the absorbance at 490 nm was measured. Data plotted represent mean of triplicate wells ± SD and are representative of multiple experiments.

### 5.3.2 Neutralisation ability of serum against the N- and C-terminus of FMDV VP4

Unexpectedly the sandwich ELISA in section 5.7 shows that both termini of FMDV VP4 are externalised from the capsid, potentially through the process of virus breathing. As both termini of VP4 are being externalised it is possible that either could be a target for neutralising antibodies. Despite the lack of neutralising ability of the VP4N15-specific antibodies shown in section 5.2.4, the VP4N45-specific serum generated in the rabbits could still be able to neutralise FMDV infectivity as it had been raised against a much longer peptide and utilises a different presentation method. In addition, as both the peptides used to immunise the rabbits are 45 amino acids in length, essentially dividing VP4 in half, the antibodies generated should span the length of VP4. The ability of the rabbit serum to neutralise virus infection was assessed using the plaque reduction neutralisation assay as used in section 5.2.4.

The rabbit serum against the N- or C-terminal 45 amino acids of FMDV VP4 was pre-incubated with O1M lysate and the titre of the virus was determined by plaque assay. FMDV was incubated with PBS and preimmune rabbit serum as negative controls and a neutralising O1M bovine serum was used as a positive control.

Neither the anti-KLHN45 or anti-KLHC45 serum reduced the titre of FMDV (figure 5.13). This is unexpected as for other picornaviruses neutralising serum has been identified against VP4. As the aphthoviruses and enteroviruses are different genera of picornaviruses is possible that, whilst VP4 plays a conserved role in genome transfer, the differences in these mechanisms results in differences in the ability of VP4 to be a target for neutralising antibodies.

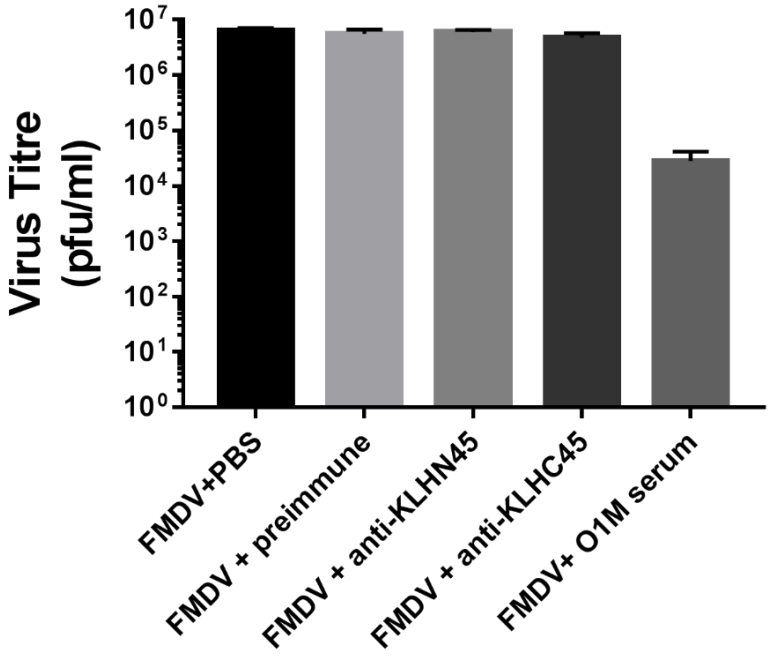


**Figure 5. 13: Antibodies against the N- or C-terminal 45 amino acids of FMDV VP4 have no effect on FMDV infectivity.**

Plaque reduction neutralisation assays were carried out to assess the effect of the anit-KLHN45 and anti-KLHC45 serum on virus infectivity. FMDV O1M was incubated with PBS, anti-KLHN45, anti-KLHC45 serum, preimmune serum or anti-O1M serum for 1 hr at 37 °C and titrated by plaque assay. Data plotted represent mean of triplicate experiments ± SEM.

## 5.3.3 Effect of antibodies against the N- and C-terminus of VP4 on FMDV- induced membrane permeability

Previous studies using HRV VP4 has shown that neutralising antibodies against the N- terminus of VP4, the region identified to induce size-selective membrane permeability, reduced HRV-induced membrane permeability (Panjwani *et al*., 2016). This results shows that the membrane permeabilisation induced by HRV is solely attributed to the N-terminus of HRV VP4 and was successfully blocked by antibodies against this region. In contrast the data presented in section 3.2 shows that both termini of FMDV VP4 have the ability to induce size-selective membrane permeability independent of each other. The data in section 5.2.5 shows that antibodies against the N-terminal 15 amino acids of FMDV VP4 have no effect on FMDV-induced membrane permeability. This could be due either the lack of membrane permeability induced by the N-terminal 15 amino acids (section 3.3) or it could indicate that FMDV-induced membrane permeability is not completely reliant on the N-terminus of VP4.

If the latter is the case then it is possible that the C-terminus may be essential for FMDV-induced membrane permeability. In order to investigate further which termini of FMDV VP4 might be vital for FMDV-induced membrane permeability the experiments described for the VP4N15-specfic antibodies were repeated (section 5.2.5) using IgG purified from serum against either the N- or C-terminal 45 amino acids. These experiments were undertaken twice due to time constraints and therefore the CF release presented is preliminary.

After incubation of FMDV with N- or C-terminus specific IgG there was no change to the FMDV induced CF release, showing that antibodies against the N- or C-terminus of FMDV VP4 have no effect on FMDV-induced membrane permeability (figure 5.14). This result is unexpected as it implies that neither termini of VP4 is solely responsible for FMDV-induced membrane permeability, which would be a considerable difference from the membrane permeability described for HRV.

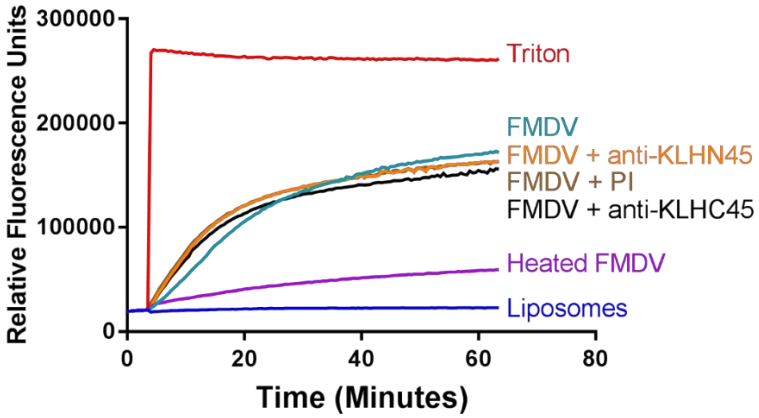


**Figure 5. 14: Antibodies that recognise the N- or C-terminal 45 amino acids of FMDV VP4 have no effect on virus-induced membrane permeability.**

Liposomes containing carboxyfluorescein (CF) at self-quenching concentrations were mixed with 1 µg of FMDV O1M that had been preincubated with 0.1 µg of IgG purifed from the anti-KLHN45, anti-KLHC45 or preimmune serum for at 37°C 1 hr. FMDV only was incubated for 1 hr with liposome buffer and as a negative control FMDV was heated at 60°C to dissociate the virus. Membrane permeability resulting in leakage and dequenching of CF was detected by fluorescence measurements (excitation 492 nm/ emission 512 nm) recorded every 30 seconds. Data shown are representative of two experiments.

## 5.4 Discussion and future work

In this chapter, two groups of antibodies against FMDV VP4 have been successfully generated and evaluated for their ability to detect and neutralise FMDV. Firstly, three antigen presentation methods for the N-terminal 15 amino acids of FMDV VP4 were compared. These consisted of two VLPs based on the hepatitis B core VLP (the design and production of these are described in chapter 4) and a conventional KLH-peptide display method. A VP4-specific polyclonal immune response was generated against the recombinant VLP but not the other presentation methods. Secondly, commercial polyclonal antibodies against the N- and C-terminal 45 amino acids of FDMV VP4 were generated. Both groups of polyclonal antibodies against VP4 were able to recognise intact virus particles but were non-neutralising and this highlights differences between the well-studied enteroviruses and FMDV.

After the successful production of HBc VLPs displaying the N-terminal 15 amino acids of FMDV VP4 (detailed in chapter 4) a small study in mice was conducted comparing both types of VLP and a conventional KLH-peptide display. Analysis of the study showed that only the recombinant VLP group had produced an immune response against the N-terminal 15 amino acids of FMDV VP4. The reasons for the absence of a response in the other two groups was investigated to inform future studies.

The peptide attachment group still induced a strong immune response against the native HBc VLP, the backbone of this immunogen, indicating the mice had received an adequate dose of the VLPs and there was not an issue with the administration of the immunogen. As there was no VP4N15 specific response the peptide attachment did not display the sequences as desired. It is possible that the 15 amino acid peptide was too short and when attached to the HBc VLP the orientation and display of the peptide was not sufficient to generate a strong immune response. There is only limited structural information about the orientation of the peptide spike binding sequence when bound to the top of the dimer spike. The structural information suggests the sequence lies across the dimer and due to this one peptide per spike can bind (Bottcher *et al.*, 1998). There is no information on the predicted orientation of any additional sequence beyond the spike binding sequence but from the successful Blokhina *et al.* study it seems likely the sequence is displayed adequately. The peptide here is considerably shorter than at used by Blokhina *et al.* and may have been too small to be displayed correctly and this could explain the failure to obtain an immune response.

Another possible reason for the failure to generate a VP4N15 specific immune response using the peptide attachment VLP could be due to the nature of the peptide-peptide interaction on the spike. The interaction holding the peptide onto the spike relies on charged amino acids on the spike interacting with charged amino acids within the spike binding tag sequence on the peptide. It was shown by Blokhina *et al.* this interaction was not strong enough to allow the complex to be purified by sucrose gradient. The adjuvant used for this experiment formed a thick emulsion which was formed as per the manufacture's instructions using a homogenising needle hub. The adjuvant and immunogen were homogenised through a narrow needle hub to prepare the immunogen for immunisation and it is possible that during this process the interaction between the peptide and VLP was disrupted, causing the loss of the peptide from the peptide-VLP complex. This would explain the strong response against the native HBc observed and the lack of associated VP4N15 response.

In contrast to the peptide attachment group, there was no homologous response to the KLH-peptide conjugate in the KLH group. As the mice from all groups were all immunised on the same day by the same people and all other groups generated a good immune response, it is unlikely the procedure of immunising the mice is the cause of the problem. Therefore, it is likely the lack of immune response in this group is due to a problem originating prior to the immunisation of the mice. As the KLH-peptide conjugate was purchased it was possible the immunogen was not the expected conjugate but testing of the immunogen confirmed it was the correct KLH-VP4N15 peptide conjugate.

Conjugation of the VP4N15 peptide could have affected the solubility of the KLH-peptide conjugate as the VP4N15 sequence contains about 20 % hydrophobic residues. It is possible that the KLH-conjugate may not all have been in suspension when immunised into the mice, resulting in no immune response against the KLH-peptide conjugate.

An additional issue could come from the fact that KLH-peptide conjugate are known to be less immunogenic than VLPs so it may be the amount of immunogen used that has contributed to the lack of response. The low amount of KLH-peptide conjugate used here was in order to directly compare the immune response to the same amount of immunogen. As this work shows the immune response against the same amount of HBc VLP was successful this work supports the idea that VLPs can induce a good immune response with less immunogen. For future studies, alongside

investigating other adjuvant options, it may be beneficial to increase the amount of KLH immunogen used to ensure a response is obtained.

Despite the lack of response from the 2 out of 3 experimental groups discussed above, the HBcN15 VLPs induced a VP4-specific antibody response. The serum from these mice was able to recognise both the VP4N15 peptide and FMDV but did not have any effect on virus titre. This is somewhat unexpected as previous work has shown that antibodies against the N-terminal 20 amino acids of EVA71 VP4 displayed on the HBc VLP can neutralise EVA71 infection (Zhao *et al*., 2013).

As it is important to maximise the reagents generated when animals are used, the mouse spleens were harvested after the terminal bleeds were collected. The splenocytes were obtained from the spleens and splenocytes from the mouse with the best antibody response were sent to The Roslin Institute to undergo fusions and form hybridomas to produce monoclonal antibodies. After this process there were about 70 positive clones identified and of these 28 were deemed strongly positive. The 28 strongly positive clones have been screened by Dr Joseph Newman and unfortunately these lack any neutralising ability in a virus neutralisaiton assay.

The second set of antibodies, rabbit polyclonal antibodies against the N- and C-terminal 45 amino acids of VP4, were generated as KLH-peptide conjugates by an antibody production company. These peptides cover the whole VP4 sequence, divided into two halves with a small amount of overlap between the peptides. These antibodies recognised the target peptide and FMDV. Unexpectedly, neither the serum against the N- or C-terminus of FMDV VP4 were able to neutralise FMDV when tested in the plaque neutralisation assay.

All of the antibodies tested by plaque reduction neutralisation assay in this chapter did not exhibit any neutralisation ability. However, all of the antibodies generated were able to detect intact FMDV bound to the integrin receptor. Due to time constraints it was not possible to investigate the properties of the antibodies further and as such there are several further experiments that would be beneficial for fully understanding these antibodies.

Firstly, to date all of the neutralisation studies have been carried out using inactivated serum or hybridoma supernatant and therefore it is possible the concentrations of anti-VP4 specific antibodies within these could be low low. A simple way to determine if the non-neutralising result was due to insufficient concentration of

antibodies would be to purify out VP4-specific antibodies from the serum or supernatants and repeat the neutralisation with the concentrated antibodies.

Secondly, during the neutralisation assays the cells were not pre-treated with the VP4-specific antibodies. Future work should investigate whether pre-treating cells with the VP4-specifric antibodies to ensure a sufficient endosomal concentration of antibodies changes the non-neutralising result shown here. As VP4 is released from the capsid within the endosome it is possible priming the endosomes with antibodies against VP4 would prevent infection.

Thirdly, as the data thus far shows antibodies against either the N- or C-terminus of FMDV are not able to neutralise FMDV it would be interesting to test the neutralisation of the antibodies in combination. As demonstrated in chapter 3 both termini of FMDV VP4 are able to induce membrane permeability and therefore, in order to use VP4 as a neutralising target antibodies against both termini may be required. This could be easiliy tested by repeating the neutralisation experiments and including a mix of the N- and C-terminus antibodies.

The sandwich ELISA results shown in this chapter demonstrate that all of the serum generated was able to detect FMDV when captured by the natural receptor for FMDV, αvβ6 integrin. The atomic structure of FMDV in complex with αvβ6 integrin indicates receptor binding does not drive a conformational change to the FMDV capsid (Kotecha et al., 2017). However, atomic structures do not always show the full nature of an interaction as they show a static snapshot of an interaction and this may not capture the dynamic nature of virus capsids. Therefore, the observation that the presence of αvβ6 integrin results in detection of FMDV by the VP4-specific antibodies could indicate there is a subtle effect on the structure of VP4 following receptor binding. The ELISA experiments presented here could be repeated with FMDV directly coated to the plate to determine if the detection of FMDV by the VP4-specific antibodies is dependent on the presence of the αvβ6 integrin receptor. If the interaction between the VP4-specific antibodies is dependent on αvβ6 integrin then it would be interesting to test the ability of the antibodies to prevent FMDV-induced membrane permeabilisation using liposomes decorated with αvβ6 integrin, using a similar approach as previously described for PV (Tuthill et al., 2006).

Previous studies have shown that VP4 can be the target of neutralising antibodies in picornaviruses, such as the enteroviruses HRV and EVA71 (Katpally *et al*., 2009, Zhao *et al*., 2013, Panjwani *et al*., 2016). One possible explanation for this is the

difference in VP4 membrane permeability between FMDV and HRV. As discussed in chapter 3, both termini of FMDV VP4 were able to induce membrane permeability whereas for HRV only the N-terminus (Panjwani *et al*., 2016). The neutralising antibodies against the N-terminus of HRV were also able to reduce membrane permeability, indicating these antibodies interfere with the pore-forming function of VP4 (Panjwani *et al*., 2016).

As both FMDV VP4 termini induced size-selective membrane permeability (demonstrated in section 3.2) it may be that targeting one of the termini is not sufficient to block membrane permeability and this could prevent antibodies against FMDV VP4 having any neutralising ability. Preliminary data using the real-time membrane permeability assay indicated that this may be the case as pre-incubation of FMDV with antibodies against the N- or C-terminus of VP4 has no effect on FMDV-induced membrane permeability. This was unexpected as, despite the data in section 3.2, I hypothesised that there would still need to be one predominant region that was primarily responsible for FMDV-induced membrane permeability, and therefore responsible for the transfer of the viral genome into the host cell. I hypothesised that this was most likely the N-terminus of VP4, following on from the evidence from HRV VP4 discussed above. However, this does not seem to be the case and neither antibodies against the N-terminal 15 or 45 amino acids have an effect on FMDV-induced membrane permeability.

The Preliminary data presented in this chapter suggests that antibodies against either the N- or C-terminus of FMDV VP4 have no effect on the membrane permeabilisation induced by FMDV. Following this result it would be interested to investigate combinations of antibodies to determine if the presence of antibodies against both termini have a collective effect on the membrane permeabilisation induced by FMDV. In addition, peptides could be used to purify the VP4-specific antibodies and allow the experiments to be repeated with more anti-VP4 antibodies.

Alongside concluding the membrane permeability assays to investigate the effect of antibodies against the N- and C-terminus of VP4 on FMDV-induced permeability it would be beneficial to characterise the effect these antibodies on the myrVP4N45 and VP4C45 peptides as these peptides are identical to those conjugated to the KLH carrier protein. This would confirm if the results above are due to an inability of these antibodies to prevent peptide membrane permeability or whether the preliminary results reflect the involvement of both termini in FMDV-induced membrane permeability, as discussed in the previous paragraph. This work was attempted but

thus far has not provided consistent results, therefore the effect of these antibodies on the N- and C-terminal peptides is unclear.

The characterisation of the VP4 antibodies in this chapter has also provided intriguing evidence that the FMDV capsid undergoes the process of capsid breathing, previously only described for the enterovirus genus. Previous work in enteroviruses has shown that the N-termini of VP4 and VP1 are transiently externalised during the process of virus breathing (Li *et al*., 1994) and while it seems likely a similar rearrangement occurs in FMDV, it has not been established which internal sequences are externalised. The results in this chapter show both potential similarities and differences between this process in enteroviruses and FMDV.

The data presented here indicates that the N-terminus of FMDV VP4 is externalised from the FMDV capsid and can be detected in an ELISA at physiological temperatures. This results indicates that this is a conserved process of the externalisation of VP4 between the enteroviruses and FMDV.

In contrast to previous studies with enteroviruses the data presented here shows that the C-terminus of FMDV VP4 is also displayed on the external surface of the capsid at physiological temperatures. This result was unexpected as it was hypothesised that should capsid breathing occur in FMDV, it would follow a similar pattern to the process characterised for enteroviruses, resulting in the externalisation of specifically the N-terminus of FMDV VP4. This appears to not be the case and this exciting and intriguing result warrants further investigation.

The transient externalisation of FMDV VP4 during capsid breathing could be linked to the externalisation of VP4 during the entry process, which is hypothesised to result in membrane penetration and genome release. Therefore the location of FMDV VP4 within the capsid could help to understand the site of VP4 externalisation during both breathing and membrane penetration. The structure of VP4 within the FMDV capsid is not fully resolved but the N-terminus is close to the 5-fold axis of symmetry and the C-terminus is close to the 3-fold axis of symmetry (Acharya *et al*., 1989). The FMDV capsid has been shown to have a capsid pore at the 5-fold axis and the capsid structure of the related aphthovirus ERAV shows capsid pores at the 5- and 3-fold axes of symmetry (Acharya et al., 1989, Tuthill et al., 2009). The atomic structure of the low pH ERAV structure showed that these pores in the capsid are present at low pH (Tuthill et al., 2009). As the N-terminus of FMDV VP4 is found near the 5-fold axis of symmetry this could be externalized from the 5-fold capsid pore. The structure

of PV in complex with a membrane revealed two umbilicus structures and one of these was located near the 5-fold axis of symmetry (Strauss et al., 2013). Therefore, the externalisation of FMDV VP4 from the 5-fold axis could be responsible for forming a similar structure during FMDV entry.

The site of externalisation of the C-terminus of FMDV VP4 is less clear. Due to the location of the C-terminus near the 3-fold axis of symmetry it may be the C-terminus is externalised at the 3-fold axis. However, the umbilicus structure of PV showed a second umbilicus located midway between the 5-fold axis of symmetry and a structural feature near the 3-fold axis (Strauss et al., 2013). Therefore, it is interesting to speculate that the C-terminus of FMDV VP4 is externalised at a yet undiscovered point in close proximity to the 3-fold axis of symmetry and would be able to form a similar umbilicus structure as observed in PV.

Further work to confirm the breathing phenomenon in FMDV is required and the antibodies used in this chapter will be useful resources to investigate this further. The next step would be to compare the ability of the serum against the N- and C-terminus to detect FMDV at both 37°C and 4°C as the process of breathing is known to be temperature dependent in enteroviruses (Li *et al*., 1994) and as such this should be confirmed for FMDV. This may reveal that only one terminus of VP4 is externalised in a temperature dependent manner or may confirm that both termini are exposed in the process of virus breathing. It would also be interesting to consider using the panel of non-neutralising monoclonal antibodies in structural studies to capture the N-terminus of VP4 being externalised from the capsid. A similar panel of monoclonal antibodies to the C-terminus could be a useful reagent to generate for future studies.

The work presented in this chapter shows that antibodies against FMDV VP4 have successfully been generated using a variety of presentation methods. The presentation of a small VP4 sequence on the HBc VLP was highly effective in producing a good immune response with a relatively low amount of immunogen indicating this could be an interesting VLP for future display of FMDV proteins. The characterisation of the antibodies has revealed that it is likely that FMDV undergoes a similar process of capsid breathing as have been previously identified in enteroviruses, which could suggest this is a conserved feature of picornaviruses. Unfortunately the panel of antibodies was unable to pinpoint which region of FMDV VP4 is responsible for FMDV VP4 membrane permeability but this could reflect the mechanism of permeability utilised by FMDV.

# Chapter 6 Comparison of VP4 proteins from FMDV and other picornaviruses

# 6. Comparison of VP4 proteins from FMDV and other picornaviruses

## 6.1 Introduction

Despite differences in the entry pathways of picornaviruses the delivery of the genome into the cytosol is an essential step in entry. The VP4 protein of several picornaviruses have been shown to induce membrane permeability (detailed in section 1.8.4) and FMDV VP4 peptides have now been demonstrated to contain a similar membrane permeabilising activity (section 3.2). Data presented in section 3.3 has started to map the membrane permeabilising function of FMDV VP4 using peptides of different lengths. As the membrane permeability induced by VP4 could be the formation of a portal for genome transfer, it is interesting to consider the possibility that there is a conserved membrane permeabilising region within VP4 that plays a role in this essential process.

A group of picornaviruses that lack VP4 are the VP0 picornaviruses which only contain the three capsid proteins VP0, VP3 and VP1. Some examples of these are the kobuviruses, such as aichi virus (AiV), and parechoviruses, such as Ljungan virus (LV), which have been shown to lack VP0 cleavage (Yamashita *et al*., 1998, Johansson *et al*., 2004). One hypothesis of the origin of these viruses is these viruses have lost the ability to cleave VP4 from VP0. If this hypothesis is correct then the N-terminus of VP0 is likely to possess similar abilities to the VP4 of other picornaviruses. Therefore, the VP0 viruses present an interesting target for structural studies to study the capsid rearrangements associated with entry. A recent study investigating the structural rearrangements following genome release of AiV has shown that there are structural rearrangements within VP0 but did not observed the externalisation of VP0 (Sabin *et al*., 2016). This may contradict the idea that the N-terminus of VP0 harbours VP4 function. However, this study compared the icosahedral native capsid with an icosahedral averaged empty particle and therefore it is possible some asymmetric rearrangement of VP0 may have been lost.

The work presented in this chapter identified a region within the N-terminus of the VP4 of picornaviruses from multiple genera that appears to share some similarities in sequence and structure. The region identified fits with experimental data presented within this thesis and published elsewhere and could possibly be a shared region of picornaviruses. The N-terminus of VP0 for several VP0 viruses were then compared and some similarities were observed at the N-terminus of some of the genera but not others and these differences were investigated using synthetic peptides for two VP0 sequences.

## 6.2 Identification of a conserved sequence within picornavirus VP4 sequences

VP4 proteins for picornaviruses across different genera have been shown to have membrane permeabilising activity and it is possible this is due to a conserved region of VP4. The work presented in section 3.3 demonstrated that the N-terminal 30 amino acids of FMDV were sufficient to induce membrane permeability but the N-terminal 15 amino acids were not. Previous work with HRV VP4 peptides demonstrated that VP4-induced membrane permeability was found within the N-terminal 45 amino acids (Panjwani *et al*., 2016). Therefore, an attempt to identify any similarities between picornavirus VP4 sequences was made in collaboration with Dr James Kelly (The Pirbright Institute), with a focus on similarities in the N-terminus. The sequences of VP4 from several picornavirus genera were aligned using Muscle alignment software (Edgar, 2004).

Through the alignment, a region of similarity between amino acids 20 and 35 near the N-terminus of VP4 was identified for many of the picornaviruses (shown in figure 6.1). This region, referred to as the INNY region, is composed of polar and aromatic amino acids. In the cardioviruses and some aphthoviruses there are motifs that are the same as the IINNYY motif shown in FMDV at the top of figure 6.1. Whereas in the enteroviruses there is a repeat of an INY sequence in a similar place figure (6.1). In other genera, such as the sapeloviruses and cosaviruses, there are variations of these motifs with amino acids with similar properties, such as a change from isoleucine to valine. Therefore, it was hypothesised that INNY motifs could be within a region that was shared between VP4 proteins.

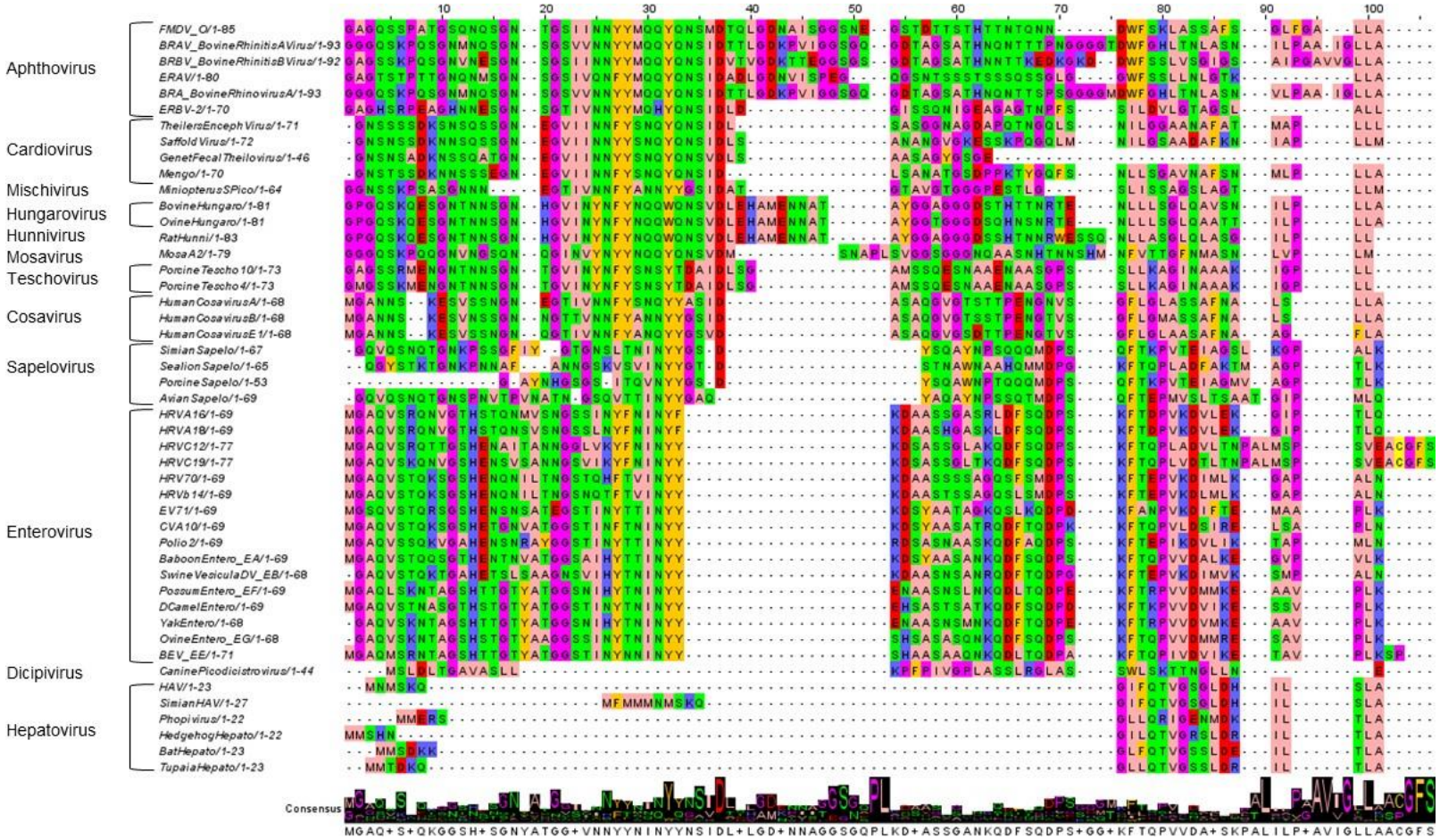


**Figure 6. 1: Alignment of picornavirus VP4 from several picornavirus genera.**

The alignment of picornavirus VP4 sequences from several genera was carried out using the MUSCLE sequence alignment tool (Edgar, 2004). The amino acids are coloured using the Zappo colour scheme as follows: aliphatic/ hydrophobic (pale pink), aromatic (orange), positively charged (purple), negatively charged (red), hydrophilic (green), conformationally special (magenta) and cysteine residues (yellow). Consensus sequence is shown below the alignment. This shows the percentage of the modal residue per column. A sequence logo showing the relative amount of residues per column is shown above the consensus sequence.

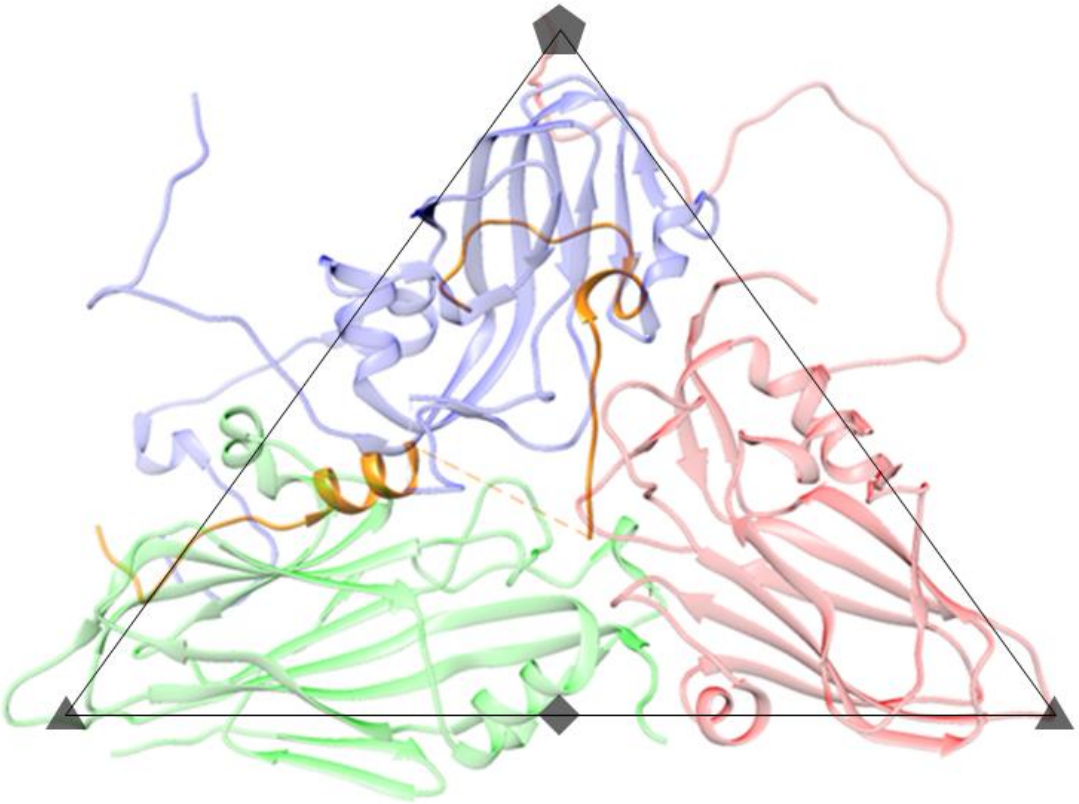

**Figure 6. 2: Location of FMDV VP4 within the capsid protomer**

The structure of FMDV VP4 (orange), shown with VP1 (blue), VP2 (green) and VP3 (red) within the capsid protomer. The axis of symmetry are shown as follows: fivefold axis (pentagon), threefold axis (triangle) and twofold axis (diamond). PDB accession used 1BBT.

As the structure of VP4 is likely to be more conserved than the amino acid sequence the structures of VP4 from within the capsid from several picornaviruses were compared. VP4 is internal within the capsid and the N-terminus of VP4 is found near the fivefold axis of symmetry and the C-terminus is found near the threefold axis of symmetry (shown in figure 6.2) (Acharya *et al*., 1989). The structure of FMDV VP4 was compared to the structures of VP4 from other genera of picornaviruses. For this comparison VP4 structures from the senecavirus Seneca Valley virus (SVV), the cardiovirus Theiler's murine encephalomyelitis virus (TMEV) and enterovirus PV were compared with VP4 from FMDV to represent the diversity of picornavirus capsid structures available. The VP4 structures of SVV and TMEV were more similar to the structure of FMDV VP4 than PV VP4 and lacked the N-terminal β sheet observed in PV VP4 (figure 6.3). The VP4 structures from SVV and TMEV have a small helix in the same location to FMDV (indicated in the box on figure 6.3). The VP4 structure of PV has a small helix in a similar place but it does not overlay completely with the helix in the FMDV VP4.

The amino acids within and before the helix were compared and for FMDV VP4 the IINNYY motif identified from the sequence alignment (figure 6.1) was found to be just before the helix (figure 6.4 A). The same region was investigated for PV VP4 and the second of the two INY sequences were found to be found in a similar location (figure 6.4 B). The position of the INNY region preceding a helix found in all VP4 sequences compared could have some conserved purpose.

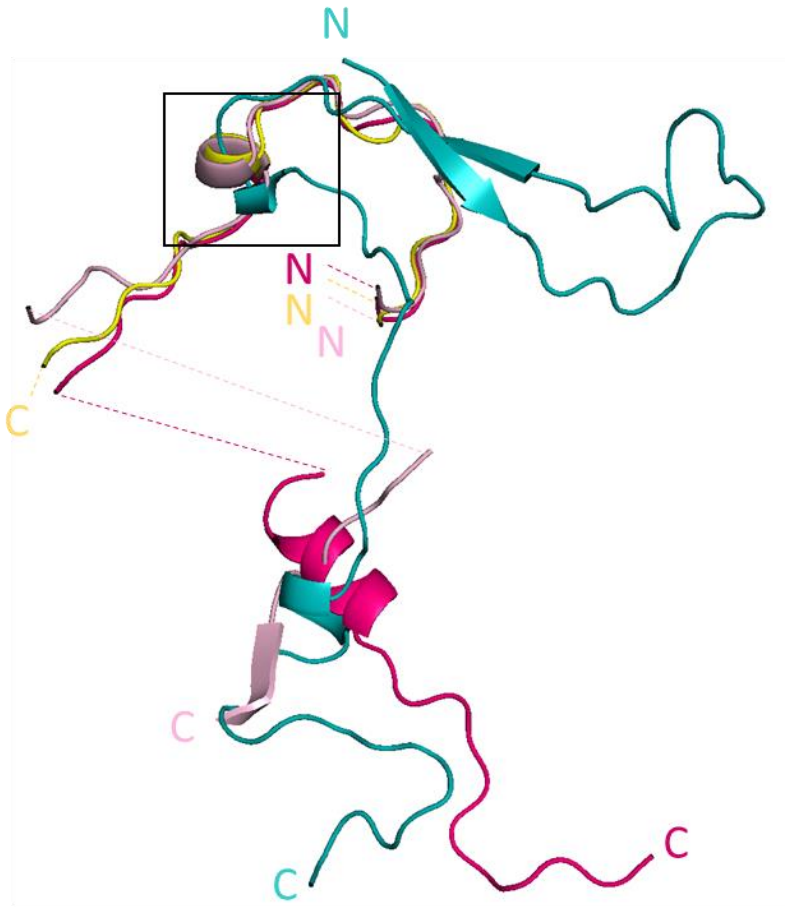


**Figure 6. 3: Comparison of VP4 structures from multiple picornaviruses**

The structures of FMDV VP4 (pink), PV VP4 (teal), SVV VP4 (pale pink) and TMEV VP4 (yellow) were compared using Pymol. The N-terminal helix is identified in the box. The N- and C-terminus of each protein is indicated by N or C in the appropriate colour. Missing structural information is indicated by the dashed lines. PDB accessions used 1BBT (FMDV), 1HXS (PV), 3CJI (SVV) and 1TME (TMEV). Image generated by Dr James Kelly (The Pirbright Institute).

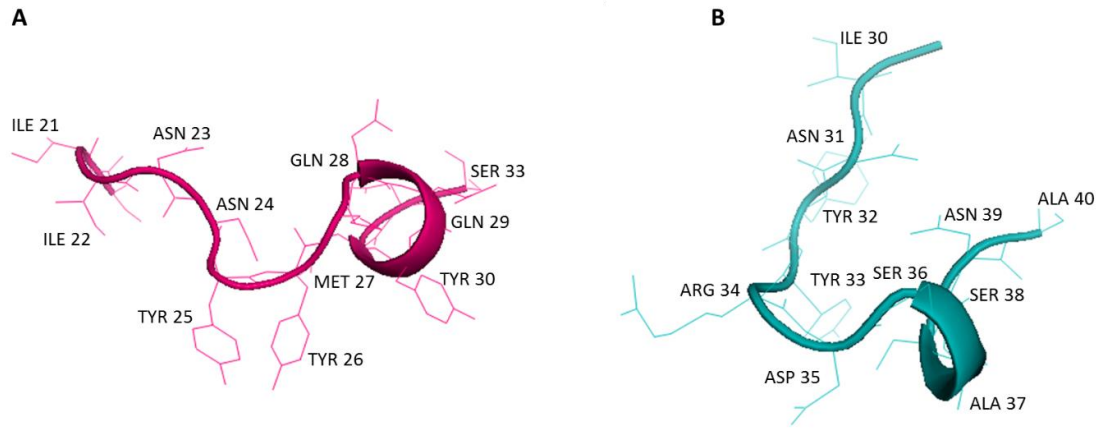


**Figure 6. 4: Comparison of the region around the N-terminal helix of FMDV and PV VP4.**

(A) Amino acids 21 to 33 of FMDV VP4 and (B) amino acids 30 to 40 of PV VP4 were annotated to show the residues surrounding the N-terminal helix. PDB accessions used 1BBT (FMDV) and 1HXS (PV). Figures made using Pymol.

## 6.3 Identification of a INNY-like region in some VP0 viruses

The VP0 picornaviruses, such as the kobuviruses and parechoviruses, are likely to have a requirement for membrane permeability during entry and genome transfer. One hypothesis for the origin of these viruses is that at some point picornaviruses lost the VP0 cleavage and therefore, the N-terminus of VP0 has retained the role of VP4. Based on the hypothesis that the INNY region (identified in section 6.2) is a conserved region between some picornavirus VP4 proteins, VP0 virus sequences were aligned with the aim of identifying a similar INNY-like region. The presence of a similar region could support the hypothesis that the N-terminus of VP0 is analogous to VP4.

The first 120 amino acids of several VP0 viruses from multiple genera were compared using a Muscle alignment (figure 6.4). The alignment shows there are some VP0 viruses that have a region which is similar to the INNY region at the N-terminus of VP0, such as amino acids 3-9 of AiV VP0. There are also several VP0 viruses that lack any sequence similarities with the INNY region in the first 120 amino acids, such as the parechovirus Ljungan virus (LV).

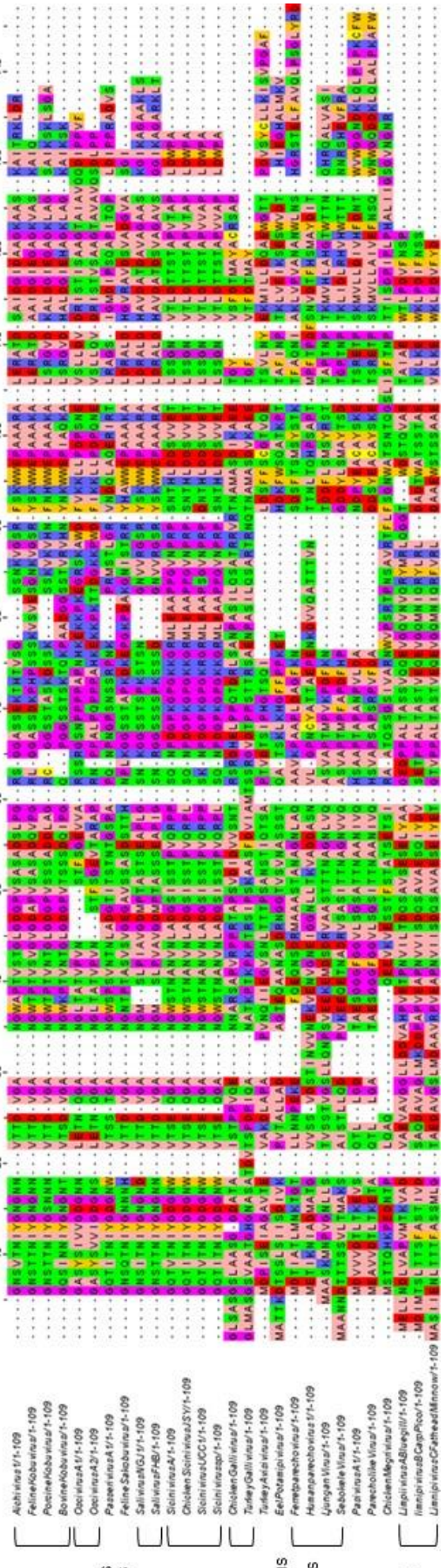


**Figure 6. 5: Alignment of picornavirus VP0 from several picornavirus genera.**

The alignment of the first 110 amino acids of picornavirus VP) sequences from several genera was carried out using the MUSCLE sequence alignment tool (Edgar, 2004). The amino acids are coloured using the Zappo colour scheme as follows: aliphatic/ hydrophobic (pale pink), aromatic (orange), positively charged (purple), negatively charged (red), hydrophilic (green), conformationally special (magenta) and cysteine residues (yellow). The genera of picornaviruses are shown on the left.

## 6.4 Peptides representing the N-terminus of Kobuvirus VP0 induce size-selective membrane permeability

The requirement for membrane permeability to allow endosomal escape is likely to be conserved across picornaviruses and work in the laboratory supports this hypothesis as Dr James Kelly (Dr James Kelly, personal communication) has shown that AiV is able to induce membrane permeability, as previously described for FMDV and HRV. The presence of the INNY-like region at the N-terminus of AiV VP0 could support the hypothesis that VP0 viruses result from a loss of VP0 cleavage and therefore, the N-terminus of VP0 is analogous to VP4 after cleavage. As some VP0 viruses had been identified to lack an identifiable INNY region, peptides of the N-terminal 45 amino acids of AiV VP0 (containing an INNY-like sequence) and LV VP0 (lacking an INNY-like sequence) were tested in membrane permeability assays to see if they shared a similar function to VP4.

Peptides representing the N-terminal 45 amino acids of LV VP0 and AiV VP0 were compared in CF release (method described in section 2.4.1). The peptide representing the N-terminus of AiV VP0 induced membrane permeability (figure 6.5). In contrast, a peptide of the N-terminus of LV induced minimal membrane permeability (figure 6.5). These experiments were undertaken twice due to time constraints and therefore the CF release presented could be considered preliminary. The CF release of the AiV VP0 peptide was characterised extensively and the data presented is representative of those experiments.

The AiV VP0 peptide was used in the FD release assay described in section 2.4.2 to establish if this peptide was able to induce size-selective membrane permeability as observed for both FMDV VP4 peptides (shown in section 3.4) and HRV VP4 peptides (Panjwani *et al*., 2016). The FD release assay showed that the AiV VP0 is able to release the smaller FD4 and some FD10 but did not release FD70 and FD250 (figure 6.6). This result indicated the membrane permeability induced by AiV VP0 is size-selective.

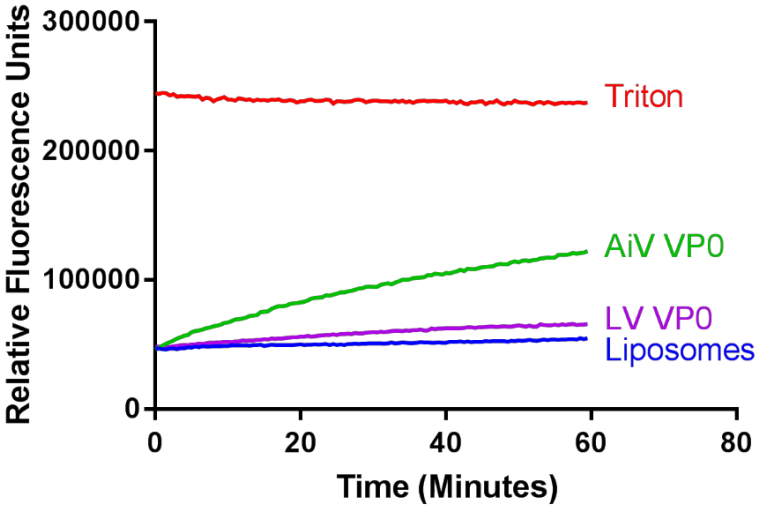


**Figure 6. 6: The N-terminus of AiV VP0 induced membrane permeability but the N-terminus of LV VP0 induces minimal membrane permeability.**

Liposomes containing carboxyfluorescein (CF) at self-quenching concentrations were mixed with AiV VP0 peptide or LV VP0 peptide at 5 µM and triton. Membrane permeability resulting in leakage and dequenching of CF was detected by fluorescence measurements (excitation 492 nm/ emission 512 nm) recorded every 30 seconds. Data shown represent n=2 experiments and data for this figure were generated by Dr James Kelly (The Pirbright Institute).

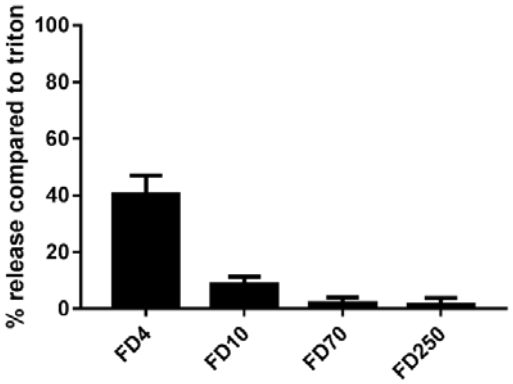


**Figure 6. 7: The N-terminus of AiV VP0 induced size-selective membrane permeability**

Liposomes containing FITC-linked dextrans (FDs) were mixed with AiV VP0 at 0.5 µM. Membrane permeability results in leakage of the FDs and fluorescence was measured in the supernatant after pelleting the liposomes. Data are presented as percentage of total release when detergent is added to the liposomes. Data shown are the mean of n=3 experiments and error bars show standard deviation.

## 6.5 Discussion

The data presented in this chapter has started to investigate the possibility of a conserved region in VP4 across picornaviruses that is important for membrane permeabilisation. Through alignment of VP4 sequences and comparison of atomic structures of VP4 within the capsid, a region at the N-terminus of VP4 containing similar amino acids has been identified and this has been termed the INNY region as it often contained a sequence containing isoleucine, asparagine and tyrosine. Investigation of the N-terminus of some VP0 picornaviruses has indicated that some VP0 viruses have an INNY-like region at the N-terminus. The kobuviruses contain an INNY-like region but the parechoviruses do not. Comparison of the membrane permeability induced by the N-terminus of AiV VP0 and LV VP0 revealed that the N-terminus of AiV VP0 is able to induce size-selective membrane permeability but the N-terminus of LV VP0 was not.

Comparison of the structure of VP4 within the capsid of several picornaviruses led to the observation that near the N-terminus there is a small helix. When the amino acids around this helix were investigated it was found they corresponded to the INNY region identified from the sequence alignments. Speculatively, the combination of a similar structural feature and region with a similar amino acid composition could point to an important role for this region within the virus lifecycle. If this is the case a conserved structure and sequence within VP4 could resemble the schematic in figure 6.8.

As VP4 plays several roles within the virus lifecycle it is possible this region is important for assembly, entry or another unknown role. The well-characterised lethal T28G mutation of PV VP4 is located within the proposed INNY region and mutant viruses were able to produce mature virus particles containing viral RNA, indicating this mutation does not renders PV assembly deficient (Danthi *et al*., 2003). The study by Danthi *et al.* shows evidence of a single mutation for PV so this result could differ between picornaviruses.

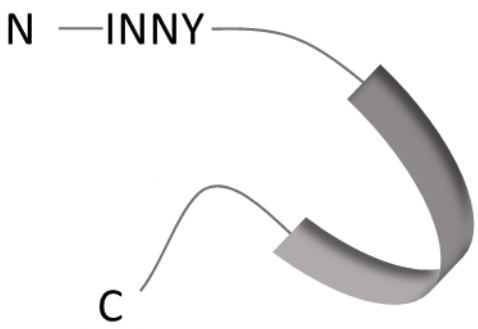


**Figure 6. 8: Schematic representative of the INNY region and helix within VP4.**

Near the N-terminus of the VP4 an INNY region would be located. INNY here refers to the region rather than the amino acid sequence. After the INNY region would be the small helix identified from comparison of VP4 structures within the capsid. There may be a 1-3 amino acid linker between a tyrosine residue and the beginning of the helix.

The hypothesis that the INNY region is involved in membrane permeability is supported by two observations. Firstly, the data presented in section 3.3 show that a short peptide ofthe first 15 amino acids of FMDV VP4 is not able to induce membrane permeability whereas longer peptides (30 or 45 amino acids) can induce membrane permeability. This suggests that the membrane permeabilising region could be located between amino acids 16-30, which would fit with the INNY region identified in section 6.2. Secondly, mutant PV with the well-characterised T28G mutation produces mature RNA-containing virus particles which are unable to form virus-induced channels and are unable to deliver the viral genome into cells, prevents PV infection (Danthi *et al*., 2003). The T28G mutation suggests there may be a link between the INNY region and a conserved region for membrane permeability, perhaps suggesting this region is essential for entry.

The atomic structure of FMDV VP4 shows that the N-terminus of VP4 is located near the fivefold axis of symmetry, where there is a capsid pore present (Acharya et al., 1989). Therefore, it could be predicted that the N-terminus of VP4 is being externalised through this pore, allowing it to be detected on the exterior of the capsid by VP4-specific antibodies (sections 5.2.3 and 5.3.2). The externalisation of the N-terminus of VP4 would allow FMDV to penetrate the endosomal membrane as the data in sections 3.2 and 3.4 show the N-terminus of FMDV VP4 is able induce size-selective membrane permeabilisation that would be a sufficient size for unfolded RNA to pass though. As the INNY region is at the N-terminus, this region could be a

conserved pore forming motif and would fit with the experimental data presented in this thesis.

Based on the analysis of the VP4 sequence, shown in chapter 3, there are no predicted transmembrane domains at the N-terminus of VP4 and there are no strongly hydrophobic stretches for amino acids at the N-terminus. However, the atomic structure of FMDV VP4 show that there is a helical region at the N-terminus, which is near the INNY region. The helical structure at the N-terminus of VP4 shows this sequence could have the ability to form a helical structure that could be involved in membrane permeability.

Within the mature FMDV capsid there are 60 copies of VP4, which are lost during the dissociation of the capsid during entry (Acharya et al., 1989). The low pH intermediate particle of ERAV shows that there are some copies of VP4 left within the capsid (Tuthill et al., 2009). This could suggest that while all VP4 proteins are able to induce pore formation there is not a requirement for all copies of VP4 to be lost from the capsid and that membrane penetration by FMDV VP4 does not require 60 copies of VP4.

However, there are picornaviruses that do not align at the N-terminus with the hypothesised INNY region (figure 6.1). Most of these are from the hepatovirus genus and the VP4 of HAV from this genus has been shown to induce size-selective membrane permeability (Shukla *et al*., 2014). Structural phylogenetic analysis of the HAV capsid compared to the discistrovirus and picornavirus capsids have shown that HAV shares capsid features with both picornaviruses and discistroviruses (Wang *et al*., 2015). The phylogenetic tree based on the P1 region of picornavirus capsids (shown in section 1.2) shows that the hepatoviruses belong to a more divergent branch of the picornaviruses compared to the aphthoviruses and enteroviruses. The VP4 protein from the distantly related triatomavirus, a member of the family *discistroviridae* within the order *Picornavirales*, has also been shown to induce size-selective membrane permeability (Sanchez-Eugenia *et al*., 2015). Therefore, it is possible that the VP4 protein of the hepatoviruses could share similarity with discistrovirus VP4.

The identification of INNY-like regions in VP0 sequences suggests that for some VP0 viruses the N-terminus of VP0 is similar to VP4 and could indicate that in these cases the N-terminus of VP0 contains VP4 membrane penetrating activity. Peptides representing the N-terminus of VP0 for AiV (containing an INNY-like region) and LV

(lacking an INNY-like region) were compared in membrane permeability assays. The AiV VP0 peptide was able to induce membrane permeability while the LV peptide induced minimal membrane permeability. Work within the laboratory has shown that AiV is able to induce membrane permeability in CF release assays (Dr James Kelly, personal communication) and this could be due to the membrane permeability induced by the N-terminus of VP0.

The concentration of AiV VP0 used in the CF membrane permeability assay was higher than previously used for FMDV peptides in chapter 3. The AiV VP0 peptide lacked myristoylation and as this post translational modification has been shown to enhance membrane permeability of the FMDV VP4N45 peptide and HRV VP4 this could explain why the membrane permeability is so low. A lower concentration of the AiV peptide was used in the FD release and showed size-selective membrane permeability, suggesting the CF experiments should be attempted at a lower concentration. The membrane permeability induced by the N-terminus of AiV VP0 could be further investigate using peptides of different lengths from the N-terminus to begin to map the membrane permeabilising function of this peptide.

The atomic structure of an AiV empty particle has been obtained and this does not show any externalisation of the N-terminus of VP0 (Sabin *et al*., 2016). However, in this structure the N-terminal 11 amino acids are not resolved and it is within these residues the INNY-like sequence was identified. Therefore, despite the lack of observable VP0 externalisation, it is possible the N-terminus of VP0 is playing a role in genome transfer and following RNA release the capsid could undergo a further rearrangement.

The atomic structure of the LV capsid has been determined and comparison of the LV capsid with other picornaviruses capsid structures has shown it shares most similarity with HAV (Zhu *et al*., 2015). As LV VP0 did not induce membrane permeability a piece of interesting future work would be to determine if LV induced size-selective membrane permeability and then carry out studies with peptides spanning the length of VP0.

The work presented in this chapter is preliminary but could warrant further work to investigate the observations relating to the INNY region and small helix discussed here. It would seem unlikely that all picornaviruses have independently evolved the ability to penetrate the endosomal membrane and therefore, it may be possible that there is a shared functional region of VP4. Whether the proposed region fulfils this role

remains to be characterised further but it presents an interesting target for future studies.

# Chapter 7 Discussion and future perspectives

# 7. Discussion and future perspectives

A critical step in cell entry of any virus is the delivery of the viral genome to the site of replication. This is vital to allow the production of new progeny virus particles and therefore onward spread of infection. Following receptor-mediated endocytosis, the lipid bilayer of the endosome presents a physical barrier that prevents infection of the cell. Therefore, it is unsurprising that strategies for crossing the endosomal membrane have arisen. Non-enveloped viruses have developed mechanisms that allow them to penetrate this membrane and continue the lifecycle. Several non-enveloped viruses have been shown to utilise a small, often internal, capsid protein that when triggered facilitates the penetration of the host membrane through several mechanisms (described in section 1.7.2). It is particularly striking that, regardless of the diversity of non-enveloped viruses, a common theme for non-enveloped virus entry is emerging.

In the case of picornaviruses, the small internal capsid protein VP4 of HRV and HAV has been shown to permeabilise membranes and therefore is proposed to play a role in the penetration of the endosomal membrane (Panjwani *et al*., 2014, Shukla *et al*., 2014). In the case of HRV, this activity has been demonstrated to be found in the N-terminus of VP4 (Panjwani *et al*., 2016). The work presented here is the first study looking at the membrane permeability induced by the VP4 of an aphthovirus and showed that both the N- and C-terminus of FMDV VP4 were able to induce membrane permeability. Antibodies that targeted either terminus of VP4 did not prevent FMDV-induced membrane permeability. Additionally, through characterisation of the VP4-specific antibodies generated in this work there is evidence that FMDV undergoes the process of capsid breathing, similar to that previously described for other picornaviruses (described in section 1.6.3).

In this thesis, the membrane permeability induced by synthetic peptide representing the N- and C-terminus of FMDV VP4 was characterised. In contrast to previous work with HRV VP4, the work presented here shows that both the N- and C-terminus of FMDV VP4 are able to induce size-selective membrane permeability that is similar to that attributed to the N-terminus of HRV VP4 (sections 3.2 and 3.4) (Panjwani *et al*., 2016). Further studies using a full length VP4 protein would help to characterise how VP4 as a whole permeabilises membranes. Comparison of the membrane permeability induced by full length VP4 with the membrane permeability induced by FMDV and VP4 peptides could help to complete the picture. It is possible that the membrane permeability induced by full length VP4 could link increase permeability by VP4 peptides described in section 3.2 and other work in the laboratory which has

demonstrated that FMDV-induced membrane permeability increases with decreasing pH.

Previous work within the laboratory demonstrated that bacterial expression of a recombinant FMDV VP4 did not yield significant amounts of protein and was not viable for large scale production of FMDV VP4 (Dr Anusha Panjwani, unpublished data). The purification of VP4 may be more achievable in the future by using immunoprecipitation utilising the panel of VP4-specific antibodies described in this thesis to isolate VP4 from inactivated virus.

The work in section 3.4 suggests that either termini of FMDV VP4 could be forming a membrane pore similar to that described for HRV VP4 (Panjwani *et al*., 2014). The structure of FMDV VP4 is not fully resolved. Therefore, carrying out structural studies using the full length VP4 isolated from virus could help to understand if FMDV VP4 multimerises and shed light on how VP4 permeabilises membranes. Preliminary studies using native non-denaturing mass spectrometry were attempted in collaboration with the mass spectrometry facility at the University of Leeds but these did not indicate multimerisation. The lack of multimerisation observed could be due to the inability of VP4 peptides to multimerise in solution and may suggest a lipid mimetic environment is required to allow the peptides to fully multimerise. Therefore, future studies using mass spectrometry could be attempted as there has been some success spraying membrane proteins for native mass spec from detergents or amphipols. This would help us to understand if FMDV multimerises and through comparisons of the multimerisation by full length VP4 and the peptides characterised here it may be possible to determine if both termini are biologically relevant.

Alongside the characterisation of membrane permeability, antibodies against FMDV VP4 have been generated through display on hepatitis B core virus-like particles (HBc VLPs) and through conventional peptide-KLH conjugates. Two approaches for the display of the N-terminal 15 amino acids of FMDV VP4 on the HBc VLPs were compared. The first approach was the formation of a recombinant VLP and the second approach was a native HBc VLP decorated with VP4N15 peptides. Following immunisation into mice the recombinant VLP induced VP4-specific antibodies whereas the peptide decorated VLP did not (shown in section 5.2.2). The peptide attachment approach was unsuccessful and the possible reasons for this are discussed in section 5.4. Unfortunately, the antibodies generated by the recombinant VLPs failed to produce a neutralising antibody response (section 5.2.4). This could be due to the conformation of VP4 within the HBc VLP preventing neutralising

conformational antibodies being produced. However, this may be unlikely because the data in section 5.2.3 demonstrate that the VP4-specific antibodies are in a conformation that can detect VP4 in a FMDV sandwich ELISA.

The panel of VP4 antibodies presented here were unable to neutralise FMDV infection (sections 5.2.4 and 5.3.3) and this was unexpected compared to previous neutralising antibodies discovered against the VP4 proteins of HRV and PV (Li *et al*., 1994, Panjwani *et al*., 2016). The evidence from other picornaviruses, discussed in section 1.9, suggests that neutralisation by VP4 antibodies against PV occurs through the binding of these antibodies to the transiently externalised VP4 sequence, exposed as a result of breathing (Li *et al*., 1994). The evidence from neutralising antibodies against HRV VP4 suggests that these antibodies can also bind to VP4 at the stage of membrane permeability and this could indicate a second mechanism of neutralisation (Panjwani *et al*., 2016).

All of the antibodies generated in this thesis against FMDV VP4 were able to detect FMDV captured by recombinant integrin in an ELISA (sections 5.2.3 and 5.3.1). This provides the first evidence that the process of capsid breathing occurs in FMDV. The process of capsid breathing in FMDV appears to result in the externalisation of both the N- and C-terminus of VP4, in contrast to data demonstrating the N-terminus of enteroviruses is externalised (Li *et al*., 1994). It is possible that this result does not fully reflect breathing in free virus because the FMDV in this assay was captured with the natural FMDV receptor, integrin. The structure of FMDV in complex with integrin has been solved and no externalisation of VP4 was observed. Therefore, this supports the idea that in contrast to PV, receptor binding by FMDV does not drive a conformational change to an entry intermediate and integrin is not required for entry (Kotecha *et al*., 2017). This suggests the ELISA results here are not due to a receptor binding-induced conformational change.

Monoclonal antibodies against the N-terminus of FMDV VP4 have been generated (section 5.2.6) and it would be interesting to characterise these for FMDV binding and utilise them in structural studies to capture the externalisation of FMDV VP4. The presence of breathing in FMDV indicates this process could be a conserved mechanism across picornaviruses, which would fit with the notion that all picornavirus capsids should exist in a state that is both protecting the viral RNA and also primed to undergo uncoating following environmental triggers.

The purified IgG against the N- and C-termini of FMDV VP4 was unable to prevent FMDV-induced membrane permeability (section 5.2.5 and 5.3.3). This could be because the immunodominant region of these peptides is not the portion of VP4 required for membrane permeability or the VP4 structure during membrane permeability is different from the KLH-peptide conjugate. The IgG against the N- and C-terminus of FMDV VP4 was not used in combination but this may be an interesting way to evaluate if the VP4 activity in FMDV can be blocked though antibody binding. If antibodies against both termini can inhibit FMDV-induced membrane permeability it is possible that future VLP display approaches should utilise the entire VP4 sequence.

As membrane permeability has been demonstrated in the VP4 sequence of several picornaviruses from different genera an attempt to identify similarities between picornavirus RNA sequences was made (Shukla *et al*., 2014, Panjwani *et al*., 2014). Alignment of VP4 sequences from several picornaviruses showed that there was a similar region within the N-terminus of VP4 proteins from several genera of picornaviruses and this was termed the INNY sequence (section 6.2). A similar region was identified in the N-terminus of some VP0 containing picornaviruses but not all of them. The presence of the INNY region at the N-terminus of VP0 may be linked to the ability of synthetic VP0 peptides to induce membrane permeability. Therefore, this may support the hypothesis that for some VP0 containing picornaviruses the N-terminus of VP0 has retained VP4 activity. The hypothesis that the INNY region is involved with membrane permeability could be investigated by mutating individual amino acids within this region to identify other mutations like the T28 mutations in PV that prevent virus entry (Moscufo *et al*., 1993).

If there is a conserved mechanism of VP4 permeability, resulting from the INNY region within the N-terminus of VP4, it would appear that FMDV VP4 has developed an additional membrane penetrating capability at the C-terminus. This C-terminal membrane permeability may be biologically relevant could be linked to the acid instability of the FMDV capsid. The requirement of both termini and could be investigated further using techniques such as alanine scanning to identify key mutations. Alternatively, site saturation mutagenesis could be used to investigate which amino acid substitutions can be tolerated and this might elude to the role of the amino acid in this position. Any mutations that did not produce virus or produced an attenuated virus could then be investigated to see if the mutation was affecting the virus through the role of VP4 in entry or assembly. Mutagenesis experiments targeting in the INNY region in FMDV to see if a similar key residue to the T28 in PV could be identified, as that may show more similarities between the N-terminus of FMDV and

PV VP4.

In conclusion the work presented in this thesis contributes to expanding the understanding of the role of VP4 in picornavirus capsid breathing and membrane permeability by studying the VP4 protein of the aphthovirus FMDV. Studying more diverse picornaviruses is particularly important to prevent bias in the field towards the enteroviruses and further the understanding of shared mechanisms. The model proposed here is a shared mechanism across picornaviruses, starting with a metastable capsid, which transiently externalises the internal capsid protein VP4 through the process of capsid breathing. The transient externalisation of VP4 is important as it would allow the virus to be primed for genome release should the virus become in close proximity of a membrane. When the virus is in close proximity to the membrane, as would occur through receptor binding, an external stimuli (receptor binding or pH) results in VP4 release from virus. As the virus is in close proximity to the membrane, the released VP4 inserts into the endosomal membrane and forms an umbilicus structure between the virus and the membrane, possibly involving other capsid proteins. Therefore, it seems that there is a shared requirement for VP4-induced membrane permeability, which may share common features. However, individual members of the picornavirus family have evolved variations of VP4-induced membrane permeability to meet the requirements of the individual virus entry pathway. Genome transfer then proceeds through a pore formed by VP4, allowing controlled and protected release of the genome. Following safe delivery of the genome the virus capsid is not required to maintain its stability and may end up dissociating or remaining as an empty particle.

# References


Acharya, R., Fry, E., Stuart, D., Fox, G., Rowlands, D. & Brown, F. 1989. The three-dimensional structure of foot-and-mouth disease virus at 2.9 A resolution. *Nature,* 337**,** 709-16.

Agosto, M. A., Ivanovic, T. & Nibert, M. L. 2006. Mammalian reovirus, a nonfusogenic nonenveloped virus, forms size-selective pores in a model membrane. *Proceedings of the National Academy of Sciences of the United States of America* 103**,** 16496-501.

Akbarzadeh, A., Rezaei-Sadabady, R., Davaran, S., Joo, S. W., Zarghami, N., Hanifehpour, Y., Samiei, M., Kouhi, M. & Nejati-Koshki, K. 2013. Liposome: classification, preparation, and applications. *Nanoscale Research Letters,* 8**,** 102-102.

Alexandersen, S., Zhang, Z., Donaldson, A. I. & Garland, A. J. M. 2003. The Pathogenesis and Diagnosis of Foot-and-Mouth Disease. *Journal of Comparative Pathology,* 129**,** 1-36.

Andreev, D. E., Fernandez-Miragall, O., Ramajo, J., Dmitriev, S. E., Terenin, I. M., Martinez-Salas, E. & Shatsky, I. N. 2007. Differential factor requirement to assemble translation initiation complexes at the alternative start codons of foot-and-mouth disease virus RNA. *RNA,* 13**,** 1366-74.

Ao, D., Guo, H. C., Sun, S. Q., Sun, D. H., Fung, T. S., Wei, Y. Q., Han, S. C., Yao, X. P., Cao, S. Z., Liu, D. X. & Liu, X. T. 2015. Viroporin Activity of the Foot-and-Mouth Disease Virus Non-Structural 2B Protein. *PLOS ONE,* 10**,** e0125828.

Arnold, E., Luo, M., Vriend, G., Rossmann, M. G., Palmenberg, A. C., Parks, G. D., Nicklin, M. J. & Wimmer, E. 1987. Implications of the picornavirus capsid structure for polyprotein processing. *Proceedings of the National Academy of Sciences of the United States of America,* 84**,** 21-5.

Bajaj, S., Dey, D., Bhukar, R., Kumar, M. & Banerjee, M. 2016. Non-Enveloped Virus Entry: Structural Determinants and Mechanism of Functioning of a Viral Lytic Peptide. *Journal of Molecular Biology,* 428**,** 3540-56.

Banerjee, M. & Johnson, J. E. 2008. Activation, exposure and penetration of virally encoded, membrane-active polypeptides during non-enveloped virus entry. *Current Protein and Peptide Science,* 9**,** 16-27.

Baumann, G. & Mueller, P. 1974. A molecular model of membrane excitability. *Journal of Supramolecular Structure,* 2**,** 538-57.

Baxt, B. & Bachrach, H. L. 1980. Early interactions of foot-and-mouth disease virus with cultured cells. *Virology,* 104**,** 42-55.

Beard, C. W. & Mason, P. W. 2000. Genetic determinants of altered virulence of Taiwanese foot-and-mouth disease virus. *Journal of Virology,* 74**,** 987-91.

Belnap, D. M., Filman, D. J., Trus, B. L., Cheng, N., Booy, F. P., Conway, J. F., Curry, S., Hiremath, C. N., Tsang, S. K., Steven, A. C. & Hogle, J. M. 2000. Molecular tectonic model of virus structural transitions: the putative cell entry states of poliovirus. *Journal of Virology,* 74**,** 1342-54.

Belsham, G. J. & Bostock, C. J. 1988. Studies on the infectivity of foot-and-mouth disease virus RNA using microinjection. *Journal of General Virology,* 69 ( Pt 2)**,** 265-74.

Belsham, G. J. & Brangwyn, J. K. 1990. A region of the 5' noncoding region of foot-and-mouth disease virus RNA directs efficient internal initiation of protein synthesis within cells: involvement with the role of L protease in translational control. *Journal of Virology,* 64**,** 5389-95.

Bergelson, J. M., Cunningham, J. A., Droguett, G., Kurt-Jones, E. A., Krithivas, A., Hong, J. S., Horwitz, M. S., Crowell, R. L. & Finberg, R. W. 1997. Isolation of a common receptor for Coxsackie B viruses and adenoviruses 2 and 5. *Science,* 275**,** 1320-3.

Berryman, S., Clark, S., Monaghan, P. & Jackson, T. 2005. Early events in integrin alpha v beta 6-mediated cell entry of foot-and-mouth disease virus. *Journal of Virology,* 79**,** 8519-8534.

Birtley, J. R., Knox, S. R., Jaulent, A. M., Brick, P., Leatherbarrow, R. J. & Curry, S. 2005. Crystal structure of foot-and-mouth disease virus 3C protease. New insights into catalytic mechanism and cleavage specificity. *Journal of Biological Chemistry,* 280**,** 11520-7.

Blokhina, E. A., Kuprianov, V. V., Stepanova, L. A., Tsybalova, L. M., Kiselev, O. I., Ravin, N. V. & Skryabin, K. G. 2013. A molecular assembly system for presentation of antigens on the surface of HBc virus-like particles. *Virology,* 435**,** 293-300.

Blumenthal, R., Seth, P., Willingham, M. C. & Pastan, I. 1986. pH-dependent lysis of liposomes by adenovirus. *Biochemistry,* 25**,** 2231-7.

Bodkin, D. K., Nibert, M. L. & Fields, B. N. 1989. Proteolytic digestion of reovirus in the intestinal lumens of neonatal mice. *Journal of Virology,* 63**,** 4676-81.

Bong, D. T., Janshoff, A., Steinem, C. & Ghadiri, M. R. 2000. Membrane partitioning of the cleavage peptide in flock house virus. *Biophysical Journal,* 78**,** 839-45.

Bong, D. T., Steinem, C., Janshoff, A., Johnson, J. E. & Reza Ghadiri, M. 1999. A highly membrane-active peptide in Flock House virus: implications for the mechanism of nodavirus infection. *Chemistry & Biology,* 6**,** 473-81.

Bostina, M., Levy, H., Filman, D. J. & Hogle, J. M. 2011. Poliovirus RNA is released from

the capsid near a twofold symmetry axis. *Journal of Virology,* 85**,** 776-83.

Bottcher, B., Tsuji, N., Takahashi, H., Dyson, M. R., Zhao, S., Crowther, R. A. & Murray, K. 1998. Peptides that block hepatitis B virus assembly: analysis by cryomicroscopy, mutagenesis and transfection. *The EMBO Journal,* 17**,** 6839-45.

Brandenburg, B., Lee, L. Y., Lakadamyali, M., Rust, M. J., Zhuang, X. & Hogle, J. M. 2007. Imaging poliovirus entry in live cells. *PLOS Biol,* 5**,** e183.

Breuss, J. M., Gillett, N., Lu, L., Sheppard, D. & Pytela, R. 1993. Restricted distribution of integrin beta 6 mRNA in primate epithelial tissues. *The Journal of Histochemistry and Cytochemistry,* 41**,** 1521-7.

Brown, F. & Cartwright, B. 1961. Dissociation of foot-and-mouth disease virus into its nucleic acid and protein components. *Nature,* 192**,** 1163-4.

Bubeck, D., Filman, D. J., Cheng, N., Steven, A. C., Hogle, J. M. & Belnap, D. M. 2005. The Structure of the Poliovirus 135S Cell Entry Intermediate at 10-Angstrom Resolution Reveals the Location of an Externalized Polypeptide That Binds to Membranes. *Journal of Virology,* 79**,** 7745-7755.

Burroughs, J. N., Rowlands, D. J., Sangar, D. V., Talbot, P. & Brown, F. 1971. Further evidence for multiple proteins in the foot-and-mouth disease virus particle. *Journal of General Virology,* 13**,** 73-84.

Caspar, D. L. & Klug, A. 1962. Physical principles in the construction of regular viruses. *Cold Spring Harbor Symposia on Quantitative Biology,* 27**,** 1-24.

Chambers, M. A., Dougan, G., Newman, J., Brown, F., Crowther, J., Mould, A. P., Humphries, M. J., Francis, M. J., Clarke, B., Brown, A. L. & Rowlands, D. 1996. Chimeric hepatitis B virus core particles as probes for studying peptide-integrin interactions. *Journal of Virology,* 70**,** 4045-52.

Chandran, K., Farsetta, D. L. & Nibert, M. L. 2002. Strategy for nonenveloped virus entry: a hydrophobic conformer of the reovirus membrane penetration protein micro 1 mediates membrane disruption. *Journal of Virology,* 76**,** 9920-33.

Chandran, K., Walker, S. B., Chen, Y., Contreras, C. M., Schiff, L. A., Baker, T. S. & Nibert, M. L. 1999. In vitro recoating of reovirus cores with baculovirus-expressed outer-capsid proteins mu1 and sigma3. *Journal of Virology,* 73**,** 3941-50.

Chow, M., Newman, J. F., Filman, D., Hogle, J. M., Rowlands, D. J. & Brown, F. 1987. Myristylation of picornavirus capsid protein VP4 and its structural significance. *Nature,* 327**,** 482-6.

Cicala, C., Arthos, J. & Fauci, A. S. 2011. HIV-1 envelope, integrins and co-receptor use in mucosal transmission of HIV. *Journal of Translational Medicine,* 9 Suppl 1**,** S2.

Clavijo, A., Wright, P. & Kitching, P. 2004. Developments in diagnostic techniques for differentiating infection from vaccination in foot-and-mouth disease. *Veterinary Journal,* 167**,** 9-22.

Crooks, G. E., Hon, G., Chandonia, J. M. & Brenner, S. E. 2004. WebLogo: a sequence logo generator. *Genome Research,* 14**,** 1188-90.

Curry, S., Chow, M. & Hogle, J. M. 1996. The poliovirus 135S particle is infectious. *Journal of Virology,* 70**,** 7125-31.

Curry, S., Fry, E., Blakemore, W., Abu-Ghazaleh, R., Jackson, T., King, A., Lea, S., Newman, J. & Stuart, D. 1997. Dissecting the roles of VP0 cleavage and RNA packaging in picornavirus capsid stabilization: the structure of empty capsids of foot-and-mouth disease virus. *Journal of Virology,* 71**,** 9743-52.

D'souza, S. E., Ginsberg, M. H. & Plow, E. F. 1991. Arginyl-glycyl-aspartic acid (RGD): a cell adhesion motif. *Trends in Biochemical Sciences,* 16**,** 246-50.

Danthi, P., Tosteson, M., Li, Q. H. & Chow, M. 2003. Genome Delivery and Ion Channel Properties Are Altered in VP4 Mutants of Poliovirus. *Journal of Virology,* 77**,** 5266-5274.

Davis, M. P., Bottley, G., Beales, L. P., Killington, R. A., Rowlands, D. J. & Tuthill, T. J. 2008. Recombinant VP4 of human rhinovirus induces permeability in model membranes. *Journal of Virology,* 82**,** 4169-74.

De Sena, J. & Mandel, B. 1977. Studies on the in vitro uncoating of poliovirus. II. Characteristics of the membrane-modified particle. *Virology,* 78**,** 554-66.

Dechecchi, M. C., Melotti, P., BONIZZAto, A., Santacatterina, M., Chilosi, M. & Cabrini, G. 2001. Heparan sulfate glycosaminoglycans are receptors sufficient to mediate the initial binding of adenovirus types 2 and 5. *Journal of Virology,* 75**,** 8772-80.

Devaney, M. A., Vakharia, V. N., Lloyd, R. E., Ehrenfeld, E. & Grubman, M. J. 1988. Leader protein of foot-and-mouth disease virus is required for cleavage of the p220 component of the cap-binding protein complex. *Journal of Virology,* 62**,** 4407-9.

Dicara, D., Burman, A., Clark, S., Berryman, S., Howard, M. J., Hart, I. R., Marshall, J. F. & Jackson, T. 2008. Foot-and-mouth disease virus forms a highly stable, EDTA-resistant complex with its principal receptor, integrin alpha v beta 6: Implications for infectiousness. *Journal of Virology,* 82**,** 1537-1546.

Diouri, M., Keyvani-Amineh, H., Geoghegan, K. F. & Weber, J. M. 1996. Cleavage efficiency by adenovirus protease is site-dependent. *Journal of Biological Chemistry,* 271**,** 32511-4.

Donnelly, M. L., Luke, G., Mehrotra, A., Li, X., Hughes, L. E., Gani, D. & Ryan, M. D. 2001. Analysis of the aphthovirus 2A/2B polyprotein 'cleavage' mechanism indicates not a proteolytic reaction, but a novel translational effect: a putative ribosomal 'skip'. *Journal of General Virology,* 82**,** 1013-25.

Duque, H., Larocco, M., Golde, W. T. & Baxt, B. 2004. Interactions of foot-and-mouth disease virus with soluble bovine alphaVbeta3 and alphaVbeta6 integrins.

*Journal of Virology,* 78**,** 9773-81.

Edgar, R. C. 2004. MUSCLE: multiple sequence alignment with high accuracy and high throughput. *Nucleic Acids Research,* 32**,** 1792-1797.

Farazi, T. A., Waksman, G. & Gordon, J. I. 2001. The biology and enzymology of protein N-myristoylation. *Journal of Biological Chemistry,* 276**,** 39501-4.

Ferrer-Orta, C., Arias, A., Agudo, R., Pérez-Luque, R., Escarmís, C., Domingo, E. & Verdaguer, N. 2006. The structure of a protein primer–polymerase complex in the initiation of genome replication*. The EMBO Journal,* 25**,** 880-888.

Ferrer-Orta, C., Arias, A., Perez-Luque, R., Escarmis, C., Domingo, E. & Verdaguer, N. 2004. Structure of foot-and-mouth disease virus RNA-dependent RNA polymerase and its complex with a template-primer RNA. *Journal of Biological Chemistry,* 279**,** 47212-21.

Filman, D. J., Syed, R., Chow, M., Macadam, A. J., Minor, P. D. & Hogle, J. M. 1989. Structural factors that control conformational transitions and serotype specificity in type 3 poliovirus. *The EMBO Journal,* 8**,** 1567-1579.

Fisher, A. J. & Johnson, J. E. 1993. Ordered duplex RNA controls capsid architecture in an icosahedral animal virus. *Nature,* 361**,** 176-9.

Fricks, C. E. & Hogle, J. M. 1990. Cell-induced conformational change in poliovirus: externalization of the amino terminus of VP1 is responsible for liposome binding. *Journal of Virology,* 64**,** 1934-1945.

Fry, E. E., Stuart, D. I. & Rowlands, D. J. 2005. The structure of foot-and-mouth disease virus. *Current Topics in Microbiology and Immunology,* 288**,** 71-101.

Galloux, M., Libersou, S., Morellet, N., Bouaziz, S., Da Costa, B., Ouldali, M., Lepault, J. & Delmas, B. 2007. Infectious bursal disease virus, a non-enveloped virus, possesses a capsid-associated peptide that deforms and perforates biological membranes. *Journal of Biological Chemistry,* 282**,** 20774-84.

Gao, Y., Sun, S. Q. & Guo, H. C. 2016. Biological function of Foot-and-mouth disease virus non-structural proteins and non-coding elements. *Journal of Virology,* 13**,** 107.

Garcia-Nunez, S., Gismondi, M. I., Konig, G., Berinstein, A., Taboga, O., Rieder, E., Martinez-Salas, E. & Carrillo, E. 2014. Enhanced IRES activity by the 3'UTR element determines the virulence of FMDV isolates. *Virology,* 448**,** 303-13.

Goodwin, S., Tuthill, T. J., Arias, A., Killington, R. A. & Rowlands, D. J. 2009. Foot-and-mouth disease virus assembly: processing of recombinant capsid precursor by exogenous protease induces self-assembly of pentamers in vitro in a myristoylation-dependent manner. *Journal of Virology,* 83**,** 11275-82.

Gorbalenya, A. E., Koonin, E. V. & Lai, M. M. 1991. Putative papain-related thiol proteases of positive-strand RNA viruses. Identification of rubi- and aphthovirus

proteases and delineation of a novel conserved domain associated with proteases of rubi-, alpha- and coronaviruses. *FEBS Letters,* 288**,** 201-5.

Göttlinger, H. G., Sodroski, J. G. & Haseltine, W. A. 1989. Role of capsid precursor processing and myristoylation in morphogenesis and infectivity of human immunodeficiency virus type 1. *Proceedings of the National Academy of Sciences of the United States of America,* 86**,** 5781-5785.

Gregson, A. L., Oliveira, G., Othoro, C., Calvo-Calle, J. M., Thorton, G. B., Nardin, E. & Edelman, R. 2008. Phase I Trial of an Alhydrogel Adjuvanted Hepatitis B Core Virus-Like Particle Containing Epitopes of Plasmodium falciparum Circumsporozoite Protein. *PLOS ONE,* 3**,** e1556.

Groppelli, E., Levy, H. C., Sun, E., Strauss, M., Nicol, C., Gold, S., Zhuang, X., Tuthill, T. J., Hogle, J. M. & Rowlands, D. J. 2017. Picornavirus RNA is protected from cleavage by ribonuclease during virion uncoating and transfer across cellular and model membranes. *PLOS Biology,* 13**,** e1006197.

Grubman, M. J. & Baxt, B. 2004. Foot-and-Mouth Disease. *Clinical Microbiology Reviews,* 17**,** 465-493.

Grubman, M. J., Robertson, B. H., Morgan, D. O., Moore, D. M. & Dowbenko, D. 1984. Biochemical map of polypeptides specified by foot-and-mouth disease virus. *Journal of Virology,* 50**,** 579-86.

Harrison, S. C. 2008. Viral membrane fusion. *Nature Structural and Molecular Biology,* 15**,** 690-8.

Harrison, S. C. 2015. Viral membrane fusion. *Virology,* 479-480**,** 498-507.

Harutyunyan, S., Kumar, M., Sedivy, A., Subirats, X., Kowalski, H., Kohler, G. & Blaas, D. 2013. Viral uncoating is directional: exit of the genomic RNA in a common cold virus starts with the poly-(A) tail at the 3'-end. *PLOS Biology,* 9**,** e1003270.

Herod, M. R., Gold, S., Lasecka-Dykes, L., Wright, C., Ward, J. C., Mclean, T. C., Forrest, S., Jackson, T., Tuthill, T. J., Rowlands, D. J. & Stonehouse, N. J. 2017. Genetic economy in picornaviruses: Foot-and-mouth disease virus replication exploits alternative precursor cleavage pathways. *PLOS Biology,* 13**,** e1006666.

Hewat, E. A., Neumann, E. & Blaas, D. 2002. The concerted conformational changes during human rhinovirus 2 uncoating. *Molecular Cell,* 10**,** 317-26.

Hildebrand, P. W., Preissner, R. & Frömmel, C. 2004. Structural features of transmembrane helices. *FEBS Letters,* 559**,** 145-151.

Hinnebusch, A. G. 2014. The scanning mechanism of eukaryotic translation initiation. *Annual Review of Biochemistry,* 83**,** 779-812.

Hosur, M. V., Schmidt, T., Tucker, R. C., Johnson, J. E., Gallagher, T. M., Selling, B. H. & Rueckert, R. R. 1987. Structure of an insect virus at 3.0 A resolution. *Proteins,* 2**,** 167-76.

Hu, Y.-B., Dammer, E. B., Ren, R.-J. & Wang, G. 2015. The endosomal-lysosomal system: from acidification and cargo sorting to neurodegeneration. *Translational Neurodegeneration,* 4**,** 18.

Hutt-Fletcher, L. M. & Chesnokova, L. S. 2010. Integrins as triggers of Epstein-Barr virus fusion and epithelial cell infection. *Virulence,* 1**,** 395-8.

Hynes, R. O. 1992. Integrins: versatility, modulation, and signaling in cell adhesion. *Cell,* 69**,** 11-25.

Irudayam, S. J. & Berkowitz, M. L. 2011. Influence of the arrangement and secondary structure of melittin peptides on the formation and stability of toroidal pores. *Biochimica et Biophysica Acta,* 1808**,** 2258-66.

Jackson, T., Clark, S., Berryman, S., Burman, A., Cambier, S., Mu, D. Z., Nishimura, S. & King, A. M. Q. 2004. Integrin alpha v beta 8 functions as a receptor for foot-and-mouth disease virus: Role of the beta-chain cytodomain in integrin-mediated infection. *Journal of Virology,* 78**,** 4533-4540.

Jackson, T., Ellard, F. M., Ghazaleh, R. A., Brookes, S. M., Blakemore, W. E., Corteyn, A. H., Stuart, D. I., Newman, J. W. & King, A. M. 1996. Efficient infection of cells in culture by type O foot-and-mouth disease virus requires binding to cell surface heparan sulfate. *Journal of Virology,* 70**,** 5282-7.

Jackson, T., Mould, A. P., Sheppard, D. & King, A. M. 2002. Integrin alphavbeta1 is a receptor for foot-and-mouth disease virus. *Journal of Virology,* 76**,** 935-41.

Jackson, T., Sheppard, D., Denyer, M., Blakemore, W. & King, A. M. Q. 2000. The Epithelial Integrin αvβ6 Is a Receptor for Foot-and-Mouth Disease Virus. *Journal of Virology,* 74**,** 4949-4956.

Jamal, S. M. & Belsham, G. J. 2013. Foot-and-mouth disease: past, present and future. *Veterinary Research,* 44**,** 116.

James, A. D. & Rushton, J. 2002. The economics of foot and mouth disease. *Revue Scientifique et Technique,* 21**,** 637-44.

Jegerlehner, A., Tissot, A., Lechner, F., Sebbel, P., Erdmann, I., Kundig, T., Bachi, T., Storni, T., Jennings, G., Pumpens, P., Renner, W. A. & Bachmann, M. F. 2002. A molecular assembly system that renders antigens of choice highly repetitive for induction of protective B cell responses. *Vaccine,* 20**,** 3104-12.

Johansson, E. S., Ekstrom, J. O., Shafren, D. R., Frisk, G., Hyypia, T., Edman, K. & Lindberg, A. M. 2004. Cell culture propagation and biochemical analysis of the Ljungan virus prototype strain. *Biochemical and Biophysical Research Communications,* 317**,** 1023-9.

Joklik, W. K. 1972. Studies on the effect of chymotrypsin on reovirions. *Virology,* 49**,** 700-15.

Katpally, U., Fu, T. M., Freed, D. C., Casimiro, D. R. & Smith, T. J. 2009. Antibodies to

the buried N terminus of rhinovirus VP4 exhibit cross-serotypic neutralization. *Journal of Virology,* 83**,** 7040-8.

Kestler, H. W., 3rd, Ringler, D. J., Mori, K., Panicali, D. L., Sehgal, P. K., Daniel, M. D. & Desrosiers, R. C. 1991. Importance of the nef gene for maintenance of high virus loads and for development of AIDS. *Cell,* 65**,** 651-62.

Kienberger, F., Zhu, R., Moser, R., Blaas, D. & Hinterdorfer, P. 2004. Monitoring RNA release from human rhinovirus by dynamic force microscopy. *Journal of Virology,* 78**,** 3203-9.

King, A. M., Sangar, D. V., Harris, T. J. & Brown, F. 1980. Heterogeneity of the genome-linked protein of foot-and-mouth disease virus. *Journal of Virology,* 34**,** 627-34.

Kirkegaard, K. 1990. Mutations in VP1 of poliovirus specifically affect both encapsidation and release of viral RNA. *Journal of Virology,* 64**,** 195-206.

Kloc, A., Diaz-San Segundo, F., Schafer, E. A., Rai, D. K., Kenney, M., De Los Santos, T. & Rieder, E. 2017. Foot-and-mouth disease virus 5'-terminal S fragment is required for replication and modulation of the innate immune response in host cells. *Virology,* 512**,** 132-143.

Knight-Jones, T. J. & Rushton, J. 2013. The economic impacts of foot and mouth disease - what are they, how big are they and where do they occur? *Preventive Veterinary Medicine,* 112**,** 161-73.

Knowles, N. J. & Samuel, A. R. 2003. Molecular epidemiology of foot-and-mouth disease virus. *Virus Research,* 91**,** 65-80.

Kotecha, A., Wang, Q., Dong, X., Ilca, S. L., Ondiviela, M., Zihe, R., Seago, J., Charleston, B., Fry, E. E., Abrescia, N. G. A., Springer, T. A., Huiskonen, J. T. & Stuart, D. I. 2017. Rules of engagement between alphavbeta6 integrin and foot-and-mouth disease virus. *Nature Communications,* 8**,** 15408.

Kratz, P. A., Bottcher, B. & Nassal, M. 1999. Native display of complete foreign protein domains on the surface of hepatitis B virus capsids. *Proceedings of the National Academy of Sciences of the United States of America,* 96**,** 1915-20.

Krogh, A., Larsson, B., Von Heijne, G. & Sonnhammer, E. L. 2001. Predicting transmembrane protein topology with a hidden Markov model: application to complete genomes. *Journal of Molecular Biology,* 305**,** 567-80.

Kumar, S., Stecher, G. & Tamura, K. 2016. MEGA7: Molecular Evolutionary Genetics Analysis Version 7.0 for Bigger Datasets. *Molecular Biology and Evolution,* 33**,** 1870-4.

Kyte, J. & Doolittle, R. F. 1982. A simple method for displaying the hydropathic character of a protein. *Journal of Molecular Biology,* 157**,** 105-32.

Lawrence, P. & Rieder, E. 2009. Identification of RNA helicase A as a new host factor in the replication cycle of foot-and-mouth disease virus. *Journal of Virology,* 83**,**

11356-66.

Le Gall, O., Christian, P., Fauquet, C. M., King, A. M., Knowles, N. J., Nakashima, N., Stanway, G. & Gorbalenya, A. E. 2008. Picornavirales, a proposed order of positive-sense single-stranded RNA viruses with a pseudo-T = 3 virion architecture. *Archives of Virology,* 153**,** 715-27.

Le, S. Q. & Gascuel, O. 2008. An improved general amino acid replacement matrix. *Molecular Biology and Evolution,* 25**,** 1307-20.

Lea, S., Hernandez, J., Blakemore, W., Brocchi, E., Curry, S., Domingo, E., Fry, E., Abu-Ghazaleh, R., King, A., Newman, J. & *Et al*. 1994. The structure and antigenicity of a type C foot-and-mouth disease virus. *Structure,* 2**,** 123-39.

Lee, H., Shingler, K. L., Organtini, L. J., Ashley, R. E., Makhov, A. M., Conway, J. F. & Hafenstein, S. 2016. The novel asymmetric entry intermediate of a picornavirus captured with nanodiscs*. Science Advances*, 2**,** e1501929.

Levy, H. C., Bostina, M., Filman, D. J. & Hogle, J. M. 2010. Catching a virus in the act of RNA release: a novel poliovirus uncoating intermediate characterized by cryo-electron microscopy. *Journal of Virology,* 84**,** 4426-41.

Li, H., Dou, J., Ding, L. & Spearman, P. 2007. Myristoylation Is Required for Human Immunodeficiency Virus Type 1 Gag-Gag Multimerization in Mammalian Cells. *Journal of Virology,* 81**,** 12899-12910.

Li, Q., Yafal, A. G., Lee, Y. M., Hogle, J. & Chow, M. 1994. Poliovirus neutralization by antibodies to internal epitopes of VP4 and VP1 results from reversible exposure of these sequences at physiological temperature. *Journal of Virology,* 68**,** 3965-3970.

Liemann, S., Chandran, K., Baker, T. S., Nibert, M. L. & Harrison, S. C. 2002. Structure of the Reovirus Membrane-Penetration Protein, μ1, in a Complex with Its Protector Protein, σ3. *Cell,* 108**,** 283-295.

Lin, J., Lee, L. Y., Roivainen, M., Filman, D. J., Hogle, J. M. & Belnap, D. M. 2012. Structure of the Fab-labeled "breathing" state of native poliovirus. *Journal of Virology,* 86**,** 5959-62.

Logan, D., Abu-Ghazaleh, R., Blakemore, W., Curry, S., Jackson, T., King, A., Lea, S., Lewis, R., Newman, J., Parry, N. & *Et al*. 1993. Structure of a major immunogenic site on foot-and-mouth disease virus. *Nature,* 362**,** 566-8.

Lopez De Quinto, S. & Martinez-Salas, E. 1997. Conserved structural motifs located in distal loops of aphthovirus internal ribosome entry site domain 3 are required for internal initiation of translation. *Journal of Virology,* 71**,** 4171-5.

Lopez De Quinto, S. & Martinez-Salas, E. 2000. Interaction of the eIF4G initiation factor with the aphthovirus IRES is essential for internal translation initiation in vivo. *RNA,* 6**,** 1380-92.

Mahapatra, M., Seki, C., Upadhyaya, S., Barnett, P. V., La Torre, J. & Paton, D. J. 2011. Characterisation and epitope mapping of neutralising monoclonal antibodies to A24 Cruzeiro strain of FMDV. *Veterinary Microbiology,* 149**,** 242-7.

Maier, O., Galan, D. L., Wodrich, H. & Wiethoff, C. M. 2010. An N-terminal domain of adenovirus protein VI fragments membranes by inducing positive membrane curvature. *Virology,* 402**,** 11-9.

Maier, O. & Wiethoff, C. M. 2010. N-terminal alpha-helix-independent membrane interactions facilitate adenovirus protein VI induction of membrane tubule formation. *Virology,* 408**,** 31-8.

Mason, P. W., Bezborodova, S. V. & Henry, T. M. 2002. Identification and characterization of a cis-acting replication element (cre) adjacent to the internal ribosome entry site of foot-and-mouth disease virus. *Journal of Virology,* 76**,** 9686-94.

Moffat, K., Howell, G., Knox, C., Belsham, G. J., Monaghan, P., Ryan, M. D. & Wileman, T. 2005. Effects of foot-and-mouth disease virus nonstructural proteins on the structure and function of the early secretory pathway: 2BC but not 3A blocks endoplasmic reticulum-to-Golgi transport. *Journal of Virology,* 79**,** 4382-95.

Moffat, K., Knox, C., Howell, G., Clark, S. J., Yang, H., Belsham, G. J., Ryan, M. & Wileman, T. 2007. Inhibition of the secretory pathway by foot-and-mouth disease virus 2BC protein is reproduced by coexpression of 2B with 2C, and the site of inhibition is determined by the subcellular location of 2C. *Journal of Virology,* 81**,** 1129-39.

Mohapatra, J. K., Subramaniam, S., Pandey, L. K., Pawar, S. S., De, A., Das, B., Sanyal, A. & Pattnaik, B. 2011. Phylogenetic structure of serotype A foot-and-mouth disease virus: global diversity and the Indian perspective. *Journal of General Virology,* 92**,** 873-9.

Moonen, P. & Schrijver, R. 2000. Carriers of foot-and-mouth disease virus: a review. *Veterinary Quarterly*

22**,** 193-7.

Morgan, C., Rosenkranz, H. S. & Mednis, B. 1969. Structure and Development of Viruses as Observed in the Electron Microscope: X. Entry and Uncoating of Adenovirus. *Journal of Virology,* 4**,** 777-796.

Moscufo, N., Yafal, A. G., Rogove, A., Hogle, J. & Chow, M. 1993. A mutation in VP4 defines a new step in the late stages of cell entry by poliovirus. *Journal of Virology,* 67**,** 5075-8.

Moyer, C. L., Wiethoff, C. M., Maier, O., Smith, J. G. & Nemerow, G. R. 2011. Functional genetic and biophysical analyses of membrane disruption by human adenovirus. *Journal of Virology,* 85**,** 2631-41.

Mullapudi, E., Novacek, J., Palkova, L., Kulich, P., Lindberg, A. M., Van Kuppeveld, F. J. & Plevka, P. 2016. Structure and genome release mechanism of human cardiovirus Saffold virus-3. *Journal of Virology*.

Nayak, A., Goodfellow, I. G. & Belsham, G. J. 2005. Factors required for the Uridylylation of the foot-and-mouth disease virus 3B1, 3B2, and 3B3 peptides by the RNA-dependent RNA polymerase (3Dpol) in vitro. *Journal of Virology,* 79**,** 7698-706.

Nemerow, G. R. 2000. Cell receptors involved in adenovirus entry. *Virology,* 274**,** 1-4.

Neumann, R., Chroboczek, J. & Jacrot, B. 1988. Determination of the nucleotide sequence for the penton-base gene of human adenovirus type 5. *Gene,* 69**,** 153-7.

Newman, J., Asfor, A. S., Berryman, S., Jackson, T., Curry, S. & Tuthill, T. J. 2018. The Cellular Chaperone Heat Shock Protein 90 Is Required for Foot-and-Mouth Disease Virus Capsid Precursor Processing and Assembly of Capsid Pentamers. *Journal of Virology,* 92.

Newton, S. E., Carroll, A. R., Campbell, R. O., Clarke, B. E. & Rowlands, D. J. 1985. The sequence of foot-and-mouth disease virus RNA to the 5' side of the poly(C) tract. *Gene,* 40**,** 331-6.

Nibert, M. L. & Fields, B. N. 1992. A carboxy-terminal fragment of protein mu 1/mu 1C is present in infectious subvirion particles of mammalian reoviruses and is proposed to have a role in penetration. *Journal of Virology,* 66**,** 6408-18.

Nibert, M. L., Schiff, L. A. & Fields, B. N. 1991. Mammalian reoviruses contain a myristoylated structural protein. *Journal of Virology,* 65**,** 1960-7.

Nurani, G., Lindqvist, B. & Casasnovas, J. M. 2003. Receptor priming of major group human rhinoviruses for uncoating and entry at mild low-pH environments. *Journal of Virology,* 77**,** 11985-91.

O'donnell, V., Larocco, M., Duque, H. & Baxt, B. 2005. Analysis of foot-and-mouth disease virus internalization events in cultured cells. *Journal of Virology,* 79**,** 8506-18.

O'donnell, V. K., Pacheco, J. M., Henry, T. M. & Mason, P. W. 2001. Subcellular distribution of the foot-and-mouth disease virus 3A protein in cells infected with viruses encoding wild-type and bovine-attenuated forms of 3A. *Virology,* 287**,** 151-62.

Odegard, A. L., Chandran, K., Zhang, X., Parker, J. S., Baker, T. S. & Nibert, M. L. 2004. Putative autocleavage of outer capsid protein micro1, allowing release of myristoylated peptide micro1N during particle uncoating, is critical for cell entry by reovirus. *Journal of Virology,* 78**,** 8732-45.

Odegard, A. L., Kwan, M. H., Walukiewicz, H. E., Banerjee, M., Schneemann, A. & Johnson, J. E. 2009. Low endocytic pH and capsid protein autocleavage are

critical components of Flock House virus cell entry. *J Virol,* 83**,** 8628-37.

Olson, E. N. & Spizz, G. 1986. Fatty acylation of cellular proteins. Temporal and subcellular differences between palmitate and myristate acylation. *Journal of Biological Chemistry,* 261**,** 2458-66.

Pan, L., Zhao, Y., Yuan, Z. & Qin, G. 2016. Research advances on structure and biological functions of integrins. *Springerplus,* 5**,** 1094.

Panjwani, A., Asfor, A. S. & Tuthill, T. J. 2016. The conserved N-terminus of human rhinovirus capsid protein VP4 contains membrane pore-forming activity and is a target for neutralizing antibodies. *Journal of General Virology,* 97**,** 3238-3242.

Panjwani, A., Strauss, M., Gold, S., Wenham, H., Jackson, T., Chou, J. J., Rowlands, D. J., Stonehouse, N. J., Hogle, J. M. & Tuthill, T. J. 2014. Capsid Protein VP4 of Human Rhinovirus Induces Membrane Permeability by the Formation of a Size-Selective Multimeric Pore. *PLOS Pathogens,* 10**,** 12.

Park, S. C., Kim, J. Y., Shin, S. O., Jeong, C. Y., Kim, M. H., Shin, S. Y., Cheong, G. W., Park, Y. & Hahm, K. S. 2006. Investigation of toroidal pore and oligomerization by melittin using transmission electron microscopy. *Biochemical and Biophysical Research Communications,* 343**,** 222-8.

Peyret, H., Gehin, A., Thuenemann, E. C., Blond, D., EL Turabi, A., Beales, L., Clarke, D., Gilbert, R. J. C., Fry, E. E., Stuart, D. I., Holmes, K., Stonehouse, N. J., Whelan, M., Rosenberg, W., Lomonossoff, G. P. & Rowlands, D. J. 2015. Tandem Fusion of Hepatitis B Core Antigen Allows Assembly of Virus-Like Particles in Bacteria and Plants with Enhanced Capacity to Accommodate Foreign Proteins. *PLoS ONE,* 10**,** e0120751.

Pilipenko, E. V., Pestova, T. V., Kolupaeva, V. G., Khitrina, E. V., Poperechnaya, A. N., Agol, V. I. & Hellen, C. U. 2000. A cell cycle-dependent protein serves as a template-specific translation initiation factor. *Genes & Development,* 14**,** 2028-45.

Plemper, R. K. 2011. Cell entry of enveloped viruses. *Current Opinion in Virology,* 1**,** 92-100.

Pumpens, P. & Grens, E. 1999. Hepatitis B core particles as a universal display model: a structure-function basis for development. *FEBS Letters,* 442**,** 1-6.

Pumpens, P. & Grens, E. 2001. HBV core particles as a carrier for B cell/T cell epitopes. *Intervirology,* 44**,** 98-114.

Qian, S., Wang, W., Yang, L. & Huang, H. W. 2008. Structure of the Alamethicin Pore Reconstructed by X-Ray Diffraction Analysis. *Biophysical Journal,* 94**,** 3512-3522.

Raghava, S., Giorda, K. M., Romano, F. B., Heuck, A. P. & Hebert, D. N. 2013. SV40 late protein VP4 forms toroidal pores to disrupt membranes for viral release.

*Biochemistry*, 52**,** 3939-48.

Ray, A., Jatana, N. & Thukral, L. 2017. Lipidated proteins: Spotlight on protein-membrane binding interfaces. *Progress in Biophysics and Molecular Biology,* 128**,** 74-84.

Rincon, V., Rodriguez-Huete, A., Lopez-Arguello, S., Ibarra-Molero, B., Sanchez-Ruiz, J. M., Harmsen, M. M. & Mateu, M. G. 2014. Identification of the structural basis of thermal lability of a virus provides a rationale for improved vaccines. *Structure,* 22**,** 1560-70.

Rueckert, R. R. & Wimmer, E. 1984. Systematic nomenclature of picornavirus proteins. *Journal of Virology,* 50**,** 957-959.

Sabin, C., Fuzik, T., Skubnik, K., Palkova, L., Lindberg, A. M. & Plevka, P. 2016. Structure of Aichi virus 1 and its empty particle: clues towards kobuvirus genome release mechanism. *Journal of Virology*.

Saiz, M., Gomez, S., Martinez-Salas, E. & Sobrino, F. 2001. Deletion or substitution of the aphthovirus 3' NCR abrogates infectivity and virus replication. *Journal of General Virology,* 82**,** 93-101.

Sanchez-Eugenia, R., Goikolea, J., Gil-Carton, D., Sanchez-Magraner, L. & Guerin, D. M. A. 2015. Triatoma Virus Recombinant VP4 Protein Induces Membrane Permeability through Dynamic Pores. *Journal of Virology,* 89**,** 4645-4654.

Sangar, D. V., Rowlands, D. J., Harris, T. J. & Brown, F. 1977. Protein covalently linked to foot-and-mouth disease virus RNA. *Nature,* 268**,** 648-50.

Schneemann, A., Zhong, W., Gallagher, T. M. & Rueckert, R. R. 1992. Maturation cleavage required for infectivity of a nodavirus. *Journal of Virology,* 66**,** 6728-34.

Shukla, A., Padhi, A. K., Gomes, J. & Banerjee, M. 2014. The VP4 peptide of hepatitis A virus ruptures membranes through formation of discrete pores. *Journal of Virology,* 88**,** 12409-21.

Sila, M., Au, S. & Weiner, N. 1986. Effects of Triton X-100 concentration and incubation temperature on carboxyfluorescein release from multilamellar liposomes. *Biochimica et Biophysica Acta (BBA) - Biomembranes,* 859**,** 165-170.

Stgelais, C., Tuthill, T. J., Clarke, D. S., Rowlands, D. J., Harris, M. & Griffin, S. 2007. Inhibition of hepatitis C virus p7 membrane channels in a liposome-based assay system. *Antiviral Research,* 76**,** 48-58.

Strauss, M., Levy, H. C., Bostina, M., Filman, D. J. & Hogle, J. M. 2013. RNA transfer from poliovirus 135S particles across membranes is mediated by long umbilical connectors. *Journal of Virology,* 87**,** 3903-14.

Strebel, K. & Beck, E. 1986. A second protease of foot-and-mouth disease virus. *Journal of Virology,* 58**,** 893-9.

Sweeney, T. R., Cisnetto, V., Bose, D., Bailey, M., Wilson, J. R., Zhang, X., Belsham, G.

J. & Curry, S. 2010. Foot-and-mouth disease virus 2C is a hexameric AAA+ protein with a coordinated ATP hydrolysis mechanism. *Journal of Biological Chemistry,* 285**,** 24347-59.

Thompson, D., Muriel, P., Russell, D., Osborne, P., Bromley, A., Rowland, M., Creigh-Tyte, S. & Brown, C. 2002. Economic costs of the foot and mouth disease outbreak in the United Kingdom in 2001. *Revue Scientifique et Technique Office International des Epizooties,* 21**,** 675-87.

Tiley, L., King, A. M. Q. & Belsham, G. J. 2003. The Foot-and-Mouth Disease Virus cis-Acting Replication Element (cre) Can Be Complemented in trans within Infected Cells. *Journal of Virology,* 77**,** 2243-2246.

Tuthill, T. J., Bubeck, D., Rowlands, D. J. & Hogle, J. M. 2006. Characterization of early steps in the poliovirus infection process: receptor-decorated liposomes induce conversion of the virus to membrane-anchored entry-intermediate particles. *Journal of Virology,* 80**,** 172-80.

Tuthill, T. J., Harlos, K., Walter, T. S., Knowles, K. J., Groppelli, E., Rowlands, D. J., Stuart, D. I. & Fry, E. E. 2009. Equine Rhinitis A Virus and Its Low pH Entry Particle: Clues Towards an Aphthovirus Entry Mechanism. *PLOS Pathogens,* 5**,** 11.

Vakharia, V. N., Devaney, M. A., Moore, D. M., Dunn, J. J. & Grubman, M. J. 1987. Proteolytic processing of foot-and-mouth disease virus polyproteins expressed in a cell-free system from clone-derived transcripts. *Journal of Virology,* 61**,** 3199-207.

Veronese, F. D., Copeland, T. D., Oroszlan, S., Gallo, R. C. & Sarngadharan, M. G. 1988. Biochemical and immunological analysis of human immunodeficiency virus gag gene products p17 and p24. *Journal of Virology,* 62**,** 795-801.

Vogel, H. & Jähnig, F. 1986. The structure of melittin in membranes. *Biophysical Journal,* 50**,** 573-582.

Vogel, M., Vorreiter, J. & Nassal, M. 2005. Quaternary structure is critical for protein display on capsid-like particles (CLPs): efficient generation of hepatitis B virus CLPs presenting monomeric but not dimeric and tetrameric fluorescent proteins. *Proteins,* 58**,** 478-88.

Walukiewicz, H. E., Johnson, J. E. & Schneemann, A. 2006. Morphological changes in the T=3 capsid of Flock House virus during cell entry. *Journal of Virology,* 80**,** 615-22.

Wang, X., Ren, J., Gao, Q., Hu, Z., Sun, Y., Li, X., Rowlands, D. J., Yin, W., Wang, J., Stuart, D. I., Rao, Z. & Fry, E. E. 2015. Hepatitis A virus and the origins of picornaviruses. *Nature,* 517**,** 85-88.

Wernery, U. & Kaaden, O. R. 2004. Foot-and-mouth disease in camelids: a review.

*Veterinary Journal*, 168**,** 134-42.

Wetherill, L. F., Holmes, K. K., Verow, M., Muller, M., Howell, G., Harris, M., Fishwick, C., Stonehouse, N., Foster, R., Blair, G. E., Griffin, S. & Macdonald, A. 2012. High-risk human papillomavirus E5 oncoprotein displays channel-forming activity sensitive to small-molecule inhibitors. *Journal of Virology,* 86**,** 5341-51.

White, J. M., Delos, S. E., Brecher, M. & Schornberg, K. 2008. Structures and Mechanisms of Viral Membrane Fusion Proteins: Multiple Variations on a Common Theme. *Critical Reviews in Biochemistry and Molecular Biology,* 43**,** 189-219.

Wickham, T. J., Mathias, P., Cheresh, D. A. & Nemerow, G. R. 1993. Integrins alpha v beta 3 and alpha v beta 5 promote adenovirus internalization but not virus attachment. *Cell,* 73**,** 309-19.

Wiethoff, C. M. & Nemerow, G. R. 2015. Adenovirus Membrane Penetration: Tickling the Tail of a Sleeping Dragon. *Virology,* 0**,** 591-599.

Wiethoff, C. M., Wodrich, H., Gerace, L. & Nemerow, G. R. 2005. Adenovirus protein VI mediates membrane disruption following capsid disassembly. *Journal of Virology,* 79**,** 1992-2000.

Wilen, C. B., Tilton, J. C. & Doms, R. W. 2012. HIV: cell binding and entry. *Cold Spring Harb Perspectives in Medicine,* 2.

Wilkins, M. R., Gasteiger, E., Bairoch, A., Sanchez, J. C., Williams, K. L., Appel, R. D. & Hochstrasser, D. F. 1999. Protein identification and analysis tools in the ExPASy server. *Methods in Molecular Biology,* 112**,** 531-52.

Yamashita, T., Sakae, K., Tsuzuki, H., Suzuki, Y., Ishikawa, N., Takeda, N., Miyamura, T. & Yamazaki, S. 1998. Complete nucleotide sequence and genetic organization of Aichi virus, a distinct member of the Picornaviridae associated with acute gastroenteritis in humans. *Journal of Virology,* 72**,** 8408-12.

Yang, L., Harroun, T. A., Weiss, T. M., Ding, L. & Huang, H. W. 2001. Barrel-Stave Model or Toroidal Model? A Case Study on Melittin Pores. *Biophysical Journal,* 81**,** 1475-1485.

Zell, R. 2018. Picornaviridae-the ever-growing virus family. *Archives of Virology,* 163**,** 299-317.

Zha, J., Weiler, S., Oh, K. J., Wei, M. C. & Korsmeyer, S. J. 2000. Posttranslational N-myristoylation of BID as a molecular switch for targeting mitochondria and apoptosis. *Science,* 290**,** 1761-5.

Zhang, L., Agosto, M. A., Ivanovic, T., King, D. S., Nibert, M. L. & Harrison, S. C. 2009. Requirements for the formation of membrane pores by the reovirus myristoylated micro1N peptide. *Journal of Virology,* 83**,** 7004-14.

Zhao, M., Bai, Y., Liu, W., Xiao, X., Huang, Y., Cen, S., Chan, P. K., Sun, X., Sheng, W.

& Zeng, Y. 2013. Immunization of N terminus of enterovirus 71 VP4 elicits cross-protective antibody responses. *BMC Microbiology,* 13**,** 287.

Zhou, W., Parent, L. J., Wills, J. W. & Resh, M. D. 1994. Identification of a membrane-binding domain within the amino-terminal region of human immunodeficiency virus type 1 Gag protein which interacts with acidic phospholipids. *Journal of Virology,* 68**,** 2556-2569.

Zhu, L., Wang, X., Ren, J., Porta, C., Wenham, H., Ekstrom, J. O., Panjwani, A., Knowles, N. J., Kotecha, A., Siebert, C. A., Lindberg, A. M., Fry, E. E., Rao, Z., Tuthill, T. J. & Stuart, D. I. 2015. Structure of Ljungan virus provides insight into genome packaging of this picornavirus. *Nature Communications,* 6**,** 8316.

Zibert, A., Maass, G., Strebel, K., Falk, M. M. & Beck, E. 1990. Infectious foot-and-mouth disease virus derived from a cloned full-length cDNA. *Journal of Virology,* 64**,** 2467-2473.